Microporous and Mesoporous Materials 312 (2021) 110751

Contents lists available at ScienceDirect

Microporous and Mesoporous Materials

journal homepage: http://www.elsevier.com/locate/micromeso

Influence of surface modification on selective CO_2 adsorption: A technical review on mechanisms and methods

Ben Petrovic, Mikhail Gorbounov, Salman Masoudi Soltani *

Department of Chemical Engineering, Brunel University London, Uxbridge UB8 3PH, United Kingdom

ARTICLE INFO

Keywords:
CO_2
Adsorbent
Adsorption
Surface modification
Functional groups

ABSTRACT

The mitigation of climate change, abatement of greenhouse gas emissions and thus, fundamentally, the separation of CO_2 from various gas streams are some of the most pressing and multifaceted issues that we face as a society. De-carbonising our entire civilisation will come at a great cost and requires vast amounts of knowledge, initiative and innovation; yet, no matter how much time or money is spent, some sectors simply cannot be decarbonised without the deployment of carbon capture and storage technologies. The technical challenges associated with the removal of CO_2 are not universal – there exists no single solution. Capturing the CO_2 on solid sorbents has been gaining traction in recent years given its cost-effectiveness as a result of its ease of application, relatively small energy requirements and applicability in a wide range of processes. Even with the myriad materials such as zeolites, carbons, metal organic frameworks, mesoporous silicas and polymers, the challenge to identify a sorbent with optimal capacity, kinetics, selectivity, stability and ultimately, viability, still persists. By tailoring these solid materials through comprehensive campaigns of surface modification, the pitfalls of each can be mollified and the strengths enhanced. This highly specific tailoring must be well informed so as to understand the mechanisms by which the CO_2 is adsorbed, the surface chemistry that has influence on this process, and what methods exist to facilitate the improvement of this. This review endeavours to identify the surface functional groups that interact with the CO_2 molecules during adsorption and the methods by which these functional groups can be introduced. It also provides a comprehensive review of the recent attempts and advancements made within the scientific community in the experimental applications of such methods to enhance CO_2 capture *via* adsorption processes. The primary search engine employed in this critical review was Scopus. Of the 421 references cited that embody the literature focussed on surface modification for enhancing the selective adsorption of CO_2, 370 are original research papers, 43 are review articles and 7 are conference proceedings.

1. Introduction

The unavoidable concerns surrounding global warming and climate change can clearly be seen in every aspect of society from technology to politics. As a result of sustained public pressure in the UK in the early summer of 2019 the UK government's response was to declare a climate emergency in June thereby announcing a target of net zero greenhouse gas emissions compared to the 1990 levels by the year 2050 [1]. If we are to successfully avoid a global rise in temperature of less than 2 °C as set out in the Paris Agreement targets [2], technologies such as Carbon Capture and Storage (CCS) are indispensable. Most integrated assessment models are unable to find a solution to meet these targets without the use of CCS [3]. CCS as defined by the Intergovernmental Panel on Climate Change is a three-stage strategy for reducing CO_2 emissions [4] encompassing the: separation; transportation; and storage of CO_2. The first accounting for around two thirds of the total cost [5]. This high cost has rendered its large-scale deployment insurmountable [6] even with governmental incentives and regulatory drivers the promise to mitigate large volumes of CO_2 has not been met. CCS is the only available technology that can deliver significant reductions in anthropogenic emissions not only from the use of fossil fuels in power generation but also from those sectors that are proving to be notoriously difficult to decarbonise such as cement manufacturing, iron and steel production, refining and the petrochemical industry [7].

Among many available CCS technologies, absorption has been the most conventional and industrialised option for large-scale applications with economic feasibility [8]. The limitations of this process however, are far reaching and include substantial energy costs, regeneration

* Corresponding author.
E-mail address: Salman.MasoudiSoltani@brunel.ac.uk (S. Masoudi Soltani).

https://doi.org/10.1016/j.micromeso.2020.110751
Received 1 September 2020; Received in revised form 9 October 2020; Accepted 2 November 2020
Available online 7 November 2020

difficulties among concerns of toxicity and further pollution with the majority of existing, conventional solvents [9]. To date, a number of separation technologies have been explored, including physical absorption, chemical absorption, cryogenics, oxyfuel combustion, membranes and adsorption. As a basic, yet effective tool for the separation of gaseous mixtures in industrial processes, adsorption, a surface energy phenomenon, has often been favoured over other methods such as absorption, decomposition or precipitation due to its advantages that include precursor accessibility, ease of handling in regeneration and cost-effectiveness [8]. The success of this approach depends on the development of an optimum adsorbent with high uptake, fast kinetics, good selectivity, low-cost, high-availability, cyclic stability, mechanical and chemical strength and an easy regeneration regime [7,10–12]. Throughout the literature there are myriad materials used for the selective capture of CO_2 such as: activated carbon (AC) [13–20], activated carbon fibre (ACF) [21–23], carbon nano-tubes (CNT) [24–31], graphene and graphene-based materials [32–39], organic polymers [40–43], molecular sieves [44–47], zeolites [48–56], metal organic frameworks (MOFs) [57–62], microporous coordination polymers (MCPs), zeolitic imidazolate frameworks (ZIFs) [63–67] and metal oxides [68–70]. Despite all these advancements, it has been learnt that zeolites suffer from issues when gas streams contain moisture or impurities [71]; MOFs can be costly and difficult to produce at scale therefore deemed less feasible for industrial applications [72]; and carbons can suffer from significant reductions in capacity at elevated temperatures. Evidently and undeniably, each type of material has its own individual limitations hindering their large-scale deployments, hence, surface modifications may be employed to provide improved sorption characteristics.

Physical adsorption is caused mainly by van der Waals force and electrostatic forces between adsorbate molecules and the atoms that compose the adsorbent surface [73]. The surface properties of the adsorbent such as polarity corresponds to its affinity with polar substances. Zeolites, a class of porous crystalline aluminosilicates are built of a periodic array of TO_4 tetrahedra (T = Si or Al), the presence of aluminium atoms in the these silicate-based molecular sieve materials introduces negative framework charges that are compensated with exchangeable cations in the pore space (often alkali cations) [74]. These characteristics enable them to adsorb gases such as CO_2. The physical adsorption of CO_2 onto zeolites is predominantly influenced by the CO_2 molecules interacting with the electric field generated by the charge-compensating cations; by exchanging these ions with various alkali or alkaline earth species the capacity can be increased [75]. Alongside zeolites in the physical adsorbent class are carbons. Here, the physical adsorption of CO_2 relies on the existence of suitable porosity but can be influenced quite significantly by the presence of various functional groups. It has been shown that carbons with basic surface groups can be more resistant to moisture and possess more active sites for the adsorption of CO_2 [76]. The importance of basic sites in the facilitation of CO_2 adsorption can be seen in metal-based sorbents, especially those that possess a low charge/radius ratio which possess a more ionic nature and present more strongly basic sites [10]. With metal-based adsorbents such as magnesium oxide or calcium oxide the CO_2 reacts to form metal carbonates where 1 mol of oxide can chemically adsorb the stoichiometric equivalent of CO_2. These alkali metal ions can also be doped into the framework of hydrotalcite materials with a view to modify their chemistry and improve the relatively low capacities. Evidently, multiple parameters affect the overall process performance and economics of adsorption [74]. With physical adsorbents, generally their capacities are a function of surface area and surface affinity towards CO_2 while chemical sorbents can possess wildly varying properties based upon the nature of their interactions with CO_2.

Enhancement of the interactions between CO_2 molecules and the sorbent can be achieved through various campaigns of surface modification techniques. Among the new directions for these modifications is pore functionalisation using polar groups such as hydroxy, nitro, amine, sulphonate, imidazole, triazine, imine, *etc.* [77]. When considering these surface functional groups (SFGs) for the purpose of adsorbent modification, a thorough understanding of their effects and synergistic relationships with one another, the adsorbent and the adsorbate, is key before attempting to identify the method with which to incorporate them. These SFGs can either be introduced prior to adsorbent synthesis *via* careful selection or modification of the precursors where CO_2-philic moieties would then form during the synthesis protocol or alternatively, through post-synthesis modification (PSM) where functional groups are attached to the surface of the adsorbent. PSM often negates the drawbacks associated with the former at the expense of fully controlled loading of the SFGs, although this can be avoided. With the pre-synthesis protocol where the introduction of SFGs occurs prior to severe acidic/basic chemical activations or extreme thermal treatments, it becomes time-consuming and nontrivial to protect the selected SFGs. This is before considering that a number of side reactions may occur due to competition with other functional groups in the reaction media [78]. The advantage then lies with post-synthetic modification [79] especially when considering the convenient scale-up of production [80].

The identification and characterisation of the functional groups present on the surface of adsorbents is just as complex, owing to the convoluted behaviour that SFGs possess. Conventionally, elemental analysis would be used as the primary method for qualitative and quantitative analyses; however, it lacks the capacity to identify SFGs. Various techniques can be used such as Boehm titration [81,82], temperature programmed desorption (TPD) [83,84], x-ray photoelectron spectroscopy (XPS) [85–87], Fourier transform infrared spectroscopy (FTIR), Raman spectroscopy [88–90] and nuclear magnetic resonance (NMR) [58,91,92]. The authors direct the reader to a number of reviews published on the use of these techniques for surface characterisation published by Wepasnick et al. [93], González-García [94], Igalavithana et al. [95], Lopez-Ramon et al. [96] and Zhou et al. [97] although this list is not exhaustive and the body of literature available on the topic is vast.

This review will provide a comprehensive evaluation and assessment of the mechanisms by which CO_2 is selectively adsorbed and the routes to the enhancement of this surface phenomena. By giving precedence to the specific surface functional groups that can facilitate the adsorption of CO_2, the scope of this work is to describe the functionalities that give rise to the interactions between the adsorbent and CO_2. Thereon, an extensive and thorough discussion of the materials and methods that promote their introduction is made. In the following section (Section 2) the mechanisms of adsorption, both physical and chemical will first be identified. The subsequent section (Section 3) will then endeavour to discuss the interactions that arise as a result of the presence of specific functional groups in the context of O-heteroatom(s) (Section 3.1), N-heteroatom(s) (Section 3.2), S-heteroatom(s) (Section 3.3) and a selection of others (Sections 3.4 and 3.5). The sections thereafter will focus on the experimental methods employed in introducing the aforementioned groups (Section 4) with respect to physical (Section 4.1) and chemical (Section 4.2) modifications and finally the reagents that can be used for this purpose (Section 5).

2. Adsorption mechanisms

The overall process of adsorption consists of a series of steps. When the fluid flows past the particle the solute first diffuses from the bulk fluid to the gross exterior of the surface, then the solute diffuses inside the pore to the surface of the pore where the solute will then be adsorbed onto the surface [98]. Since adsorption can only occur on the surface, increasing porosity can increase the available space for adsorption to occur. Pore sizes can be classified as either macropores (>50 nm), mesopores (2 nm–50 nm) and micropores (<2 nm) [99]. The mechanisms of adsorption then can be divided into two stages: the diffusive mechanisms, *i.e.* how the CO_2 molecule is transported to the active sites in the pores of the adsorbent; and the adsorption mechanisms, *i.e.* how

the CO_2 molecule is adsorbed on the surface *via* molecular reactions or interactions with various functional groups.

With respect to the first stage, four distinct mechanisms of mass transport exist: molecular or bulk diffusion; Knudsen diffusion; surface diffusion; and Poiseuille flow [100–102]. Aside from Poiseuille flow which is a function of pressure difference across the adsorbent the other transport mechanisms are a function of temperature: molecular proportional to $T^{3/2}$, while Knudsen diffusion is a function of $T^{1/2}$. Surface diffusion is more significant at higher surface loadings but will decrease as temperature increases in physisorption as a result of the decrease in the surface loading and increase in diffusional flux in the gas phase as a result of faster molecular diffusion [103]. Depending on the structure of the adsorbent several of these mechanisms can occur and compete or cooperate with one another [73]. The simplest mechanism of diffusion is Knudsen diffusion which occurs when the diameter of the pore is less than the mean free path of the molecules. In the case of molecular diffusion, if this takes place in the macropores it is known as pore diffusion. When the molecules on the surface of the adsorbent are mobile, typically when adsorbed components form two or more layers they can migrate, and this is termed surface diffusion and, in some cases, can contribute more to intraparticle diffusion than pore diffusion. When the adsorbate molecule is close to the size of the micropore, the rate of diffusion can be limited, the diffusion becomes an activated process depending heavily on the adsorbate properties.

When looking at the second stage of CO_2 adsorption, the majority of solid surfaces preferentially adsorb CO_2 over N_2 *via* a physisorption mechanism, owing to the greater polarizability and quadrupole moment of CO_2 [104]. However, the addition of an SFG can lead to an increasing importance of the chemical interaction. Normally, the introduction of Lewis bases increases the affinity of the material towards CO_2, as carbon dioxide can act as a weak Lewis acid. Therefore, adding basic N-containing functional groups to the surfaces of classical adsorbents (*i.e.* activated carbons, zeolites and *etc.*) is one of the most popular ways of improving sorption properties. However, the addition of functional groups may lead to the blockage of the access of the adsorbate molecules to the pores [105] by clogging the outermost layer of the framework in MOFs upon grafting [104] or filling and/or damaging the pores following impregnation of AC or other mesoporous supports [106] by potentially covering the mesopore, thereby adversely denying further diffusion into the pore. Therefore, steric hindrance should also be considered when choosing the appropriate functionalisation. Disordered micropores tend to have a slower gas diffusion rate; the presence of mesopores promotes gas diffusion and transport into the micropores by reducing the pathway distance and the resistance to diffusion [107]; a low diffusion coefficient leads to a high activation energy of diffusion [108].

3. Surface functional groups

3.1. O-Heteroatom(s)

The acidic nature of the surface of the adsorbent is usually determined by the presence of oxygen. The strong electronegativity of this atom draws the electron density from less electronegative atoms towards itself, thereby creating localised nucleophilic and electrophilic centres [8]. Alongside this, the oxygen containing functional groups are often polar in nature and that increases the degree of hydrophilicity of the adsorbent and the affinity towards water [109]. Such hydrophilicity can be explained by the hydrogen bonds between water molecules and the surface oxygen atoms [110]. In spite of this, oxygen functionalities can improve sorption properties. An increase of 26% in carbon uptake (at 298 K and 1 bar) compared to the unmodified adsorbent has been reported by Plaza et al. [111]. Nevertheless, the use of such functional groups in the context of carbon capture has been investigated thoroughly; the results of which and their adsorption mechanisms will be discussed hereafter.

3.1.1. Phenol

A porous carbon surface was grafted with hydroquinone (*para*-hydroxyphenol) by Wang et al. [89]. The resulting material demonstrated an adsorption capacity of 3.46 $mmol_{CO2}/g$ at 1 bar and 298 K, whereas the unmodified carbon used in the study corresponded to a CO_2 uptake capacity of 3.02 $mmol_{CO2}/g$. At 273 K and 1 bar, the capacity was 5.41 $mmol_{CO2}/g$ and 4.78 $mmol_{CO2}/g$, for the modified and unmodified carbon, respectively. Enhancements in CO_2 uptake for the modified carbon were also realised at 323 K. Alongside this, an increase of 58.7% in CO_2/N_2 selectivity and a considerable uptake of 1.33 $mmol_{CO2}/g$ at 273 K and 0.1 bar (absolute) was observed. This was despite a lower Brunauer–Emmett–Teller (BET) surface area and pore volume for the modified sample, 925 m^2/g vs 1006 m^2/g and 0.53 cm^3/g vs 0.57 cm^3/g, respectively. In this work, the modification lead to a negligible decrease in isosteric heat of adsorption: from 23.8 kJ/mol to 23.5 kJ/mol. This implies that the cost of regeneration for the modified materials will be significantly lower than for other materials [112,113]; interestingly modified ACs tend to present higher values of adsorption heat but it was concluded that the value is not only determined by the introduced groups rather a combination of these with specific surface area and pore structure. The impact of decreasing specific area on the hydroquinone modified samples may offset the impact of oxygen doping [89].

3.1.2. Carboxylic

A high density of surface carboxylic (-COOH) groups make carbonaceous adsorbents highly dispersible in water [109]. A surface carboxylic group should lead to enhancement in physisorption, as it increases the binding energy (if the bond is non-chemical). This effect is caused by lone pair donation of the oxygen in the group and the carbon in CO_2 and by hydrogen bond interactions of the acidic protons and the CO_2 oxygen [114]. Therefore, it is understood that the two types of interactions are attributed to the two different parts of the carboxylic group: the carbonyl (which can act as a Lewis base) and the hydroxy group (which can use the acidic proton to act as a Lewis acid). An investigation of such functionalisation on a conjugated microporous polymer (CMP) [40] showed an increase of sorption heat and a decline in volumetric CO_2 uptake as well as the surface area and pore volume. The same rise of enthalpy has been observed for a MOF (MIL-53) when modified with the carboxylic group, this rise however, was accompanied by an elevation in CO_2 uptake [62]. Modifying the MOF, UiO-66 with the same SFG has also been shown to lead to an uptake in capacity: 6.4 $mmol_{CO2}/g$ at 25 bar and 33 °C compared to 5.6 $mmol_{CO2}/g$ [115]. Therefore, –COOH is considered to be a great substitute for ligand modification for CO_2 adsorption in MOFs [116]. However, such free functionalities could negatively coordinate with the metal ions in the framework [40]. Additionally, free carboxylic acid sites decompose to CO_2 upon heat treatment forming uncoordinated carbon sites that can easily adsorb CO_2; those sites have been shown to provide additional CO_2 adsorption capacity in the impregnated adsorbent as reported by Caglayan et al. [117].

3.1.3. Quinone

Quinone functionalisation has been investigated in the work of Wang et al. [89], the modified carbon demonstrated an adsorption capacity of 2.22 $mmol_{CO2}/g$ at 1 bar and 298 K. The unmodified carbon was shown to exhibit a capacity of 3.02 $mmol_{CO2}/g$ under the same conditions. When decreasing the temperature to 273 K, as to be expected the capacity increases to 3.44 $mmol_{CO2}/g$ and 4.78 $mmol_{CO2}/g$ for the modified and unmodified carbon, respectively. This trend was also observed at 323 K, rendering the uptake of quinone-functionalised carbon consistently lower than that of the unmodified. This poorer performance may be a result of the modified sample possessing significantly lower BET surface area and pore volumes, 653 m^2/g and 0.38 cm^3/g, respectively; half that of the parent, 1006 m^2/g and 0.57 cm^3/g. When considering the CO_2 uptake with respect to the surface area, the normalised values are greater for the modified sample thus elucidating to

the stronger interactions of CO_2 with the O-decorated carbon framework. Furthermore, functionalising the surface with quinone lead to a marginal decrease in the isosteric heat of adsorption: from 23.8 kJ/mol to 23 kJ/mol. Improvements in CO_2/CH_4 selectivity were also achieved, the quinone-modified sample demonstrating a selectivity of 4.6 (at 298 K and 1 atm), which represents a 28.4% improvement over the parent material. A similar increase was noted for CO_2/N_2 selectivity.

3.1.4. Lactone

Lactones are a functional group that is considered to be acidic [118] and non-polar [119]. This group can be found on the surfaces of carbonaceous adsorbents and is commonly formed during the chemisorption of CO_2 [120]. Though, generally, not a functionality used to modify the adsorbing material, lactones are not believed to be adverse or detrimental for the capture of carbon dioxide. However, other functional groups discussed in this review are considered to be better for these purposes. The same observation has been made by Bai et al. [119] in that alternative polar groups (*e.g.* hydroxyl and carboxyl) can lead to enhancements in both adsorption capacity and selectivity.

3.1.5. Carbonyl

The unpaired electrons of oxygen that exist in groups such as carbonyl enhance the adsorption of polar and polarisable species, through Lewis acid-base (or electron acceptor-donor) interactions [121], most probably of Lewis acid-base nature. A recent first principles study indicated that it could in fact be a functionality for CO_2 capture by porous adsorbents [122]. Carbonyl can also be found in one of the two pyridone group tautomers [123] (which will be discussed in a later section), the carbonyl form is the most abundant. Groups such as ketone and aldehyde also contain an electron donating oxygen atom that can interact electrostatically with CO_2 [111] leading to a Lewis acid-base interaction between carbon dioxide (acting as a Lewis acid) and the carbonyl oxygen being the preferred binding site for the adsorbate [124]. The interaction between carbonyls and CO_2 involves greater electron transfer than that of a benzene group and $_{CO2}$. The influence of this group has been investigated in the work of He *et al.* [41] which involved the development of a microporous organic polymer (MOP) based on triptycene that was formyl-functionalised (-HC═O). Interestingly the adsorbent performed poorly in comparison to an analogous amino-modified sorbent: 1.1 $mmol_{CO2}/g$ vs 2.1 $mmol_{CO2}/g$ at 298 K and 1 bar. In the work of Kim et al. [125] again on MOPs, the carbonyl groups of cucurbit(6)uril (CB(6)) were shown to have a strong interaction with CO_2. Of the three sites that CO_2 was adsorbed, that with the carbonyl present included two CO_2 molecules, interacting with the SFG but also with each other in a slipped-parallel geometry. The influence of carbonyl can also be seen in indole-based MOPs [126]; the indole and carbonyl groups developing a synergistic improvement to the favourability of CO_2 adsorption. This can be observed in the value of the isosteric heat of adsorption, 35.2 kJ/mol. The capacity of this adsorbent was demonstrated to be 6.12 $mmol_{CO2}/g$ at 1 bar and 273 K with a CO_2/N_2 selectivity of 76 and CO_2/CH_4 of 20, the BET surface was 1628 m^2/g. The performance postulated to be a result of indole and CO_2 showing strong local dipole-π (out-plane) stacking interactions with each other, whereas they cannot form an in-plane conformation [127] and carbonyl only being able to form in-plane conformations with CO_2. The adjacent carbonyl groups are also more polar due to the resonance effect by the indole group.

3.1.6. Ethers

Ethers contain an electron donating oxygen atom that could interact electrostatically with CO_2 [111]. In the work of He et al. [41], an acetyl (-C-O-CH_3) functionalised triptycene MOP was evaluated alongside a similar aminotriptycene MOP. The two sorbents exhibited comparable results at 273 K at 1 bar (3.2 $mmol_{CO2}/g$ and 3.4 $mmol_{CO2}/g$, respectively) with the ether-substituted polymer surpassing the –NH_2 modified analogue at 298 K and 1 bar. The uptake of the former being 2.2 $mmol_{CO2}/g$ and the latter 2.1 $mmol_{CO2}/g$. It was learned in the work of Zeng et al. [128] however, that the replacement of an ether group in a 5-fold interpenetrated covalent organic framework (COF) with a CH_2 group would result in a 32% decrease in CO_2 capacity at 1 bar. Cmarik et al. [129] demonstrated that adding two methoxy groups (O–CH_3) to the ligand of UiO-66 has been shown to improve CO_2/N_2 selectivity and uptake at 298 K and 1 bar from 1.786 $mmol_{CO2}/g$ for the non-functionalised framework to 2.631 $mmol_{CO2}/g$. These improvements achieved despite a significant decrease in surface area from approximately 1105 m^2g to 868 m^2/g and pore volume from 0.55 cm^3/g to 0.38 cm^3/g. However, the performance of this functionality was worse than that of the amine group investigated in the same study. This fact was attributed to a reduced pore volume and surface area as the methoxy group is bulkier compared to –NH_2. Epoxy groups, a cyclic ether of three atoms, has also been investigated in the context of surface modification and has been shown to provide reasonable results [130]. In the work of Kronast et al., UiO-66-epoxide demonstrated a capacity of 2.26 $mmol_{CO2}/g$ at 1 bar and 35 °C.

3.1.7. Esters

Esters are a close but more polar relative of ethers; both esters and ethers are less polar than alcohol. This property has been associated with the promotion of CO_2 adsorption, as the capacity and selectivity of such functionalised materials should increase due to the chemisorption of carbon dioxide by dipole-quadrupole interactions. Molavi et al. [131] has investigated a MOF with a variety of functional groups including esters *via* grafting. By comparing these with the parent MOF that possessed just a primary amine ligand functionalisation the results indicated a rise in CO_2 uptake of 36% at 298 K and 1 bar from 3.14 to 4.28 $mmol_{CO2}/g$. It is noteworthy, that the selectivity over nitrogen was higher for the ester-modified adsorbent than for the amine-modified. However, one must also note that the resulting material was grafted by glycidyl methacrylate and, therefore, included not only the above discussed functionalisation but also secondary amines, hydroxyls and alkenes compared to the parent material that possessed merely the primary amine group. Nevertheless, we can partially attribute the enhancement of CO_2 affinity to the ester present and assume that it is not detrimental to post-combustion carbon capture with solid adsorbents as it is able to interact with the adsorbate; other functionalities are better suited for these purposes.

3.1.8. Hydroxyl

The interaction between the hydroxyl group and CO_2 is typically considered to be a result of hydrogen-bonding interactions or electrostatic interactions [132]. These mechanisms have been found in the adsorption mechanisms of a MOF-like MIL-53 where the adsorption was directed by the formation of relatively weak hydrogen bonds between CO_2 and the corner-sharing hydroxyl groups [133,134]. This interaction suggests that the main mechanism is in fact a result of hydrogen bonding between the $H_{(OH)}$ and the $O_{(CO2)}$ but when considering the high electrostatic potential, there is the possibility that the $O_{(OH)}$ could donate electrons to CO_2 [107]. Additional interactions have been identified when functionalising the ligands of MOFs in the work of Torrisi et al. [116]. Alongside the aforementioned interactions, there were cases of monopole interactions between the same atoms reinforced by a mutual inductive effect. This judgement is based on the angle measurements of the C═ O···H bond (93°), the value of which is too low for this interaction to be characteristic of hydrogen-bonding. Even with this, we can assume that both types of bonding can occur simultaneously or separately within adsorbent-adsorbate system. This statement however does not hold when considering modifications involving alcohol groups since the adsorption characteristics and therefore overall performance of the process vary depending on the type of bond. The alcohol group of diethanolamine (DEA) was shown to enhance the adsorption of CO_2 in an amine-mixed metal-oxide hybrid adsorbent developed by Ravi et al. [135] as a result of Lewis acid-base interactions between the $H_{(OH)}$ and

the $O_{(CO2)}$ [136]. The synergistic effect between alcohol groups and amines facilitates the reaction between amines and CO_2 molecules [131]. It has been shown by Kronast et al. that at 308 K an amino alcohol-substituted UiO-66 could adsorb approximately 2.2 $mmol_{CO2}/g$ at 1 bar and 11.67 $mmol_{CO2}/g$ at 20 bar. This corresponds to a CO_2 loading of 51 wt% in combination with a high selectivity over nitrogen. The BET measurements have indicated only 3 m^2/g of accessible surface area. Hydroxyl groups have also been shown to form bicarbonate type complexes [137]. Ma et al. reported [107] that the adsorption of CO_2 increases linearly with an increase in surface hydroxyl groups at ambient temperature and pressured up to 0.5 bar. This linearity, however, is lost at elevated pressures or decreased temperatures. In contrast, Dawson et al. [40] was able to identify a decrease in adsorption capability of a CMP that was modified with a view to produce a "di-ol" network. The decrease in capacity was around 10% (to 1.07 $mmol_{CO2}/g$ at 298 K and 1 bar) despite a significant increase both surface area and pore volume. Adsorption capacity calculated from the isotherms of dihydroxy modified MIL-53 demonstrated the opposite trend, a significant enhancement in both capacity and selectivity (CO_2/N_2) compared to the original at pressures above 0.2 bar and room temperature [62]. In this work it was also found that the presence of metal coordinated –OH groups could inhibit CO_2 adsorption near $–NH_2$ sites; both qualities evidencing the crucial role of polar groups in CO_2 capture and the particularly penalising impact of bulky, non-polar groups. The influence of polar –OH groups on the adsorption capacity has also been reported for organic salicylisimine cage compounds by Mastalerz et al. [138]. Hydroxyl group derivatives can also be beneficial for CO_2 adsorption; Zhao et al. investigated introducing extra framework cations such as K^+ with a view to promote CO_2 adsorption through electrostatic interactions with carbonaceous materials in the same way as for MOFs and zeolites [139]. The hydroxyl derivative, $-OK^+$ facilitated a capacity for the carbon of 1.62 $mmol_{CO2}/g$ at 0.1 bar and 25 °C; the highly ionic nature of the bond led to high polarization and charge transfer along the carbon surface. This phenomenon resulted in an adsorption energy of 36.04 kJ/mol, much higher than for that of pyridinic (19.03 kJ/mol) or amino groups (17.22 kJ/mol) substituted analogues. Hydrolysis into the hydroxyl group can also lower the adsorption energy (to 11.15 kJ/mol).

3.2. N-Heteroatom(s)

Theoretically, introducing nitrogen will improve the electron density of the carbon framework or in other words increase the basicity of the carbon framework which in turn will anchor the electron deficient carbon of the CO_2 to the carbon pore surface by Lewis acid-base (N atom) interactions [114]. Nitrogen containing SFGs are capable of providing a lone pair of electrons, which can act as an attractive site for the electron-deficient carbon atom of the CO_2 molecule due to the high electron-withdrawing properties of the oxygen atoms [8]. The basicity of the materials can also enhance the dipole-dipole interactions and hydrogen-bonding to the surface. This property should also increase the selectivity over non-polar gases such as CH_4 [139] and N_2 [140]. At the same time, polar nitrogen functionalities will generate an increase in the sorbent's hydrophilicity. It has been shown in myriad studies [141–143] that H_2O molecules are trapped inside the narrow micropore space of carbonaceous materials due to an enhancement in hydrogen bonding with H_2O. With this, the assumption can be made that functionalisation with these groups may be better suited to systems with a dry flue gas. Reports of a massive drop in competitive adsorption on N-doped carbons are widely known; the molecular simulations in the work of Psarras et al. elucidated to this. Under a humidity of 10% the CO_2 loading was at the very least compromised by pyridonic and pyrrolic groups. However, regardless of the type of N-containing SFGs, it is commonplace to reveal enhancements in CO_2 binding energies [144] and heats of adsorption [140,145] although not necessarily in adsorption capacity [146] in the context of carbonaceous materials.

3.2.1. Amine

Amine groups do not necessarily simply polarise the CO_2 molecules; rather they strongly and selectively bind it *via* chemisorptive interactions. Conventionally, a CO_2 molecule combines with amine groups to form a carbamate [106,108,131,147,148]; there are debates on the specific mechanism of that reaction but the general belief is in the intermediate formation of a zwitterion [149] followed by deprotonation by a Brønsted base [150] *i.e.* an amine. The prevalence of chemisorption can be discovered through considering the heats of adsorption, amine-functionalised materials tend to possess higher values than that of the non-functionalised analogues. There are also reports of a combination of mechanisms underpinning the adsorption: *e.g.* the material adsorbs CO_2 *via* formation of not only ammonium carbamates but also carbamic acid pairs [151]; this fact however is often dismissed as a result of the instability of carbamic acid. In some cases, amine moieties can play an indirect role in the capture of CO_2. Stavitski et al. [133] reported that the shifting of the electric potential of the adsorbent may create more attractive alternative sites for the CO_2 molecule, suggesting that the dominant force for adsorption is the van der Waals force inherent to the adsorbent. In this case, the absence of any chemisorption mechanism would lead to reduced regeneration cost and hence, better potential for applications in pressure-swing adsorption (PSA) systems. Saha and Kienbaum [110] however, postulated that hydrogen-bonding appears to be the key element in CO_2 adsorption. Generally, amine-functionalised materials will promote high CO_2 selectivity and enhanced performance under moist conditions but they often exhibit slow adsorption kinetics and require relatively high temperatures to regenerate [151]. It is important to remember that excessive amine loading has potential to cause agglomeration on the support's surface resulting in the blockage of pores. This blockage effect will lower the CO_2 molecule's accessibility to the active sites [70] and cause a diminution of micropore volume, further reducing the materials capacity. These assumptions have been confirmed by Plaza et al. [152] and Heidari et al. [146]. Cases that describe reductions in surface area and/or pore volume post amine-modification can be found throughout the literature [40,104,106,134,153–155]; this effect though, is not limited to amine modifications. The reduction in these two properties normally arises from pore blockage or the collapse of pore walls, examples can be found for oxides (mainly carboxyls, hydroxyls and carbonyls) [109], fluorines [156], carboxyls [40] and glycidyl methacrylate (which includes hydroxyl, ester and alkane groups) [131] and polycarbosilane [157]; these examples however, are by no means exhaustive.

The term amines described a number of groups that can be classified based on the number of substitutes there are connected to the nitrogen atom of the group. If there exists a single substitution the group belongs to primary amines; in the case of two substitutions then the classification is secondary amines; three substitutions belongs to tertiary amines; and four for quaternary amines, this class can also be referred to as graphitic although this is not always an accurate description. With respect to their application in post-combustion carbon capture (PCC), secondary amines are reported to have more favourable adsorption characteristics [149,158]. This is a result of the electron donating effect of the R substitutes that exhibit higher reactivity and stronger basicity than their primary relatives [131]. The addition of tertiary amines can increase the reactivity of the composite acting simultaneously to improve the adsorbents' stability [108]. The quaternary group of nitrogen atoms have been identified as irrelevant for CO_2 capture in carbon fibres [159]; attributed to the involvement of the 2 S^2 electrons in a dative covalent bond with the neighbouring carbon atoms [160] thereby curtailing its potential as a Lewis base. Quaternary-N often acts to suppress the efficiency of other basic nitrogen groups [161].

The amine group, $–NH_2$ is considered to be a great substitute for ligand modification of MOFs for CO_2 adsorption [116], however, this does not always yield better sorption characteristics. Abid et al. [134] demonstrated that despite normally increasing the adsorption capacity of amino-functionalised zeolites at moderate temperatures [148] the

adsorption on NH_2-MIL-53 (Al) decreased at 1 bar and 273 K from 2.856 $mmol_{CO2}/g$ to 2.143 $mmol_{CO2}/g$ for the unmodified and amino-functionalised MOF, respectively. A decline in the heat of adsorption was also observed for the materials from 39 kJ/mol to 28 kJ/mol, respectively. At lower pressures in the range of 0–0.5 bar, simulations by Torrisi et al. [62] concluded that both binding energies and enthalpies as well as CO_2 uptake were higher for an NH_2-MIL-53 sorbent than that of the unmodified parent material. The work of Cmarik et al. [129] corroborates this conclusion, the uptake of the developed UiO-66-NH_2 at 298 K and 1 bar was 2.973 $mmol_{CO2}/g$, the greatest value for all evaluated modifications (-NO_2, -$(OMe)_2$ and -Naphtyl). The selectivity (CO_2/N_2) was also demonstrated to be highest with the –NH_2 modification. These improvements are not limited just to MOFs, Liu et al. [162] demonstrated that a 5 A zeolite-based mesoporous silica hybrid adsorbent could adsorb 5.05 $mmol_{CO2}/g$ at 298 K. The sorbent was impregnated with 30 wt% polyethylenimine (PEI) and captured the CO_2 from a moist, simulated flue gas and performed significantly better than the pristine zeolite (0.73 $mmol_{CO2}/g$) and zeolite/silica hybrid (0.82 $mmol_{CO2}/g$).

3.2.2. Nitro

The nitro group, when present during the adsorption of CO_2 tends the CO_2 to be positioned adjacently thus allowing an electrostatic interaction between the two oxygens of the SFG and the electron deficient carbon atom of the CO_2 [116]. In this work, Torrisi et al. identified that the binding energy of the modified sorbent was lower than the parent; consistent with the electron withdrawal properties of the nitro group. He et al. [41] compared a nitro-substituted and formyl-substituted triptycene-based polymer, at 298 K and 1 bar, the nitro-sorbent demonstrated a capacity of 1.8 $mmol_{CO2}/g$ vs 1.1 $mmol_{CO2}/g$ for the formyl-sorbent. This result despite the lower BET surface area: 140 m^2/g vs 525 m^2/g for the nitro- and formyl-substituted polymers, respectively; opposite to the trend where a higher surface area leads to a greater capacity. This observation, however, can be ascribed to the fact that –NO_2 groups possess a higher polarity than the –HC═O (keto/aldehyde/-formyl/carbonyl) group. Considering polarity, both –NH_2 and –SO_3H groups have higher polarity (in that order) than the nitro group and it has been shown that at pressures up to 1 bar, a Zr-based MOF exhibits the same trend [163]. In this case however, the trend is not noticeable only in the uptake but also with adsorption energy and working capacity. Zhang et al. were able to demonstrate the same with a UiO-66 MOF modified with -Br, –NO_2 and –NH_2, again in ascending polarity [164]. The UiO-66 sorbent produced by Cmarik et al. [129] was able to capture 1.786 $mmol_{CO2}/g$ while the nitro-functionalised derivative far exceeded this at 2.573 $mmol_{CO2}/g$ at ambient temperature and pressure. The selectivity (CO_2/N_2) was also shown to improve. Generally, the functionalisation of materials with –NO_2 is not considered as effective in the context of CO_2 capture than modification with the amino group. This can be attributed the reduced polarity and acidic nature of the nitro group as well as the larger size of the nitro group which may lead to a greater possibility of pore blockage [165].

3.2.3. Amide

The basicity of amides tends to be much smaller than alkylamines, pyridines and ammonia. This a result of the delocalisation of the lone pair of electrons in the nitrogen atom through resonance with the carbonyl oxygen. Interestingly though, this group may have potential for PCC applications due to the presence of two different adsorption sites: the –C═O and -NH_x. The former can act as an electron donor (Lewis base) and the latter as an acceptor (Lewis acid) for the CO_2 molecule [166]. Ratvijitvech et al. [105] modified MOPs in which an amine functionalised CMP was modified to produce amide functionalised networks. The resulting material demonstrated a reduced surface area and pore volume when compared to the parent amine network. When increasing the alkyl chain length of the amide from 1 to 5 (not counting the carbon with the double bond to oxygen and the σ bond to the amino group), both parameters decreased from 316 m^2/g to 37 m^2/g and 0.21 m^2/g to 0.04 m^2/g, respectively as a result of pore filling. Decreases in capacity and isosteric heat of adsorption was also observed when going from amine to amide group functionalisation and when increasing the alkyl chain length. At 1 bar and 273 K the amine group CMP exhibited a capacity of 1.65 $mmol_{CO2}/g$ vs 1.51 $mmol_{CO2}/g$, 1.46 $mmol_{CO2}/g$ and 0.87 $mmol_{CO2}/g$ for the acetamide, propenamide and decanoic acid amide functionalised relatives, respectively. Similar observations were made at 298 K but for all cases, the selectivity (CO_2/N_2) was between 8.5 and 12, less than the 14.6 exhibited by the parent –NH_2 network. Safarifard et al. [166] investigated the applications of either the amide or imine groups in MOFs. They were able to demonstrate that the incorporation of the amide group rather than the imine does not necessarily improve the adsorbents performance. The CO_2 capacity, selectivity (CO_2/N_2) and the heat of adsorption were shown to increase in a fashion depending on the position and orientation of the functional group; the –NH moieties established hydrogen bonds and NH···π interactions with the surrounding network. It was concluded that the accessibility of the functional group is crucial to the enhancement of CO_2 adsorption, especially when introduced in interpenetrated networks.

3.2.4. Imine

Imine nitrogen is in the sp^2 hybridisation state, which makes it comparable to the nitrogen of pyridine since the lone pair there does not contribute to the aromatic ring but instead occupies a hybrid orbital. The assumption can be made then, that the basicity of this atom be close to that of a pyridinic-N. The double bond between the carbon atom and the nitrogen should strongly attract the CO_2 molecule *via* Lewis interactions. The work of Zeng et al. on COFs [128] investigated the impact of imine-based COFs in comparison to triazine-based and boron-based analogues. Their findings suggest such materials are promising candidates for CO_2 capture as they have moderate heats of adsorption, high selectivity over N_2 and a large capacity for CO_2. For instance, the adsorption isotherms of one sample termed TRITER-1 were studied at 273 K and 298 K at 5 bar, under these conditions the capacity demonstrated was 13.38 $mmol_{CO2}/g$ and 3.11 $mmol_{CO2}/g$, respectively. This performance postulated to be a result of high surface area, super-microporosity and the presence of nitrogen-rich basic 1,3, 5-triazine ring and imine functionalities [128]. Mastalerz et al. [138] demonstrated that when reducing imine bonds to amine, the thermal stability of a porous organic cage compound was compromised. Moreover, Gajula et al. [167] were able to achieve lower capacities in a covalent organic cage after a similar transformation of the imine group to an amine group, attributed to the greater surface area of the imine-functionalised sorbent (12.8 m^2/g) than the amine alternative (5.7 m^2/g).

3.2.5. Nitrile

In the nitrile group (-C≡N), the nitrogen atom is in a sp hybridisation state which means that the lone pair electrons are position closely to the nucleus, thus the nitrile group is not significantly basic. The investigation of polymethylmethacrylate (PMMA) by Jo et al. [168] involved impregnating the support with amine functionalities. The primary amine was replaced by a secondary amine with acrylonitrile connected to the nitrogen atom. Such a modification should be better for the adsorption of CO_2 as detailed earlier. Conversely, it was realised that the modification leads to a decrease in capacity, pore volume and surface area in the modified PMMA (–NH–$(CH_2)_2$–C≡N) compared to the original –NH_2 SFG. The observation was the same when transforming the secondary amine to a tertiary with the same alkylnitrile end group. The reduction in surface area and pore volume can be attributed to the difference in size of the functional groups. Patel and Yavuz [169] were able to demonstrate this weaker interaction of the C≡N-containing materials than those containing amines and amidoximes. In their work a nitrile group was substituted with an amidoxime, which led to an increase in the CO_2 adsorption properties. These results suggest that the

cyano or nitrile functional groups is not the most sought after SFG for PCC. An amidoxime, (–(NH_2)C═N–OH) functionality is an interesting candidate for surface modification of an adsorbent as the molecule's terminal functional groups resemble those of monoethanolamine (MEA), the conventional benchmark for CO_2 absorption. Upon capture the CO_2 molecule can bind with both –NH_2 and –OH simultaneously [170], as a result this group is considered CO_2-philic. The results of this modification are reported to be an increase in capacity of up to 17% at ambient temperature and pressure for the amidoxime substituted polymer of intrinsic microporosity [169]. This was achieved despite a decrease in BET surface area from 771 m^2/g for the nitrile-containing parent to 531 m^2/g for the amidoxime substituted derivative. The explanation for this reduction concluded to be a result of the intermolecular interaction of neighbouring amidoximes forming hydrogen-bonding. With this, they also noted a clear dipole-quadrupole interaction between the adsorbent and CO_2. Mahurin et al. were able to successfully graft amidoxime onto the surface of a porous carbon [171] which facilitated a 65% improvement in CO_2/N_2 selectivity. Interestingly, the overall capacity decreased slightly from 4.97 $mmol_{CO2}/g$ to 4.24 $mmol_{CO2}/g$ at 273 K and 1 bar and from 2.87 $mmol_{CO2}/g$ to 2.49 $mmol_{CO2}/g$ at 298 K and 1 bar. This reduction being a result of the reduction in BET surface area from 1857 to 1288 m^2/g; the isosteric heats of adsorption however, were shown to increase from 23.3 kJ/mol to 24 kJ/mol indicating an enhanced interaction between CO_2 and the sorbent.

3.2.6. Pyrrole

Pyrrole is a weak basic N-containing functional group as the lone pair of electrons is used in sustaining the aromaticity of the molecule. CO_2 molecules interact with the hydrogen and the nitrogen atoms of the functional group therefore, two types of interaction take place: the Lewis acid/base; and the hydrogen-bonding [107]. The works of Lim et al. [144] however, suggest that the interaction mainly happens between the positive hydrogen atom of the HN-functionality and the oxygen of the CO_2. The authors describe a larger distance between the oxygen of CO_2 and the hydrogen of the pyrrole group (2.135 Å) in comparison to the pyridone group with a hydroxy-functionalisation (1.943 Å). This may indicate a stronger affinity towards CO_2 of the latter than is found with pyrrole. They were also able to identify that the difference between the adsorption energy of the unmodified and pyrrole-functionalised surfaces is negligible [144]. Nevertheless, there have been suggestions that the pyrrolic nitrogen serves as an attractive site for CO_2 capture, one example would be the work of Hao et al. [172]. In this work, porous carbons were activated at different temperatures resulting in various SFGs. It was realised by the authors that the pyrrole group (and/or amides) are prevalent in the samples pyrolysed at 400 °C–500 °C. A significant decrease was observed at temperatures of 700 °C and above where protonated quaternary-N and pyridine-N-oxides become more prevalent. The sample pyrolysed at 400 °C demonstrated a capacity of 1.87 $mmol_{CO2}/g$ whereas those produced at temperatures between 500 °C and 800 °C all demonstrated similar capacities around 3.13 $mmol_{CO2}/g$. The 400 °C sample possessed a negligible BET surface area (42 m^2/g) and micropore volume (0.032 cm^3/g); at 500 °C this increased to 467 m^2/g and 0.210 cm^3/g, respectively. The importance of the pyrrolic group then is quite significant; the 500 °C sample possessed roughly half the specific surface area and micropore volume of steam activated coconut carbon yet, a capacity 20% higher.

3.2.7. Pyridine

Pyridine is one of the most basic SFGs used for the surface modification of adsorbents for use within post-combustion carbon capture [144]. During the process of adsorption, the CO_2 molecule locates closely to the nitrogen atom of the pyridine group for two reasons. The first being a Lewis acid-base interaction by charge transfer where the lone pair electron of the nitrogen atom donates the charge to the electron-deficient carbon atom of CO_2 resulting in a decrease in bond angle [110]. The second being steric hindrance of the interaction between the functional group and CO_2 [144] which results in oxidation of the nitrogen atoms and in the release of some of them as N_2 [173]. It is believed that pyridine and pyridone functionalities have the strongest influence on carbon dioxide adsorption [110] and despite the lack of the hydroxyl group, this functionality is considered by some [144] to be a more suitable surface modification in the context of carbon dioxide adsorption. Bae et al. [174] modified the MOF, Ni-DOBDC with pyridine molecules in an attempt to make the normally hydrophilic internal surface more hydrophobic. The success of this modification was estimated to be around 33%, i.e. 33 % of the open metal sites were coordinated by pyridine. It was realised that the introduction of pyridine could reduce H_2O adsorption while retaining considerable CO_2 capacity at typical flue gas conditions. The selectivity (H_2O/CO_2) was demonstrated to be 1844 for the Ni-DOBDC but a remarkable 308 for the pyridine modified MOF. The benefit of pyridine presence was also identified by Zhang et al. [175]. The coexistence of adjacent pyridinic-N and –OH/-NH_2 species was proposed to make an important contribution to high CO_2 adsorption performance, especially CO_2/N_2 selectivity. The porous activated carbon (PAC) demonstrated a capacity up to 5.96 $mmol_{CO2}/g$ at 25 °C and 1 bar, a result of the pyridinic-N and adjacent –OH or –NH_2 possessing the lowest hydrogen bonding energies for CO_2 thereby playing an anchoring role in adsorbing CO_2 molecules.

3.2.8. Pyridone

As previously mentioned, pyridone exists in two tautomers with the carbonyl form as the most abundant, hence the chemical environment of the nitrogen atom in pyridone is similar to pyrrolic-N [123]. So, for pyridone as for pyrrolic-N, the nitrogen atom contributes two *p*-electrons to the π-system, and a hydrogen atom is bound in the plane of the ring. It is important to remember that within the accuracy of XPS measurements pyridone-N cannot be distinguished between pyrrolic-N [123] and so is often grouped together in adsorbent characterisation. Lim et al. have reported exceptional hydrogen bonding between this functional group and the CO_2 molecule with an adsorption energy of −0.224 eV (21.58 kJ/mol) compared to the −0.218 eV for the pyridine SFG and −0.098 eV for the unmodified material [144]. During adsorption, CO_2 locates closely to the hydroxyl group of pyridone due to hydrogen bonding. The implication being that this type of interaction may contribute more than just the Lewis interaction in the case of the pyridine SFG. Their results suggest that both the pyridine and pyridone groups are suitable for the selective adsorption of CO_2 with the latter having a slightly higher binding energy. In the work of Sevilla et al. [176], porous carbons from polypyrrole were activated using potassium hydroxide (KOH) at different temperatures ranging from 600 °C to 850 °C. The authors noted that with the increase in activation temperature and the amount of oxidising agent the nitrogen content decreased dramatically from nearly 10 wt% of nitrogen species for the mildest conditions to less than 1% for the harshest. The dominating nitrogen SFG was pyridone with a small proportion of pyridinic-N groups. The sample with the highest content of such functionalities was reported to have a CO_2 uptake of 6.2 $mmol_{CO2}/g$ at 1 atm and 0 °C, whereas the least N-containing adsorbent adsorbed 4.3 $mmol_{CO2}/g$. These figures were attributed by the authors to two factors: 1) narrower micropore sizes; and 2) larger amounts of pyridone SFGs in the AC with better CO_2 sorption characteristics.

3.2.9. Additional N-containing SFGs

Aside from the conventional and well discussed nitrogen containing SFGs, there exists additional groups such as quaternary amines, pyridine-N-oxides and cyanides. These groups tend not to show a big influence in the adsorption of CO_2 when compared to the non-functionalised surfaces [144]. Therefore, they are not immensely interesting in the context of this review paper. An example of this would be amidine (R–C(=NH)–NH_2) which has been introduced within a mesoporous silica sorbent by Zhao et al. The adsorbent demonstrated a

low CO_2 uptake and thereby declared less useful for the separation of CO_2 from flue gases, especially when compared to amine-functionalised materials [177].

3.3. S-Heteroatom(s)

Sulphones, sulphoxides and sulphonic acids have been found to attract CO_2 *via* polar interactions and hydrogen bonding [173]. Given the size of the sulphur atom compared to carbon, its presence tends to protrude out and induce strain and defects, this arrangement in carbons helps to localise charge and generate favourable CO_2 adsorption [178]. The large and polarisable d-orbitals and the sole pair of electrons of S atoms can easily interact with the oxygen in CO_2 [179,180]. They have also indicated a very high degree of pore utilisation for CO_2. It is believed that sulphur in thiophenic configurations transfers electrons to the carbon dioxide molecule which can result in oxidation of the surface group and in the release of some SO gas.

Sulphonic groups (SO_3H) are another interesting candidate for surface functionalisation. A feature of this group is its flexibility, both in terms of the rotation about the C–S bond and in the directionality of the –OH bond, allowing it to orient itself to maximise the strength of intermolecular interactions [116]. Although, lone pair donation is at play here, the main interaction in this case is hydrogen-bonding between the acidic proton of the functional group and the oxygen in carbon dioxide [114] (the distances confirm this assumption [163]). These two simultaneous interactions lead to strong binding of the molecules. The sulphonate group is considered to be a great substitute for ligand modification for CO_2 adsorption in a MOF [116]. For instance, Biswas et al. [115] have added this functionality to UiO-66 and demonstrated that the uptake of both the functionalised and the non-functionalised MOF at 25 bar and 33 °C was 5.6 $mmol_{CO2}/g$. Interestingly, the sulphonate containing adsorbents' uptake was less than that of the pristine MOF at lower pressures. A thioether (organic sulphide) modified MOF has also been investigated in the work of Kronast et al. [130]. The UiO-66-ethylsulfide had a surface area of 52 m^2/g and adsorbed 2.4 $mmol_{CO2}/g$ CO_2 at 1 bar and a temperature of 308 K, the highest uptake out of the SFGs evaluated at pressures below 5 bar.

3.4. Halogens

Halogens are strong electronegative atoms from the 7th group of the Mendeleev's periodic table that have significant electron withdrawing properties. A study by Torrisi et al. [181] depicted the influences of substituting various halogen atoms onto the benzene ligands of a MOF. Their findings suggest that adding such an atom(s) is unlikely to result in a substantial increase in CO_2 adsorption, as Fluorine, Chlorine, Bromine and *etc.* destabilize the π-quadrupole interaction by withdrawing the charge of the π-aromatic system. Destabilization increases with the number of halogen groups. However, this action leads to increasing acidity of the aromatic hydrogens, which can form weak hydrogen bonds with the oxygens of CO_2 molecules. The work of Biswas et al. on Iodine-modified UiO-66 [115] indicated an uptake of 5.1 $mmol_{CO2}/g$ (at 25 bar and 33 °C). A decrease of 10% compared to the unmodified framework and a dibromide-modified adsorbent [130] which had an uptake of 3.93 $mmol_{CO2}/g$ (at 20 bar and 35 °C). Cho et al. [44] claimed enhanced CO_2 adsorption from 1.61 $mmol_{CO2}/g$ to 2.07 $mmol_{CO2}/g$ at 298 K in oxy-fluorinated carbon molecular sieves. Postulated to be a result of the high electronegativity of the halogen leading to a halogen/hydrogen bond-like interaction of the functional group with the adsorbate. Most of the increase in this characteristic can, however, be attributed to the presence of oxygen containing SFGs although they did acknowledge that CO_2 interacts weakly with fluorine. It has also been reported by Shahtalebi et al. [156] that with a rise in fluorination levels, a reduction in surface area and pore volume is realised as well as a minor decrease in both the activation energy and isosteric heat of adsorption coupled with a slower CO_2 uptake.

3.5. Hydrocarbon surface functional groups

3.5.1. Alkyl

In the same study by Torrisi et al. [181] methyl substitution was shown to increase the sorbent's affinity towards CO_2 through the electron donation action of the group and a positive inductive effect (methyl being the smallest alkyl group). This substitution injects electronic charge into the aromatic system of the MOF's benzene ligand thereby improving the π-quadrupole interaction. There is also an additional stabilising, weak hydrogen bond between the oxygen of the CO_2 and the hydrogen of the CH_3. In this work, tetramethyl substitution represented the upper limit for that particular ligand. In 2010, Torrisi et al. [62] reported a drop in CO_2 capacity with the addition of two methyl groups to the ligands of a MIL-53 sorbent, accompanied by a rise in the enthalpy of adsorption. A similar dimethyl functionalisation of a CMP led to a reduction in capacity, 0.94$mmol_{CO2}/g$ at 298 K and 1 bar vs 1.18 $mmol_{CO2}/g$ for the unmodified material at the same conditions [40]. Another noteworthy aspect of surface modification with this group has been proposed by Zelenak et al. [149]. By adding a methyl radical onto 3-aminopropyl-modified mesoporous silica SBA-12 (SBA-12/AP) they anticipated an increase in CO_2 sorption capacities of the adsorbent, since 3-(methylamino)propyl is a stronger base compared to the former. Contrary to this prediction, they found a decrease in the capacity from 1.04 $mmol_{CO2}/g$ for the primary amine-modified SBA-12/AP sample to 0.98 $mmol_{CO2}/g$ for the SBA-12 with a 3-(methylamino)propyl functionality. This effect can most likely be attributed to the steric hindrance and the low accessibility of the lone electron pair of the latter. In the work of He et al. [41] alkyl-substituted amino groups were successfully incorporated into triptycene-based polymers. The resultant microporous network presented an excellent capacity, 4.17 $mmol_{CO2}/g$ at 273 K and 1 bar as well as CO_2/N_2 selectivity, 43.6 under the same conditions.

3.5.2. Alkene

Alkene groups are in a sp^2 hybrid state, which means that they are considered to be more basic than alkyl groups. Aside from this, the double bond present in such substances allows for the chemical adsorption of CO_2 through π-π interactions since the π-electron system is polarisable in the alkene group [131]. An allyl-modified UiO-66 was investigated by Kronast et al. [130] along with other various SFGs. Out of the groups analysed this group was present in the parent material and showed the worst sorption characteristics with a capacity of 13 wt% at 35 °C and 20 bar. At 1 bar the uptake was deduced to be approximately 0.4 $mmol_{CO2}/g$.

3.5.3. Arene

A naphthyl functionalised material has been shown by Cmarik et al. [129] to exhibit lower capacity than the original at around 1 bar and 298 K, a value of 1.537 $mmol_{CO2}/g$ for the modified and 1.786 $mmol_{CO2}/g$ for the parent. This fact was attributed to the bulkiness of the functionality leading to a smaller pore volume and surface area, as well as a lack of active binding sites since naphthyl is non-polar. On the other hand, a slight improvement in CO_2/N_2 selectivity was realised by the authors.

4. Experimental methods employed in the introduction of surface functional groups

Given the myriad SFGs that can be introduced onto solid sorbents in the interest of improving their performance in PCC, it is a logical assumption that the routes in which to achieve this are just as multifaceted and diverse. When considering the ideal modification for an adsorbent, it is imperative to its success that the technique is suitable for both the moieties to be introduced and the adsorbent. Before any modification then, especially with those adsorbents that are associated with a level of scarcity and consequently cost, a comprehensive understanding of their chemical properties and structure is fundamental. This

will inform not only the methods that can be used, but also what limitations exist. Throughout the literature, there is clear evidence that there exists an optimum set of conditions to achieve the most efficient and impactful modification which, in itself is highly specific and often needs tailoring to suit the needs of the adsorbent, adsorbate and the moiety to be introduced. This section will endeavour to inform those wishing to improve the CO_2 capture performance of their selected adsorbent. Before this however, it is worth highlighting that in the context of post-synthesis treatments, activation is considered to be the optimisation of sorption capacity *via* increasing specific surface area, whereas modification is the introduction of non-carbon moieties to the surface of carbonaceous materials to improve their sorption capacity for specific sorbates [182]. Although specific to carbons, this definition stands for the majority of alternative sorbents.

4.1. Physical modification

Physical activation is the partial gasification of a precursor or intermediate material to increase its porosity. In the context of carbonaceous materials, some authors distinguish two stages to physical activation [182]: the first being the oxidation of amorphous carbon-like tar opening the clogged pores; the second being the partial oxidation of carbon crystallites. The first stage primarily increases the specific surface area whilst the second both increases the specific surface area by creating new (micro) pore space or creating new interconnections between pores but also by changing the surface chemistry [182,183].

4.1.1. Pyrolysis

A chemically and physically irreversible process which involves the thermal degradation of the precursor in an inert environment at elevated temperatures under the limited or complete absence of oxygen [184]. Pyrolysis is at the core of the overall process for the conversion of biomass into value-added products such as porous carbons. The by-product (biochar) of organic wastes such as biomass waste, sludge and polymer waste can be utilised for the development of CO_2 adsorbents such as porous carbon, zeolites and mesoporous materials [185]. Table 1 details the effect of the pyrolysis conditions on the products yielded [182,184,186]; a detailed description of advanced thermal treatments can be found in the work of Spokas et al. [187]. Slow pyrolysis is considered the conventional process as it tends to produce less volatiles and a larger proportion of solid char.

4.1.2. Gaseous activation

Gaseous activation involves exposing the material to a volume of either steam, carbon dioxide or air at temperatures above 700 °C [121]. These oxidising agents penetrate into the internal structure and gasify the carbon atoms resulting in an opening and widening of inaccessible pores [191]. Materials activated this way will see an improvement in internal surface area and a larger presence of oxygen containing functional groups including phenolic, ketonic and carboxylic groups. The porosity of the activated sorbent depends on a number of factors including temperature, process duration and oxidant choice [182]. Oxidation with CO_2 tends to result in the opening of new pores, whilst steam often widens existing microporosity [121]. In addition to steam, CO_2 and oxygen, chlorine, ammonia, sulphur and sulphur dioxide can be used as agents for physical activation although the use of ammonia or sulphur dioxide can also be considered a modification. Steam and CO_2 are the most commonly used [121]. It has been demonstrated that oxidation of AC in the gas phase increases mainly the concentration of hydroxyl and carbonyl surface groups, while oxidation in liquid phase can incorporate a higher amount of oxygen in the form of carboxylic and phenolic hydroxyl groups onto the carbon surface at much lower temperatures compared to the gas phase oxidation [192,193].

Table 1
Pyrolytic conditions and corresponding product yield [184].

Pyrolysis Type	Temperature (°C)	Heating Rate (°C/min)	Residence Time	Yield (%) Bio-oil/Biochar/Syngas
Slow [91,188]	350–700	<10	min-days	35/30/35
Intermediate [189]	400–600	>10	<30s	50/25/25
Fast/Flash [190]	<650	~100 °C	<30s	75/12/13
Gasification [187]	>800	variable	Sec-min	5/10/85

The effect of activation temperature on the characteristics and adsorption properties of porous carbons prepared from polyvinylidene fluoride was investigated by Hong et al. [194]. The samples were heated to a temperature between 700 °C and 950 °C (3 °C/min) under 200 ml/min CO_2 flow. With an increase in temperature, BET surface area increased from 1023 m^2/g to 2750 m^2/g as did micropore volume. Above 800 °C the sorbents demonstrated a decrease in narrow micropores and instead developed new micro/mesoporous structures with larger (0.82 nm–1.21 nm) micropores. It was believed that the rate of pore enlargement is faster than rate of generation resulting in the formation of new micro and mesopores rather than narrow micropores [195]. At 25 °C and 1 bar, the 800 °C activated sample demonstrated a capacity of 3.84 $mmol_{CO2}/g$ a result of the dominance of narrow micropores (0.53 nm–0.70 nm). A comparison between the physical and chemical activation of vine shoot-derived biochar for PCC has been made by Manyà et al. [196]. The physically activated sample was heated to 800 °C (10 °C/min) under 100 ml/min CO_2 flow for either 1 or 3 h. The 3 h sample was shown to adsorb 1.58 $mmol_{CO2}/g$ at 25 °C and 1.013 bar after 1 min, 69% of the total CO_2 adsorbed after 10 min. The selectivity (CO_2/N_2) of the adsorbent was a strong 68.5, less than the sample activated for 1 h (115).

4.1.2.1. Air activation. The mechanism for air activation with carbonised charcoal can be described by the following reactions [197,198] where the *f* subscript denotes a free active carbon site and the parenthesis designate a surface complex:

$$2C_f + O_2(g) \rightarrow 2C(O) \text{ Oxygen chemisorption } \Delta H = -395 \text{ kJmol}^{-1} \quad (1)$$

$$C_f + O_2(g) \rightarrow CO_2 \text{ Carbon gasification } \Delta H = -395 \text{ kJmol}^{-1} \quad (2)$$

$$C(O) + O_2(g) \rightarrow CO(g) + CO_2 \text{ Oxide gasification } \Delta H = -111 \text{ kJmol}^{-1} \quad (3)$$

Applying air as a gasifying agent is an economically attractive approach for physical activation. It starts with the chemisorption of oxygen onto the carbon to form surface oxides in Eq. (1); the reaction is exothermic and so occurs rapidly even at low temperatures [121]. This is followed by the desorption of CO_2 and CO in Eq. (2) and Eq. (3), respectively.

The effect of activation conditions in the single-step oxidation of biochars has been investigated by Plaza et al. [198]. Air was used in a range of temperatures between 400 °C and 500 °C, higher temperatures were also investigated (500 °C–650 °C) with a reduced oxygen concentration (3%–5%). At low O_2 concentrations and 650 °C sorbents with high micropore volume in the narrow micropore domain (0.3 nm–0.5 nm) were obtained; capacities up to 2.11 $mmol_{CO2}/g$ were achieved at 25 °C and 1.01 bar. Nitrogen-enriched porous carbon fibres have been synthesised by Xiong et al. *via* air activation [199]. The air activation of oxidised polyacrylonitrile (PAN) fibres was carried out at between 400 °C and 500 °C at a rate of 10 °C/min for 30 min. When the heat treatment temperature is increased from 400 °C to 500 °C, BET surface area, pore volume and micropore volume all increase; at 400 °C around 57% of the pores were within the narrow micropore region (≤0.8 nm) which is the size limit established in the volume-filling mechanism for CO_2 adsorption [14,15]. Fig. 1 exhibits the surface of the porous carbon fibres (PCFs) activated under different conditions.

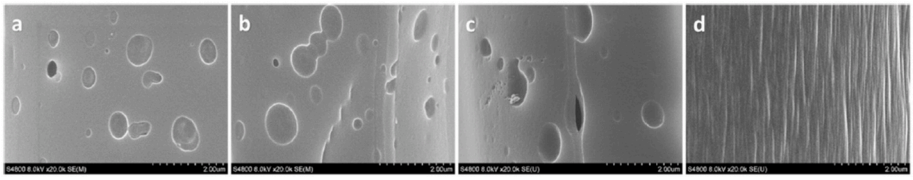

Fig. 1. Scanning electron microscope (SEM) images of (a) 400 °C air activation; (b) 450 °C air activation; (c) 500 °C air activation; and (d) nitrogen activation [199].

At 400 °C pores can be seen with various sizes with some interconnected channels, when increasing activation temperature to 450 °C these pores become larger and more prevalent. Fig. 1(c) illustrates further smaller pores alongside deep channels produced inside the carbon. Fig. 1(d) exhibits the PCF produced in the presence of nitrogen and shows grooves inherited from wet-spun polyacrylonitrile fibre that remains intact [199]. The nitrogen content of the sorbents decreased from 23.68% at 400 °C to 20.86% at 500 °C in the form of pyridinic, pyrrolic/pyridonic and pyridine-N-oxides; interestingly, pyridinic-N-oxides were not found in the sample activated under nitrogen. Therefore, air activation can not only produce higher amounts of narrow micropores but also forms of more nitrogen species favourable for CO_2 capture. The 500 °C sample demonstrated a capacity of 2.25 $mmol_{CO2}/g$ at 25 °C and 1 bar as a result of the high volume of total pores, micropores, pores below 0.8 nm and excellent contents of pyrrolic/pyridonic-N and oxygen species facilitating a selectivity (CO_2/N_2) of 183. Various activating agents were employed in a recent study by Guo et al. [200], among them were air, CO_2, phosphoric acid (H_3PO_4) and sodium hydroxide (NaOH). The air activation of waste sugarcane bagasse was carried out at 850 °C for 120 min after pyrolysis at 750 °C. The air activated sample demonstrated the lowest BET surface area (99 m^2/g) as well as the presence of pyridinic, pyrrolic/pyridonic, quaternary and pyridine-N-oxide groups as well as ketone, carbonyl and/or lactone groups, ether and/or alcohol and carboxyl groups. The capacity of the air activated sample was shown to be the lowest at 1.61 $mmol_{CO2}/g$ at 25 °C and 1 bar.

4.1.2.2. CO_2 activation. The mechanism of activation with CO_2 involves the Boudouard reaction [121,182]:

$$C_f + CO_2 \rightarrow C(O) + CO \text{ Dissociative chemisorption} \quad (4)$$

$$C(O) \rightarrow CO \text{ Desorption of surface oxide} \quad (5)$$

In this process, CO_2 undergoes dissociative chemisorption on the carbon surface to form a surface oxide and carbon monoxide as shown in Eq. (4). The surface oxide is subsequently desorbed from the surface, further developing the pore structure shown in Eq. (5) [121]. The overall reaction is shown in Eq. (6) [201,202].

$$C_{(s)} \rightarrow CO_{2(g)} \rightarrow 2CO_{(g)} \ \Delta H = +159 kJmol^{-1} \quad (6)$$

Zhang et al. evaluated the effect of different modification routes for biochar [203], one of which was to pass CO_2 through a vertical tube furnace that contained the biochar (2 g) at various pre-set temperatures (500 °C–900 °C at 10 °C/min) for 30 min. The same was conducted with pure ammonia gas and a mixture of ammonia and CO_2 *i.e.* CO_2 activation, ammonification and a combination of activation and ammonification, respectively. CO_2 activation increased the micropore surface area from 224 m^2/g to a maximum of 610 m^2/g at an activation temperature of 800 °C; this temperature also developed the largest micropore volume of 0.24 cm^3/g. At higher temperatures however, activation leads to a greater loss of nitrogen content: 0.54 wt% vs 1.09 wt% with the unmodified biochar. Interestingly, an activation temperature of 500 °C led to an increase in nitrogen content to 1.28 wt%. FTIR spectra showed the presence of phenol O–H, C–H and C–O as well as a weak presence of N–COO. The activation temperature of 800 °C facilitated a maximum CO_2 capacity at 20 °C of 2.26 $mmol_{CO2}/g$. Similarly, Zabiegaj et al. activated carbonised coconut shell particles with CO_2 [204] at a temperature of 950 °C for 6 h (at 10 °C/min) after an initial treatment at 800 °C for 1 h (at 1 °C/min) without CO_2. The capacity was found to be 4.8 $mmol_{CO2}/g$ at 0 °C with a BET surface area of 900 m^2/g and narrow micropore and micropore volumes of 0.35 cm^3/g and 0.39 cm^3/g. Mesfer et al. [205] also employed CO_2 as the activating agent to synthesise AC from walnut shells. The authors carbonised walnut shell kept at 500 °C for 4 h under CO_2 flow at 200 ml/min.

4.2. Steam activation

The smaller size of water molecule compared to CO_2 facilitates the activation by using steam. The reaction is endothermic thus, making it easier to control and therefore, better suited for gasifying carbons with high surface activity [121]. Commonly used to introduce porosity and oxygen-containing functional groups such as carboxylic, carbonyl, ether and phenolic hydroxyl groups onto carbon surfaces. The process usually takes place for between 30 min and 3 h using superheated steam (800 °C–900 °C) [206] with flow rates of between 120 ml/min [207] and 300 ml/min [208] or flow rates of water between 2.2 ml/min to 5 ml/min carried in nitrogen (300 ml/min) [209]. The reactions between carbon and steam are described in Eq. (7) - Eq. (14) [121,210].

$$C_f + H_2O \rightarrow C(O) + H_2 \text{ Chemisorption} \quad (7)$$

$$C(O) \rightarrow CO + C_f \text{ Scavenging of surface oxide} \quad (8)$$

$$CO(g) + C(O) \rightarrow CO_2(g) + C_f \text{ Carbon gasification} \quad (9)$$

$$CO + H_2O \rightarrow CO_2 + H_2 \text{ Water} - \text{gas shift reaction} \quad (10)$$

$$C_f + 2H_2O \rightarrow CO_2 + 2H_2 \text{ Carbon gasification by steam} \quad (11)$$

$$C_f + CO_2 \rightarrow 2CO \text{ Carbon gasification by carbon dioxide} \quad (12)$$

$$C_f + 2H_2 \rightarrow CH_4 \text{ Carbon gasification by hydrogen} \quad (13)$$

$$CH_4 + H_2O \rightarrow CO + 3H_2 \text{ Carbon gasification by hydrogen} \quad (14)$$

The process starts with the exchange of oxygen from the water molecule to the carbon surface creating a surface oxide in Eq. (7) which may be devolved as carbon monoxide in Eq. (8). Carbon monoxide may increase the rate of gasification by scavenging the surface oxide to produce CO_2 in Eq. (9). The process is followed by a water-gas shift reaction in which water vapour is broken down to CO_2 and hydrogen gas in Eq. (10) which may activate the surface by Eq. (12) or Eq. (13) [121]. The overall reaction can be seen in Eq. (15) [201,202].

$$C_{(s)} \rightarrow H_2O_{(g)} \rightarrow CO_{(g)} + H_{2(g)} \ \Delta H = +117 kJmol^{-1} \quad (15)$$

The procedure of pore formation is closely related to water-gas shift reactions and the depletion of carbon. Steam activation improves the porous structure by removing trapped products [206] contained within the material and develops both micropores and mesopores to produce a wider range of pore size distribution [191,211,212]. In general, the volume/radius of the pores and surface area increase with the steam temperature and treatment time due to an increase in the removal of carbon atoms from the carbon surface [121]. At low temperatures *i.e.* around 300 °C, the consumption of aliphatic hydrogen atoms occurs, whereas at higher temperatures aromatic hydrogens react to form

oxygen-containing groups [213]. Steam treatment below 300 °C isn't thought to be a good pre-treatment as it is unable to remove the strongly bonded hydroxyl groups [209]. Oxygen-containing groups that decompose between 300 °C and 600 °C give rise to the formation of new bonds and when the temperature rises above 600 °C, typical reactions such as cyclisation and condensation of carbon rings occur [213,214]. The steam activation of waste cork powder [208] using nitrogen (300 ml/min) as a carrier gas was carried out by Mestre et al. In this study, the steam was generated from the water vapour pressure at ambient temperature. The activation conditions were 750 °C for 1 h with a heating rate of 20 °C/min; the sample was shown to have present a number of oxygen functional groups such as R–OH and R = O. Steam has also been used in combinations with other reagents which includes potassium carbonate (K_2CO_3) and H_3PO_4 [207,208] among others.

4.2.1. Thermal treatment

Thermal treatments of adsorbents can describe any form of modification that involves the use of elevated temperatures but, for the purpose of this review the term will be used to describe treatments that explicitly use temperature as the method of modification. Thermal treatment in the presence of an inert atmosphere can be used to remove surface acidic functionalities from the surface of carbonaceous materials especially at elevated temperatures over 700 °C [215]. Surface acidity is often related to the presence of oxygen containing SFGs [216–218] the majority of which can be removed at temperatures between 800 °C and 1000 °C [192]. The removal of these groups will act to increase the basicity of the surface [216] as a result of strongly acidic SFGs such as carboxylic, anhydrides and lactones decomposing at lower temperatures, while weakly acidic SFGs such as carbonyl, phenol and quinone decompose at higher temperatures [215,219,220].

Thermal activation of binderless, hierarchically porous zeolite 13× monoliths has been carried out by Akhtar and Bergström [221]. The materials were heated to a temperature between 750 °C and 900 °C at 5 °C/min and held for up to 2 h. The narrow temperature range where mechanically stable monoliths could be produced without loss of surface area was identified at 750 °C–800 °C although at a holding time above 0 min at 800 °C the majority of the microporosity was lost. The 13× crystal structure collapsing to an amorphous phase at 30 min. Thermally treated graphene nanosheets (GPN) produced by Chowdhury et al. [222] were able to capture 2.89 $mmol_{CO2}/g$ at 273 K and 1 bar, significantly more than the 0.81 $mmol_{CO2}/g$ captured by the unmodified graphene. The treated sorbent displayed rapid kinetics with ultra-high selectivity (CO_2/N_2) as well as stability and readily reversible adsorption/desorption. The GPN was treated at four temperatures between 200 °C and 800 °C under N_2 flow (500 ml/min) at a rate of 5 °C/min with a holding time of 2 h. The stoichiometry of the sorbents was evaluated and included carbon sp^2, hydroxyl/carbonyl groups and carboxyl/carboxylate groups. The 800 °C sample was virtually free of all oxygen SFGs attributed to the near complete degeneration of carbonyl moieties to CO at 700 °C–770 °C [223]. The heat-treated samples exhibited a highly wrinkled external morphology due to the decomposition of the oxygen SFGs. The 800 °C temperature in an inert atmosphere for 2 h was identified as the most effective for developing highly ordered graphene sheets with high surface area and hierarchical interconnected nanoporous structure facilitating a capacity of 2.19 $mmol_{CO2}/g$ at 298 K and 1 bar in less than 3 min whilst retaining 95% of its' capacity after five cycles. Thermal treatments have also been employed by Fan et al. [224] with a view to produce annealed ZIF-8/Chitosan spheres with improved mechanical stability. A temperature of 500 °C was employed for 4 h which maintained the honeycomb structure and improved its' capacity to 0.99 $mmol_{CO2}/g$.

4.3. Chemical modification

Chemical activation can also be used to improve adsorbent performance. The process typically involves the mixing of the feedstock material with concentrated aqueous solutions of an activation agent; the vigorous mixing initiates the degradation of the feedstock. The resulting solution then requires subsequent treatment *i.e.* thermal activation or pyrolysis. The intensive mixing causes the original structure of the feedstock to degrade. In plant biomass for example, bonds between cellulose molecules loosen and ions of the activation agent occupy the resulting voids and thus, define the microporosity that is created during activation and becomes available after washing thus, avoiding the formation of tar and the blocking of pores [182]. Usually employed in place of physical activation often due to the fact that it can be used as a single step process reducing total energy requirements at the cost of extensive washing to remove any residual traces of the reagent. This washing can also lead to significant secondary pollution issues if toxic reagents are employed. The temperatures for pyrolysis can be lower than for physical activation, for zinc chloride temperatures between 600 °C–700 °C can be used but for potassium hydroxide temperatures in excess of 850 °C are still needed [182]. Feedstock to agent ratios are typically in the range of 1:0.5 to 5:1 [225]. The level of activation is dependent on the dosage used but also on the chemical itself, the intensity of mixing, and both the temperature and duration of subsequent activation. At high chemical concentration or excess reaction time, pore volume decreases due to the physical collapse of carbonaceous structures [226]. Although the mechanisms of activation vary between each agent, they possess common principles.

4.3.1. Impregnation

One of the most common forms of chemical activation involves the impregnation of raw precursors with a dehydrating agent prior to the carbonisation/activation [225]. The reagents used usually include acidic, alkaline and salt mediums. Impregnation is also often the employed method when chemically modifying the physicochemical properties of adsorbents. Although not used explicitly for the introduction of amines into the porous structure of adsorbents; a significant body of literature exists where this is method is employed [155,227–232]. The method typically involves dissolving amine species in a polar solvent (methanol or ethanol) and subsequent mixing with the porous support [233]. Parameters to consider to enhance the process include the mixing regime, temperature, reaction/contact time and any post-thermal treatments. Amine groups are typically fixed to the porous support through physical adsorption *via* dipole-dipole interaction, van der Waals force, hydrogen bonding, acid-base titration, or ion-exchange mechanisms [234]. The lack of any significant chemical bonding is considered the major drawback with this method and can lead to the loss of these groups during cyclic operation [42]. Considering that the mechanisms by which these groups are fixed within the support are the same that underpin CO_2 adsorption, there is an obvious trade-off between equilibrium capacity and functional group loading due to pore blockage. This blockage reduces internal surface area or micropore volume limiting CO_2 transport to the active sites [42], especially at lower temperatures. The impregnation method has been demonstrated to incorporate surface functionalities aside from amines [235] and is often the method by which chemical reagents are dispersed within sorbents for subsequent treatments.

A comparison between the impregnation and grafting of two amines (PEI and 3-aminopropyltriethoxysilane (APTES), respectively) onto the mesoporous silica MCM-41 has been carried out by Rao et al. [236]. The impregnation involved dissolved PEI in anhydrous ethanol (20 ml) followed by the addition of MCM-41 (1 g); the slurry was then stirred for 8 h at room temperature. The loading efficiency of impregnation far exceeded the grafting, 89.1% for 50 wt% PEI-MCM-41 and 23.18% for 50 wt% APTES-MCM-41. The impregnated sample demonstrated a 47% increase in capacity, the maximum being 3.53 $mmol_{CO2}/g$ at 25 °C and 1 atm at a rate of 0.1141 $mmol_{CO2}/s$. Diethylenetriamine (DETA) impregnation of a low-cost sepiolite adsorbent in the work of Liu et al. [237] resulted in a capacity of 1.65 $mmol_{CO2}/g$ at 35 °C and 1 atm, the working capacity being 95.2% of that after 4 cycles. The DETA was

dissolved in 20 g methanol and saw the addition of 4 g purified/acid-modified sepiolite and 1 h of stirring.

4.3.2. Grafting

Given the disadvantages associated with the impregnation method; grafting amine groups *via* covalently bonding these sorbents to the groups has been explored [42]. Dindi et al. [229] employed the method of grafting and impregnation when functionalising fly-ash derived cancrinite zeolites. The impregnation of the sorbents with MEA and DEA and grafting of APTES were compared using their CO_2 capture performance. The impregnated sorbents were prepared by mechanically mixing the zeolites with a 60 wt% amine solution in a ratio of 1.21 g:1 g (solvent:zeolite) and subsequent drying. The grafting involved dissolving the APTES in water and then mechanically mixing the zeolite with the solution in the same ratio, this was then aged for 48 h (room temp) and then 12 h at 40 °C and subsequently dried. N_2 adsorption isotherms of the pristine cancrinite and functionalised derivatives showed a decrease in pore size and surface area after modification [19]. A comparison between the effect of impregnation and grafting on the textural properties is hard to make since APTES was grafted and MEA and DEA were impregnated. The profiles produced from differential thermogravimetry (DTG) and thermogravimetric analysis (TGA) confirmed that the APTES was not just impregnated but successfully grafted; the largest peak was shown at 500 °C and not at the boiling point of APTES (217 °C) which would be where the physically adsorbed or impregnated APTES would be lost [229]. Although the capacity of the grafted sorbent was less than the two impregnated samples due to the fact that APTES is only tethered to the Si–O–Si groups through a silanization process on the pore walls and impregnated groups are packed within the support; the thermal stability of the grafted sorbent when carrying out cyclic adsorption/desorption studies makes it an appealing method for the functionalisation of porous supports. Hiyoshi et al. grafted aminosilanes onto SBA-15 [238] under three conditions: 1) calcined SBA-15 was refluxed in toluene solution of aminosilane (1.7 vol%) under Ar flow; 2) the same as in 1) but with 10 times the concentration of aminosilane solutions (17 vol%); and 3) boiling SBA-15 and then modifying with the 17 vol% solutions. The boiled support was seen to have a higher density of anchored aminosilanes suggesting that not only the isolated hydroxyl groups but also the hydrogen bonded hydroxyl groups are suitable sites for anchoring aminosilanes. This was demonstrated by the surface coverage being between 25%–38% for 1) and 57%–80% and 79%–118% for 2) and 3), respectively.

4.3.3. Solid-solid mixing

In solid-solid mixing method, both raw precursor and activator are mixed in solid state. Then the mixture is converted using a heat treatment process during which both processes (carbonisation and activation) take place simultaneously [19]. Solid-solid mixing has been revealed to formulate AC with lower surface area and pore volume [225]. This poor development of porosity can be caused by the difficulties associated with the activator penetrating into the sorbent structure [239] although this is heavily dependent on the chemical used as demonstrated by Ros et al. [240]. The size of the molecule of the modifying agent is key when implementing a solid mixing regime.

4.3.4. Ligand functionalisation

The capacity for functionalisation of organic ligands is one of the most important features of MOFs [131]. The modification of MOFs after their synthesis is a versatile method that facilitates the control of the number and variety of functional groups introduced into the MOFs *via* a variety of organic transformations [130,241]. Two UiO-67 analogues, $[Zr_6O_4(OH)_4(FDCA)_6]$ and $[Zr_6O_4(OH)_4(DTDAO)_6]$ termed BUT-10 and BUT-11 with functionalised pore surface and high stability were synthesised from two functional ligands 9-fluorenone-2,7-dicarboxylic acid (H_2FDCA) and dibenzo[b,d]thiophene-3,7-dicarboxylic acid 5,5-dioxide (H_2DTDAO), respectively, by Wang et al. [242]. The method for BUT-10 involves heating a solution of H_2FDCA (80 mg, 0.3 mmol), $ZrCl_4$ (71 mg, 0.3 mmol) and 3 ml of acetic acid in 17 ml of dimethylformamide (DMF) to 120 °C for 10 h. BUT-11 is synthesised similarly: a solution of H_2DTDAO (61 mg, 0.2 mmol), $ZrCl_4$ (47 mg, 0.2 mmol) and 1.7 ml of trifluoroacetic acid in 18 ml of DMF was heated to 120 °C for 48 h. Importantly, when synthesising zirconium-based MOFs, a modular acid is crucial, particularly for obtaining a single-crystal sample [242]. The introduction of functional groups in the ligands was demonstrated to decrease both the pore sizes and surface areas of the resulting MOFs. Interestingly, the CO_2 uptake of both BUT-10 and BUT-11 was shown to be more than double compared to the parent MOF (UiO-67) attributed to the stronger interactions between the carbonyl and sulfone groups in the two MOFs and CO_2 molecules. Grand Canonical Monte Carlo (GCMC) simulation confirmed that CO_2 molecules do in fact locate around sulfone groups. The influence of amide groups on the CO_2 capture performance on three novel functionalised MOFs was evaluated by Safarifard et al. [166]. In this investigation, a mixture of $Zn(NO_3)_2.6H_2O$ (0.297 g, 1 mmol), H_2oba (0.258 g, 1 mmol), and the corresponding amide ligand (0.5 mmol) and DMF (50 mL) was divided into seven glass vials followed by subsequent heating at 120 °C for 3 days and then cooling to room temperature. Colourless (TMU-22) and red-brown (TMU-23 and TMU-24) crystals were obtained as pure phases [166]. The activation of these crystals began with a solvent-exchange step where they were immersed in acetonitrile and dichloromethane for 3 days (solvent changed daily). Amino-functionalised UiO-66 (NH_2-UiO-66 (Zr)) was chosen as the parent MOF in a post synthesis modification campaign using glycidyl methacrylate (GMA) in the work of Molavi et al. [131]. GMA was chosen since it contains a number of functional groups including hydroxyl, ester and alkenes; the postulation being that a combination of amine and hydroxyl groups can increase the CO_2 capacity more so than if the groups were used exclusively. The amine functionalised MOF (NH_2-UiO-66) was produced by dissolving 2.27 mmol (0.53 g) of zirconium (IV) chloride ($ZrCl_4$) and 2.27 mmol (0.41 g) of 2-aminoterephthalic acid in 30 ml DMF at room temperature for an hour. The mixture is then heated to 120 °C for 24 h after which it was separated and washed with DMF and chloroform under sonication. The GMA modified MOF (GMA-UiO-66) was produced by suspending the NH_2-UiO-66 nanoparticles (60 mg) in tetrahydrofuran (THF, 5 ml) through sonication for 20 min after which 1.6 mmol GMA was added and then heated to 55 °C for 36 h. With the amine functionalised sample, the FTIR spectra showed the presence of carboxyl groups and amine groups. With the post-modified sample, the amine groups are removed and replaced by hydroxyl groups while the carboxyl groups are retained; there was also a strong peak characteristic of ester carbonyl stretching indicating successful GMA attachment. NMR was able to confirm the presence of the 2-aminoterephthalate ligand as well as a successful conversion of primary amine groups in NH_2-UiO-66 to secondary amines in GMA-UiO-66 (60%). The modification with GMA was able to enhance the chemisorption of CO_2 and hinder the physisorption of N_2, simultaneously improving the CO_2 capacity and CO_2 selectivity vs the unmodified MOF. This promotion of adsorption capacity (CO_2) is postulated to be a result of: 1) quadrupole-dipole interactions between CO_2 molecules and polar amine, hydroxyl and ester groups; and 2) π-π interaction through alkene groups. The adsorption capacities achieved were 3.15 $mmol_{CO2}/g$ and 4.28 $mmol_{CO2}/g$ for NH_2-UiO-66 and GMA-UiO-66 respectively. This improvement being the result of a successful grafting of NH_2-UiO-66 by GMA through a ring opening reaction between amino groups on the surface and the epoxy group in GMA molecules.

4.3.5. Amination

Most nitrogen-containing complexes provide basic sites with sufficient binding energies for the attachment of weak acidic species such as CO_2. The high electron-withdrawing property of the oxygen atoms present in CO_2 makes the carbon centre electron-deficient (electrophilic); hence, it binds to the electron-rich amine nitrogen [8]. Amination is an alternative term used to describe the process by which an

adsorbent is treated using ammonia gases. A form of thermal treatment, the adsorbents are heated to elevated temperatures (200 °C–1000 °C) in the presence of NH_3 prior to cooling under an inert flow. Plaza et al. studied the effect of temperature on ammonia treatment and identified that a maximum CO_2 capacity and nitrogen incorporation was reached at 800 °C without any prior oxidative treatments [243]. When treated with ammonia at high temperature the gas decomposes to free radicals such as NH_2, NH, and atomic N and H. These free radicals may attack the carbon surface to form surface nitrogen functionalities (SNFs) [8,215]. Apart from the incorporation of basic nitrogen functionalities the removal of oxygen containing functionalities can significantly improve the basicity of the treated materials [215]. The presence of any oxygen containing SFGs prior to modification can also enhance the efficacy of ammonia treatments; these groups will decompose thereby increasing the activity of the free radicals further promoting the development of surface nitrogen functionalities such as amides and pyridines.

4.3.6. Ammoxidation

Another route to enriching the nitrogen content of adsorbent is *via* ammoxidation, developed on the basis of using an ammonia-air gas mixture in contrast to the use of a pure ammonia atmosphere during amination [8]. Ammoxidation describes the simultaneous oxidation and nitrogenation of the precursor and is considered to be one of the most effective methods of nitrogen-enrichment to carbon materials [244]. The ammoxidation process typically uses air and ammonia mixtures at a ratio of around 1:10 at 100 ml/min, 350 °C and a heating rate of 5 °C/min for 5 h [245,246]. It is commonly used alongside treatment to enhance the textural properties such as pre-oxidation with hydrogen peroxide [246] or subsequent KOH activation [245,247]. Nitrogen contents upwards of 14 wt% can be realised; the predominant species being amine, amide and nitrile [248] although at higher temperatures these may transform or decompose to more stable species such as pyrrolic, pyridinic or quaternary nitrogen [246,249]. Capacities of above 4 $mmol_{CO2}/g$ have been attained at 25 °C with these treatments although this is a result of both nitrogen content and porous structure [250].

4.3.7. Hydrothermal

Hydrothermal treatments involve thermo-chemically converting the precursor in the presence of water, low amounts of oxygen, high-pressure (14 MPa–22 MPa) and temperature (120 °C–300 °C) for 1 to several hours [251]. The low energy due to mild conditions facilitates a controllable valorisation of watery wastes [18,91,252]. The hydrothermal treatment of D-glucose in the work of Yue et al. [253] involved mixing 15 g of D-glucose with 150 ml of water and subsequent heating at 180 °C for 12 h. Carboxyl-rich porous carbons (CPCs) derived from glucose were prepared by a hydrothermal method in the presence of acrylic acid and non-ionic surfactant Brij72 as structure directing agents [254]. Here glucose and acrylic acid were dissolved in deionised water and heated at 423 K overnight meanwhile Brij 72 was dissolved in hydrochloric acid (HCl) at 323 K. The two solutions were then mixed at 323 K and heated at 453 K for 16 h. The products were then solvent extracted in ethanol at 353 K for 12 h, filtered, washed and dried. Hydrothermal treatments of carbonaceous materials leads to products similar to that of pyrolysis without the need for extreme temperatures; the products tend to possess high carbon contents, numerous oxygen containing SFGs, dissolved minerals and well developed porosity [18,255–257].

4.3.8. Hydrothermal fusion

Hydrothermal fusion is often employed to synthesise zeolites from various precursors such as fly ash (FA) [258]. The methods to synthesise various types of zeolites can be found in the literature [259–262]. Cancrinite-type zeolites were synthesised by Dindi et al. [229] *via* hydrothermal fusion. In this study, raw FA was fused with NaOH at a temperature of 500 °C in a ratio of 1:1.2 for 1 h. The product was then mixed with water at a liquid/solid ratio of 3 mL/g and hydrothermally treated at 140 °C for at least 5 h and was then filtered, washed (to neutralise pH) and dried. The transformation of mullite and quartz that were the predominant phases in the FA was confirmed by x-ray diffraction (XRD) spectra which showed primarily hydroxycancrinite ($Na_g[Al_6Si_6O_{24}]OH_2{\cdot}3H_2O$) and small amounts of hydroxysodalite. Depending on the Si/Al ratio, NaOH concentration and hydrothermal temperature and time, different zeolites can be formed [229]; here the 140 °C hydrothermal temperature and relatively high NaOH concentration (~4 M) led to the formation of cancrinite. Temperatures for the fusion step can be between 550 °C [49,263] and 750 °C [50] with subsequent hydrothermal treatments in the range of 40 °C–140 °C [49,258]. A 2018 review paper has been published by Claudio Belviso that discusses in detail the various methods for zeolite synthesis from ashes [264].

4.3.9. Combinations

It has been reported that combinations of chemical and physical activation techniques can accelerate the chemical changes in the material and also, may facilitate the removal of hydrogen and oxygen [207]. A number of combined techniques have been evaluated such as H_3PO_4, ammonification and KOH [246] or nitric acid and KOH [171]. The synergies between these combinations being far reaching; their employment being highly specific to the end use of the adsorbent. Zhang et al. employed a combination of CO_2 activation and ammonification with biochar in order to improve the adsorbents CO_2 capture performance; here a mixture of CO_2 (100 ml/min) and ammonia (80 ml/min) was passed through a vertical tubular furnace containing the biochar (2 g) at various temperatures (500 °C–900 °C) [265]. The combination of CO_2 and ammonia was able to achieve the highest content of nitrogen at 600 °C (3.98 wt%) when compared to the sample prepared with solely CO_2 or ammonia modification. The ammonia-modified biochar exhibited a number of peaks within the FTIR spectra, namely: O–H, C–O, C–H and N–COO functional groups but also C═N and C–N confirming that high temperature ammonia treatment had introduced nitrogen-containing functional groups. The combination of CO_2 and ammonia led to carbamate or carbamic acid (N–COO) skeletal vibration which increased with modification temperatures [265]. It was postulated to be a result of one or two mechanisms. Mechanism A [46,266]: C–OH and C–O–C could react with ammonia to generate primary and secondary amines which would then react with CO_2 to form N–COO. If the amine of N–COO was secondary, then mechanism B [92,254,267] could be prevalent which follows the dehydration reaction of the corresponding ammonium carbamate or carbamic acid leading to the formation of pyridine C═N and C═O (lactones and ketones) which would serve as more active sites for the introduction and conversion of nitrogen functional groups [265].

5. Reagents

5.1. Acidic

Acidic modification is carried out using various oxidants with a view to increase the acidic properties of the sorbents by removing mineral elements and improving the hydrophilic nature of the surface [268]. Nitric acid (HNO_3), sulphuric acid (H_2SO_4) and H_3PO_4 are widely used for this purpose. Acid type and activation time for common acids used in

Table 2
Effect of acid type on activation time (carbons), reproduced from the work of Kandah et al. [269].

Activation Time (min)	Type of Acid
180	Acetic acid
210	Phosphoric acid
40–60	Sulphuric acid
Instantaneously	Nitric acid

the modification of adsorbents is given in Table 2 [269]. During the modification, oxygen-enriched functionalities are generated on the carbon surface including carboxylic, lactone and phenolic hydroxyl groups [270]. Oxidation by gaseous oxidants such as CO_2, O_2 and steam can also be used producing higher proportions of hydroxyl and carbonyl groups when compared to liquid-phase oxidation that increases the proportion of carboxylic and phenolic hydroxyl groups. Liquid-phase oxidation is less energy intense and can introduce a higher oxygen content than the gas-phase route.

5.1.1. Phosphoric acid – H_3PO_4

Phosphoric acid is a common reagent used for the activation of various carbon precursors and can facilitate this formation of AC at lower temperatures due to the chemical changes that it incurs. Phosphoric acid has two important functions: the promotion of pyrolytic decomposition of the initial material and the formation of a cross-linked structure [207]. Yadavalli et al. [271] investigated ammonium sulphate surface modification of phosphoric acid activated Douglas fir sawdust pellets. The precursor was first impregnated with H_3PO_4 at an impregnation ratio of 1.5:1 or 3:1 for around 48 h. The biomass was then dried and carbonised using a microwave oven (700 W) where the temperature was maintained at 410 °C for 20 min. The greatest adsorption capacity was found with the biomass derived AC that had the highest impregnation ratio and ammonium sulphate content due to the more developed pore structure that arises from the chemical activation. Highlighting the importance of pre-treatment when modifying the surface of adsorbents. Budinova et al. [207] studied the effect of H_3PO_4 impregnation on biomass with post-thermal treatments that included heating to 600 °C at 3 °C/min for 1 h under N_2 flow; heating to 600 °C at 3 °C/min for 1 h under N_2 flow and then steam; and exclusively with steam at 700 °C for 2 h. It was found that in the chemically activated sample the presence of carboxylic groups was much higher. The samples that underwent thermal treatments in the presence of steam showed much lower contents of carboxylic and lactone groups but much higher contents of hydroxyl and carbonyl groups. The pH of the sample prepared with consecutive pyrolysis was found to have the highest pH (6.5) representing it contained the highest number of basic surface functional groups. The use of H_3PO_4 was also employed in similar fashion to Budinova et al. by Girgis et al. [17]. Both studies employed this reagent in order to enhance the properties of AC for the adsorption of *p*-nitrophenol (PNP) and methylene blue (MB). Its application was found to increase the porosity where subsequent thermal treatments were used to increase the content of oxygen containing functional groups on the surface of the adsorbents. These oxygen-containing functional groups, however, were found to decompose at temperature over 800 °C whereas the phosphate acidic-type compounds persisted. Heidari et al. used phosphoric acid to produce AC from eucalyptus wood [146] with an impregnation ratio of 2 (g/g) and carbonisation temperature of 450 °C. Due to the quantity of volatile matter within the precursor (cellulose and hemicellulose), the AC consisted of a significant amount of oxygen which has a great influence on the subsequent ammonia modification that was employed. This influence arises due to the decomposition of oxygen containing groups that are then replaced with nitrogen containing groups [146,246]. The FTIR spectra for the activated sampled showed the presence of phenol, alcohol and carboxylic acid as well as ketones and secondary cyclic alcohol. This was confirmed by XPS spectra that also showed the presence of graphite, carbonyls, quinones and carbonates. Titration of this sample demonstrated that the carbon had no basic groups on the surface and was entirely acidic: 5.3 meq/g. Activated carbon prepared from pine cone by H_3PO_4 activation in the work of Khalili et al. [272] employed the impregnation of H_3PO_4 and subsequent activation temperature of 500 °C at 5 °C/min for 170 min under 100 ml/min N_2 flow. Melamine-nitrogenated mesoporous AC has also been prepared *via* a single-step chemical activation with H_3PO_4 from a rice husk precursor [273]. Yaumi et al. impregnated alkali treated risk husk with 88 wt% H_3PO_4 at a fixed reaction of 1:2 wt% (Rice Husk:H_3PO_4). The sorbents were then impregnated with melamine in the presence of ethanol, stirred, dried and then heated to 500 °C for 1 h (5 °C/min).

Fig. 2 exhibits the surface morphology of the materials as they are prepared. RH is non-porous with blocked surface whereas RHP_{AC} and RHP-M1 exhibit highly developed porosity with both micro and mesopores. It was learned that the pore development results from the evaporation of volatiles and the reagent when heated to 500 °C leaving vacant space [274]. The phosphoric acid activated sample demonstrated a capacity of 3.42 $mmol_{CO2}/g$, less than the melamine modified (4.41 $mmol_{CO2}/g$) but still significant.

5.1.2. Hydrochloric acid – HCl

Hydrochloric acid has been used in the process of acid digestion to remove ash from samples and concentrate carbon [231] or to remove impurities when synthesising zeolites from FA [275]. Its most frequent use is in the neutralisation and removal of residual traces of reagents such as KOH used for activation/modification [226,276,277]. There are instances of HCl being used for the purpose of adsorbent modification, but these tend to focus on pore development rather than surface modification. Bada and Potgieter-Vermaak compared HCl-modified and heat-treated coal FA and found that the acid was able to produce larger specific surface areas in the sorbent (5.4116 m^2/g vs 2.9969 m^2/g). This was deemed a result of the acid corroding the outer layer of the FA allowing a disintegration of its stable glassy layer. Corroborated by the SEM images that showed development of cracks that exposed the inner constituents of the FA thus, increasing micropore volume [278]. In the work of Zhao et al. [139], a number of extra-framework cations were introduced into N-doped microporous carbons and assessed as CO_2 adsorbents. It was realised that K^+ ions play in key role in promoting CO_2 adsorption *via* electrostatic interactions; HCl molecules anchored in the carbon had a similar promoting effect, contradicting conventional wisdom that neutralisation of basic sites by acids diminishes CO_2 adsorption. In this work, HCl was used to wash the developed N-doped carbon prior to washing with distilled water. The nitrogen content of this sorbent was 12.9 wt%, with 3.3 wt% Cl and could capture 4.03 $mmol_{CO2}/g$ at 25 °C and 1 bar.

5.1.3. Hydrogen peroxide – H_2O_2

Hydrogen peroxide was employed by Guo et al. as a pre-oxidation reagent for coconut shell prior to ammoxidation and KOH activation [246]. It is believed that the surface oxygen groups that are formed in the process of ammoxidation act as intermediate anchoring sites to introduce nitrogen functionalities [279]. If the introduction of additional oxygen groups can be achieved with prior oxidation, more nitrogen could be introduced with the subsequent ammoxidation. The carbonised coconut shell was treated with 10% H_2O_2 (1 g carbon:10 ml solution) for 2 h at room temperature.

The morphology of the samples through the consecutive modifications can be observed in Fig. 3. Both C and HC (Fig. 3(a) and (b)) exhibit a smooth and bulky morphology. The nitrogen doping in the sample shown in Fig. 3(c) introduces wrinkles on the surface; Fig. 3(d) illustrates the effect of KOH activation. The sorbent possesses irregular and heterogeneous types of macropores on the surface [246]. The pre-oxidation treatment increased the oxygen content of the carbon from 17.07 wt% to 22.58 wt%; after ammoxidation the pre-oxidised sample exhibited a nitrogen content of 15.58 wt% vs 14.43 wt% without the pre-oxidation. The adsorbents also possessed a much narrower microporosity than those without the pre-treatment and was able to capture 4.47 $mmol_{CO2}/g$ at 25 °C and 1 bar. The observed high capacity was a result of nitrogen content and narrow microporosity.

5.1.4. Nitric acid – HNO_3

Nitric acid treatments can break down the pore walls and expand micropores into meso or macropores thus, facilitating a greater increase in acidic functional groups such as hydroxyl, carboxylic, ketonic and other oxygen containing moieties [280–282]. In the work of Shawabkeh

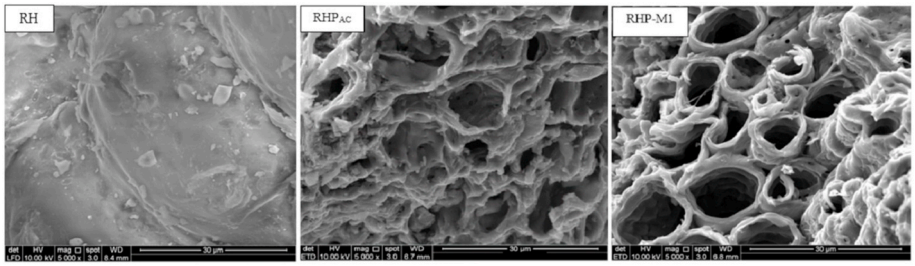

Fig. 2. SEM images of: Rice husk (RH); H3PO4 activated rice husk (RHPAC); and Melamine impregnated H3PO4 activated rice husk (RHP-M1) [273].

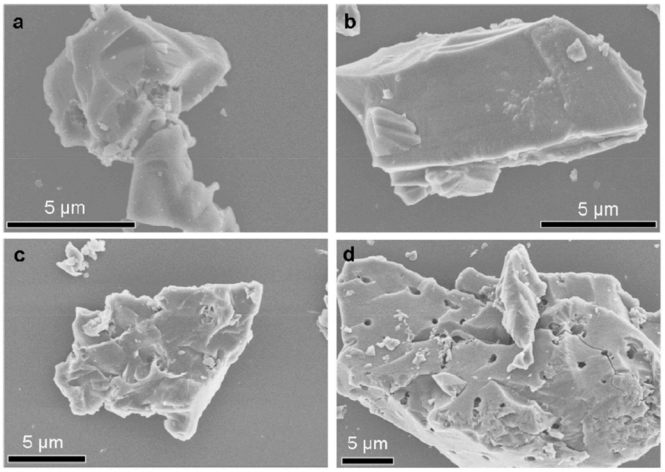

Fig. 3. SEM images of (a) Carbonised coconut shell (C); (b) H2O2 pre-treated C (HC); (c) Nitrogen-doped HC (NHC); and (d) KOH activated NHC at 650 °C (NHC-650-1) [246].

et al. [283] 100 g of oil FA was mixed with a mixture of 200 ml of concentrated sulphuric acid and nitric acid (volumetric ratios of nitric to sulphuric acid ranged from 5/95 to 20/80). The acid-ash mixture was then heated and stirred at 160 °C; further oxidation was achieved by passing a constant flow of air (5 ml/min). Heating was continued until the slurry became a black solid material. Demineralised water was added to further aid the ash activation. With the addition of sulphuric acid, no effect occurred however, when increasing the nitric acid content, a rapid increase in solution temperature was observed (up to 150 °C) thus, deeming the reaction exothermic. The treatment with acids results in several sulphonation and nitrification reactions at the surface of the ash samples [269]. When increasing the nitric acid content (0%–20%) in the acid mixture, an increase in Si content was observed, 0.99 wt% to 7 wt% as a result of the leaching of Mn, Ni and Zn from the ash. Interestingly sulphur content also increased from 71 wt% to 82 wt% with 10 wt% HNO_3, above this, the sulphur content decreased to 77 wt% due to the oxidation of organic sulphur to produce sulphur dioxide. FTIR spectra clearly elucidated that when using nitric acid, the development of oxygen containing functional groups such as carboxylic groups is enhanced. The maximum functionalisation with the carboxylic acid group was found with 15% HNO_3, above this, a decrease in the attachment was seen. Fuming nitric acid was employed by Shen and Wang [80] to functionalise tetraphenyladamantane-based microporous polyimide. Here polyimide networks (PI-ADNT) (8 g) was added to 8 ml of fuming nitric acid at −15 °C; then acetic acid (4 ml) and acetic anhydride (2.4 ml) were added into the solution followed by stirring for 3 h, 6 h or 12 h. The nitrated sorbents were termed PI-NO_2-1, PI-NO_2-2 and PI-NO_2-3, respectively. The acetic acid and acetic anhydride were added to the reaction instead of the conventional sulphuric acid to avoid the possibility of sulphonation reactions. The nitration success was confirmed by the presence of NO_2 groups within the FTIR spectra; solid-state C CP/MAS (cross-polarization with magic angle spinning) NMR spectra showed an enhanced peak characteristic of nitro-substituted carbons in phenyl or naphthalene groups. The degree of nitration increased with increased reaction time although the support was saturated as time exceeded 3 h [80]; 18.82 wt%, 20.04 wt% and 20.06 wt% for PI-NO_2-1 to 3, respectively. When increasing nitration time, a reduction in surface area and pore size is found as a result of nitro group occupation of the pores. In the samples nitrated for 6 h and 12 h, the porous channels were almost entirely blocked by these groups. The adsorption capacity of PI-NO_2-1 was shown to be the highest at 4.03 $mmol_{CO2}/g$ at 273 K and 1 bar (17.7 wt%) even with its lower surface area when compared to the unmodified sample. At 298 K the capacity was reduced to 2.02 $mmol_{CO2}/g$. The lower capacity seen in the samples with higher nitration is due to the lack of ultramicropores (pore size less than 7 Å) that are present. It was identified that the adsorption capacity relies heavily on surface area, affinity of CO_2 towards the polymer skeleton and microporous structure. The strong affinity of CO_2 may be due to the large dipole moment of C–NO_2 bonds that arises from the strong-electron-withdrawing effect of the nitro group [80]. The strength of this affinity can be seen when considering the selectivity of the sorbents. Those with higher nitrogen content demonstrated better selectivity for CO_2 when mixed with either N_2 or CH_4. Relative to meso or macroporous adsorbents, microporous materials would usually have a number of advantages for the selective adsorption of small gas molecules such as CO_2 (3.30 Å) when mixed with CH_4 (3.8 Å) and N_2 (3.64 Å) [80]. The mesoporous sorbents PI-NO_2-2 and PI-NO_2-3 showed better selectivity than the microporous PI-NO_2-1 which can only be attributed to the enhanced affinity of the nitrogen doped sorbents towards the polar CO_2 gas. Nanoporous organic frameworks (NPOF) have also been post-modified in the work of Islamoglu et al. [77] using either fuming nitric acid or sodium dithionite. The procedure for modification using fuming nitric acid follows charging a round-bottom flask with 10 ml of concentrated H_2SO_4 and cooling to 0 °C where NPOF (100 mg) was added followed by dropwise addition of 93 μL fuming HNO_3 and stirring for 90 min at the same temperature. The mixture was then poured into 75 ml of ice and stirred for 30 min at room temperature after which the powder was filtered and washed with water and ethanol to produce NPOF-1-NO_2 (108 mg). The key points of this method being the nitration of NPOF-1 at 0 °C in the presence of 2 equivalent of HNO_3 per phenyl rung for 90 min. A nitration of NPOF-1 was also performed with excess HNO_3 for 6 h at 0 °C and will be referred to as NPOF-1-NO_2(xs); interestingly this results in a much lower surface area (749 m^2/g) when compared to NPOF-1-NO_2 (1295 m^2/g). The success of the nitration was confirmed by the presence of asymmetrical and symmetrical stretching of NO_2 in the FTIR spectra. The excess nitration resulted in lower than expected levels of 1,4 substituted phenyl rings (~0.59 nitro/phenyl ring) while the controlled nitration yielded ~0.4 nitro per phenyl ring. The CO_2 capture capacity of the two nitro-functionalised NPOFs was demonstrated to be 2.00 $mmol_{CO2}/g$ and 2.52 $mmol_{CO2}/g$ (at 298 K and 1 bar) for NPOF-1-NO_2(xs) and NPOF-1-NO_2, respectively, lower than that for the amine derivatives. Sulphuric and nitric acid can also be used to incorporate amino/nitro groups on the surface of AC as demonstrated by Zhang et al. [284]. Here a two-step procedure is used, a nitration

followed by reduction as in the aforementioned study. The sulphuric/nitric acid mixture is used to tailor the surface of AC through the basic organic reaction introducing nitro groups after which these can be reduced to amino groups through reactions with acetic acid and iron powder. Sulphuric acid (60 ml, 98 wt%) and nitric acid (54 ml, 65 wt%) were mixed with deionised (DI) water (114 ml) producing 228 ml of solution; a concentrated solution was also prepared (228 ml H_2SO_4/HNO_3). The nitration was performed at 323 K with AC (2 g) suspended in 80 ml of the acid mixture and stirred for 90 min; the two prepared samples were termed AC-NO_2 and AC-NO_2(strong) corresponding to the acid strength used. The reduction in BET surface area and total pore volumes was strongest in the samples prepared with higher strength acids due to excessive oxidation and hence pore collapse [284,285]; those prepared with dilute acids only saw slight decreases. Interestingly, the average pore diameter increased suggesting that pore widening and not blockage occurred. The XPS spectra facilitated an evaluation of the atomic concentration of C, O and N; nitrated N content increased from 0 at% to 1.20 at% and O content increased from 5.85 at% to 16.11 at% indicative of the oxygen SFGs formed during nitration. Within the N content, deconvoluted peaks showed that pyrrolic and pyridonic-N were present as well as pyridine type N. The optimisation of nitric acid modification on mesoporous char derived from used cigarette filters has been demonstrated by Masoudi Soltani et al. [82]. The full factorial design of experiment sought to optimise the 2 factors: acid concentration and contact time. Nine experiments were conducted using concentrations of 2 mol/L, 5 mol/L and 8 mol/L and contact times of 2 h, 5 h and 8 h. It was realised that acid concentration had a more significant effect on BET surface area than contact time, the optimum conditions being a concentration of 5 mol/L and a contact time of 5 h facilitating a BET surface area of 439 m^2/g. The modification was seen to increase surface acidity by around 57.8% associated with the amount of carboxylic and phenolic surface groups; the oxygen content increased by a factor of around 2.5.

5.1.5. Sulphuric acid – H_2SO_4

The activation of bentonite was carried out by Wang et al. [286] using sulphuric acid where bentonite was added to different concentrations of H_2SO_4 (3, 6 and 9 M) at a fixed ratio of 10 ml to 1 g bentonite, heated to 95 °C and stirred at 600 rpm for 4 h in an oil bath. The intention was to develop a support that could be functionalised by immobilising an amine-functional polymer thus, producing a molecular basket sorbent or MBS. For all samples, an increase in pore volume and surface area along with a widening of pore size suggest that the acid treatment leads to the leaching of metal ions within the surface of smaller pores. Activation with 6 M acid was deemed optimum owing to the decrease in surface area and pore volume as a result of pore collapse and greater metal leaching at higher concentration [286]. The production of AC from molasses has been demonstrated by Legrouri et al. [287] in 2004. Molasses were treated with sulphuric acid (37 N) in a 1:1 (w/w) proportion and heated at 10 °C/min to either 120 °C under air flow (MS), 550 °C under N_2 flow (MS550 N) or 750 °C under steam flow (MS750V). The MS750S sorbent possessed a BET surface area of 1214 m^2/g while the other two were significantly lower at 343 m^2/g and 402 m^2/g for MS and MS550 N, respectively. Chen and Lu were able to improve the adsorption capacity of kaolinite through sulphuric acid treatment from 0 $mmol_{CO2}/g$ to 0.08 $mmol_{CO2}/g$ [288]. The kaolinite was added to an acid solution (either 0.5, 1, 2 or 3 M) at a ratio of 1 g–10 ml acid and were aged at 95 °C for between 3 h and 16 h. The 3 M solution was found to be the most suitable as it resulted in the highest BET surface area and pore volume to 42.4 m^2/g and 0.139 cm^3/g, respectively, after 3 h. This suggests the acid dissolves the metal ions present in the kaolinite and rearranges its crystal structure. The treatment introduced surface hydroxyl groups. Li et al. investigated the influence of nitrogen, sulphur and phosphorous doping on AC for CO_2 capture [289]. The sulphur doping was achieved by adding the carbon precursor (1.7 ml of 37 wt% formaldehyde) and template (1 g of hexagonally packed mesoporous silica) to a mixture of resorcinol (0.935 g), ethanol (21.25 ml) and various amounts of H_2SO_4 (98 wt%) followed by polymerisation and carbonisation. The SEM images of the carbons prepared with various acid catalysts are exhibited in Fig. 4; it was learned that the morphology was influenced by the type and quantity of acid. The HMS template possesses plate-like particles not seen in the derived carbon regardless of acid type [289]. The sponge-like network in the carbons may be a result of polymerisation of the outside HMS. With phosphoric acid the sorbents possess myriad interconnected particles of irregular shape forming macropores in the voids. For the sulphur doped counterparts, when increasing the amount of acid (S1 to S3) the spongy texture is lost and replaced by rod-like particles.

Sulphur doping was shown to be the most effective in improving CO_2 adsorption, the sample with the greatest sulphuric acid addition (1.128 g) reached a capacity of 3.6 $mmol_{CO2}/g$ at room temperature and 100 kPa. This postulated to be a result of the formation of strong pole-pole interactions due to the existence of sulphur SFGs with no dependence on BET surface area performing better than a commercial AC with BET surface area of 3180 m^2/g. The nitrogen and sulphur co-doping of microporous AC was achieved in the work of Sun et al. [290] by sulphonation reactions simultaneously acting as a cross-linking agent and sulphur source. The carbon was produced by sulphonated poly (styrene-vinylimidazole-divinylbenzene) macro-spheres followed by carbonisation and KOH activation. The sulphonation involved dwelling resin spheres (5 g) in 1,2-dichloroathan (10 ml) for 12 h and then treating with concentrated H_2SO_4 (10.87 ml) for 2 h at 180 °C. The treatment led to the grafting of sulphonic acid SFGs onto the benzene and imidazole rings which worked as cross-linking agents and sulphur sources during the subsequent carbonisation [291]. Of the KOH activated sample, the sulphur species were reduced, and mainly present as mono-oxidised sulphur and neutral sulphur. Without KOH activation, sulphur is present mainly as sulphonic acid and sulphoxides. Capacities upwards of 4.2 $mmol_{CO2}/g$ were achieved at 25 °C and 1 bar with the co-doped sorbents.

5.2. Basic

When the surface of a carbonaceous adsorbent contains a large number of oxygen-containing acidic groups, the contribution of resonating π-electrons to carbon basicity is overshadowed. Basic treatment induces a positive charge on the surface that enhances the adsorption of negatively-charged moieties [270]. Given the acidic role of CO_2 (weak Lewis acid); the introduction of Lewis bases onto the surface of adsorbents may favour CO_2 capture performance [7]. One way of increasing the basicity is to remove or neutralise the acidic functionalities or by replacing the acidic groups with proper basic groups (*e.g.* basic nitrogen functionalities) [215]. This can improve the interaction between the surface and acidic species *via* dipole-dipole interactions, hydrogen bonding and covalent bonding; treatment with hydrogen or ammonia at high temperatures (400 °C–900 °C) is seen most frequently [270]. When reacting with ammonia, nitrogen groups are formed on the surface. Nitrogen functionalities can also be introduced *via* reaction with nitrogen containing precursors such as ammonia, nitric acid and the multitude of amines; or chemical activation in a nitrogen enriched environment [215,271,292]. Possible forms of nitrogen that can exist include the groups: amide, imide, lactame, pyrrolic and pyridinic groups [270]. Basic treatments can also be used to produce synthetic zeolites; the main product formed during alkali activation of FA, for example, is an amorphous alumino-silicate gel or zeolite precursor [293]. The difference between zeolite synthesis or alkali modification lies with experimental conditions. For zeolite synthesis, high concentration of hydroxide ions is responsible for the decomposition of Si–O–Si and Al–O–Al bonds which then form Al–OH and Si–OH groups. These species are then condensed leading to the precipitation of zeolitic precursors. It is also well known that hydroxides open more micro and macropores in carbonaceous materials during chemical activation [294].

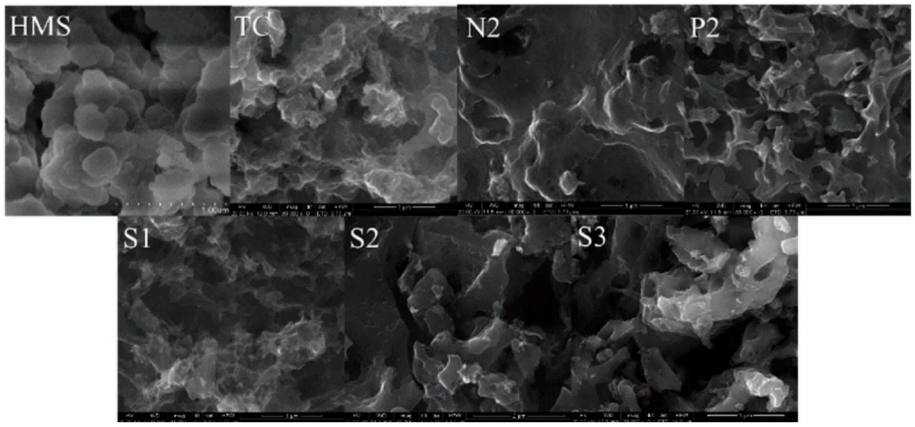

Fig. 4. SEM images of HMS and the prepared carbons with various amount of acid catalyst: (HMS) hexagonally packed mesoporous silica; (TC) pure templated carbon; (N2) N-doped; (P2) P-doped; (S1)-(S3) S-doped carbons prepared with various amounts of acid catalysts [289].

5.2.1. Potassium hydroxide – KOH

Potassium hydroxide (KOH), although basic in nature, is most often employed to generate porosity *via* either solid-solid reactions or solid-liquid reactions [7]. As a result, KOH is more suitably termed an *activation agent* rather than an agent used for surface modification; but the enhancements to pore structure and surface area [29] that can be realised, renders it an important tool in increasing the available sites for subsequent surface modification or doping [295]. Phenolic hydroxyl and carboxyl groups often become weaker after treatment with KOH and the alkaline solution may act to neutralise the acidic groups on the surface of the sorbent [296]. For activations below 700 °C, the main products are generally believed [297] to be H_2, H_2O, CO, CO_2, K_2O and K_2CO_3 as shown in the first 4 reactions (Eq. (16) - Eq. (19)). Potassium hydroxide dehydrates into K_2O at 400 °C, then carbon is consumed by the reaction of carbon and H_2O with the emission of H_2. Potassium carbonate is formed by the reaction of K_2O and CO_2 which is produced in the 3rd reaction (Eq. (18)) [298]. A number of studies indicate that K_2CO_3 forms at c.400 °C and at over 600 °C, KOH is completely consumed [299]. The as-formed K_2CO_3 in Eq. (19) and Eq. (21) decompose into CO_2 and K_2O at temperatures above 700 °C and completely disappear at c.800 °C [298]. The resulting CO_2 can be further reduced by carbon to form CO at high temperatures (Eq. (23)). The potassium compounds K_2O and K_2CO_3 can also be reduced by carbon to produce metallic K at temperatures over 700 °C (Eq. (24) and Eq. (25)).

$$2KOH \rightarrow K_2O + H_2O \text{ Dehydration} \quad (16)$$

$$C + H_2O \rightarrow H_2 + CO \text{ Water} - \text{gas reaction} \quad (17)$$

$$CO + H_2O \rightarrow CO_2 + H_2 \text{ Water} - \text{gas shift reaction} \quad (18)$$

$$K_2O + CO_2 \rightarrow K_2CO_3 \text{ Carbonate formation} \quad (19)$$

$$C + K_2O \rightarrow 2K + CO \text{ Reduction by carbon} \quad (20)$$

$$6KOH + 2C \rightarrow 2K + 3H_2 + 2K_2CO_3 \text{ Global reaction} \quad (21)$$

$$K_2CO_3 \rightarrow K_2O + CO_2 \quad (22)$$

$$CO_2 + C \rightarrow 2CO \quad (23)$$

$$K_2CO_3 + 2C \rightarrow 2K + 3CO \text{ Reduction by carbon} \quad (24)$$

$$K_2O + H_2 \rightarrow 2K + H_2O \text{ Reduction by hydrogen} \quad (25)$$

Based on these observations; three primary activation mechanisms occur within this treatment [297,298]:

1. Redox reactions between various potassium compounds and carbon etches the carbon framework generating a network of porosity.
2. The formation of H_2O and CO_2 acts to gasify the carbon further adding to the development of porosity.
3. The metallic K intercalates into the carbon matrix thereby expanding the lattice. Upon removal of this K and its compounds the expanded lattices are unable to return to their previous non-porous structure.

The process then, encompasses both chemical and physical activation along with lattice expansion. The mechanisms are highly dependent on the activation parameters (amount of KOH, temperature etc.) and the reactivity of the carbon source.

Serafin et al. [300] used potassium hydroxide to prepare ACs from a number of biomass sources in a single-step method using saturated KOH solutions for 3 h at a ratio of 1:1 (w/w) followed by carbonisation (700 °C) for 1 h (under N_2). The precursor was learned to be decisive in the textural properties of the resulting carbon. Determination of the effective pore ranges was achieved by evaluating CO_2 adsorption at various temperatures and pressures. At 273 K and 1 bar, micropores of between 0.3 nm and 0.86 nm were deemed the most effectual. At typical flue gas conditions (P_{CO2} = 0.15 bar) this range was 0.3 nm–0.57 nm facilitating a capacity of 1.25 $mmol_{CO2}/g$. The carbon precursor, although important, is not the only factor to consider when employing KOH as a reagent. Sudaryanto et al. [301] evaluated the effect of carbonisation duration (1 h–3 h), temperature (450 °C–750 °C) and impregnation ratio (1:2–5:2, w/w) when chemically activating cassava peel. With an impregnation ratio of 1:1, carbonisation temperature showed little effect on the porosity of the products; BET surface area and total pore volume were not significantly impacted although this was not evaluated at other impregnation ratios. The assumption that carbonisation temperature variation would influence pore development was demonstrated. Increasing the temperature from 450 °C to 750 °C increased the evolution of volatile matters adding to the development of porosity. It was confirmed that both micro and mesopores could be produced between 450 °C–650 °C; at 750 °C the developed pores were predominantly in the mesopore region. Increasing the impregnation ratio (at 750 °C for 1 h) led to a decrease in pore development due to the promotion of oxidation and thus, gasification of the carbon due to the elevated presence of KOH. At higher ratios the intercalation effects of metallic K are more significant thereby adding to the development of mesopores through the widening of existing micropore structure. Tseng et al. prepared high surface area AC from corncob *via* KOH etching and CO_2 gasification [302]; in a previous study [303], impregnation ratios were classified as two types (I and II). The reactions of type I include surface activation and micropore etching and type II describe solely micropore etching. The combined method employed wet impregnation

(KOH:precursor of 1:1 and 4:1 by mass) and subsequent carbonisation at 780 °C for 1 h under N_2 flow; after this the N_2 was switched to CO_2 for gasification. The CO_2 gasification post-treatment was found to be less significant for KOH ratio of 4. A ratio of precursor to KOH of 4 was also employed by Stavropoulos et al. [277]. The use of KOH often leads to the loss of nitrogen from carbon frameworks [245] and so, is often employed in combination with other reagents to increase the content of nitrogen such as urea [295,304–306]. Chen et al. [86] carbonised dried crab shells which were then impregnated with KOH solution at various ratios (KOH/C) for 2 days. The mixtures were then heated to 500 °C–700 °C for 90 min under N_2 flow and termed CS-X-Y. Increasing the ratio from 0.5 to 2 at 600 °C led to an increase and then decrease in CO_2 capacity, the optimum ratio at 0.15 bar (P_{CO2}) was identified at 1 but at 1 bar it increased to 1.5. Fixing the ratio at 1.5 and increasing temperature from 500 °C to 700 °C leads first to an increase and then a decrease in capacity; 650 °C was learned to be the optimum: 4.37 $mmol_{CO2}/g$ at 25 °C and 1 bar and 1.57 $mmol_{CO2}/g$ at 0.15 bar. Potassium hydroxide activated crab shell was transformed into a solid uniform carbon monolith. The nitrogen species on the ACs included pyridinic-N (25.6%–35.1%), pyrrolic-N (45.1%–47.3%), quaternary-N (11.7%–20.1%), and pyridinic-N-oxide (6.6%–11.3%). Although the micropore filling mechanism dominated CO_2 adsorption on the well-developed ACs, the effective N-containing groups such as pyrrolic-N on the adsorbent surface played an important role in the adsorption of CO_2 on the less-developed ACs [86]. ACFs derived from PAN saw a series of modifications either by KOH or tetraethylenepentamine (TEPA) by Chiang et al. [307] in an attempt to identify the relationship between CO_2 capture performance and the primary material parameters (porosity and nitrogen content). ACF was immersed in an aqueous KOH solution where KOH:ACF = 2:1 (w/w) and mixed in ultrasonic equipment for 10 min at room temperature, dried and then heated to 800 °C (10 °C/min) and held for 1 h under N_2 flow and termed aACF. The hydroxide treatment boosted the appearance of meso and micropores through aiding the development of porosity and forming a pore skeleton through the intercalation of K in the carbon lattice. Here, KOH was demonstrated to not only generate new micropores [308] but also widened existing pores such that all pore size ranges saw an increase in volume. The loss of a significant portion of N atoms that originated from the ACF precursor was also observed. The majority of the oxygen SFGs were of –OH and C═O groups, whereas 6 nitrogen SFGs were found, namely: pyrrolic/pyridonic-N > nitro > quaternary-N alongside aromatic-N-imines, pyridine-type N and pyridine-N-oxides. Due to the difficulties in differentiating between pyridonic and pyrrolic-N [123], it was postulated that due to the presence of oxygen on the surface and that pyrrolic-N is more unstable than pyridonic-N at elevated temperatures [85], it is likely that pyridonic-N persisted rather than pyrrolic-N during the KOH process. CO_2 capture capacity was demonstrated to be 2.74 $mmol_{CO2}/g$, higher than the unmodified and TEPA modified samples. It was suggested that this capacity was a result of the sample having the highest percentage of imine and pyridonic groups although it was identified that capacity was highly associated with micropores and especially ultramicropore volume as well as O-SFGs, indicating that O–C coordination is important. Wang et al. reported a facile synthesis procedure for nitrogen doped porous carbons (NPCs) that incorporated a combination of large surface areas, well-defined micropore sizes, and variable nitrogen by using polyimine as the carbon precursor [309]. The porous polyimine was prepared based on Schiff base condensations between building blocks with polyformyl and polyamino functionalities namely, *m*-phenylenediamine and terephthalaldehyde [310]. The subsequent KOH activation procedure followed the solid-solid mixing of polyimine and KOH pellets at a weight ratio of 2:1 and heating to between 600 °C and 750 °C for 1 h (3 °C/min) under argon flow. The polymer prepared without solvents (SFRH) by a melting-assisted method by Zhang et al. [311] involved mixing and grinding resorcinol (2.2 g) and hexamethylenetetramine (0.84 g) for 10 min at room temperature after which it is heated and cured at 160 °C for 24 h. Potassium hydroxide was then used to introduce porosity in the carbon, SFRH polymer (1 g) was immersed in aqueous KOH solution (200 ml) at various mass ratios (1–3:1), after which it was pyrolysed at between 600 °C–800 °C (10 °C/min) for an hour; hereafter it will be denoted as SNMC-x-y where x denotes mass ratio and y activation temperature.

The precursor SFRH shown in Fig. 5(a) has a bulky and smooth morphology with no visible porosity; after activation at 600 °C (Fig. 5 (b)) the particles become spongy and three-dimensional with a vast number of irregular pores. For SFRH, FTIR spectra showed the stretching vibration of C–O, methylene bridge and C–N and N–H bonds; after activation the bands of benzene rings disappeared but N–H vibrations were still visible indicating partial preservation of its nitrogen content. When the KOH/SFRH ratio is 1 or 2 the samples possess an abundance of micropores, at a ratio of 3 the pores become wider; this same trend can be seen with specific surface area and pore volume that increase with higher pyrolysis temperatures at the expense of the N-content. Binding energies of pyridine and pyrrolic/pyridonic-N were identified. The corresponding area ratios were measured to be 1:4.3, 1:6.1 and 1:2.2 for SNMC-1-600, SNMC-2-600 and SNMC-3-600, respectively - further reinforcing the greater stability of pyridonic-N vs pyrrolic-N [176] in harsher activation conditions [311]. SNMC-2-600 exhibited the best capacity at 1 bar and 298 K of 4.24$mmol_{CO2}/g$ due to adsorption being dominated by microporous channels of 0.5–1 nm at 1 bar. At 0.15 bar and 298 K, SNMC-1-600 demonstrated the highest capacity of 1.41 $mmol_{CO2}/g$ due to its higher nitrogen content which can significantly enhance performance at lower CO_2 partial pressures.

5.2.2. Sodium hydroxide – NaOH

Chemical activation using alkalis can also be achieved using NaOH. It is worth noting that in the context of carbonaceous materials, when there exists a more ordered pore structure their morphology remains unchanged with both potassium and sodium hydroxide activation. However, for poorly ordered carbons, KOH tends to destroy nanotubular morphology. This is due to the production of metallic K which has the ability to intercalate into all materials where Na can only intercalate with disorganised ones [7]. Consequently, activation with NaOH can be considered less damaging to the precursor. In this type of reaction (solid-hydroxide) the reactivity of the solid has to be a key factor. Higher temperatures are required in order to permit reactions [312] since NaOH is less reactive than the previously discussed KOH. The reaction between NaOH and carbon begins at around 570 °C vs the 400 °C for KOH and carbon [299]. The global reaction between carbon and NaOH is described in Eq. (26) [312]:

$$6NaOH + 2C \rightarrow 2Na + 3H_2 + 2Na_2CO_3 \quad (26)$$

Boujibar et al. [90] have demonstrated the use of sodium hydroxide to produce nanoporous AC sourced from argan fruit shells. The carbonised argan shells (700 °C, 10 °C/min for 1 h under N_2 flow) were either impregnated with the agents (NaOH or KOH) or mixed physically. The impregnation followed mixing the precursor (4 g) with the solution (16 g hydroxide in 50 ml distilled water) which was then ages at 60 °C for 2 h. In the latter case, NaOH or KOH beads (16 g) were mixed with the precursor (4 g) at room temperature in the absence of water. After

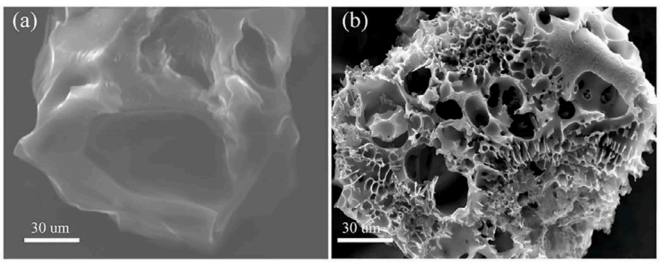

Fig. 5. SEM images of: (a) the polymer SFRH; and (b) SNMC-1-600 [311].

both processes, the samples were heated to 850 °C (5 °C/min) for 1 h under nitrogen flow. SEM images (Fig. 6) demonstrate that KOH activation leads to a honeycomb-like structure with smooth spherical voids, more prevalent with the impregnated sample. In the case of NaOH activation, the carbons exhibit irregular and inconsistent morphology perhaps a result of the less reactive chemical agent. The NaOH impregnated sample possessed a BET surface area of 1826.96 m^2/g, micropore volume of 0.23 cm^3/g and nitrogen content of 12.61 wt% facilitating a capacity of 3.73 $mmol_{CO2}/g$ at 25 °C and 1 bar. Singh et al. have investigated the effects of various agents (sodium amide ($NaNH_2$), NaOH and K_2CO_3) when synthesising modified porous carbon from polyacrylonitrile [313]. The carbonised polyacrylonitrile (800 °C, 10 °C/min, 2 h under N_2 flow) was mixed with the activating agents at four different ratios (1:1 to 1:4, carbon:agent) overnight (for NaOH and K_2CO_3) and then carbonised at 800 °C for 2 h. When increasing the ratios from 1 to 3, S_{BET}, V_{total} and V_{micro} increased from 754 m^2/g to 1020 m^2/g, 0.42 cm^3/g to 0.57 cm^3/g and 0.32 cm^3/g to 0.51 cm^3/g, respectively. At a ratio of 4, all of these properties were shown to decrease.

The SEM images exhibited in Fig. 7 illustrate the development of porosity with various reagents. Raw PAN is spherical and becomes irregular after carbonisation without the development of any pores. Activation with $NaNH_2$, NaOH or KOH produces pores as a result of the evaporation of volatile matters. When activating with this chemical, Na^+ can be introduced and will replace various phenolic and carboxylic ions [314]. The prepared carbons were able to capture up to 2.2 $mmol_{CO2}/g$ (30 °C and 1 bar), at a ratio of 4 the capacity was shown to be 1.98 $mmol_{CO2}/g$ due to a decrease in surface area. A combination of commercial adsorbents (zeolite, GAC and ACF) were modified with various alkaline agents (NaOH, K_2CO_3, DEA, aminomethyl propanol (AMP) and MEA + AMP) by Liu et al. [315]. The excess impregnation method was employed whereby the agents (1 M) were dissolved in deionised water and the adsorbent added (1.5 g per 100 ml solution) and stirred at 95 °C for 2 h. The NaOH modified ACF was demonstrated to have the highest CO_2 uptake whereas the performance of the zeolite was better enhanced with the K_2CO_3 modification. This was postulated to be a result of the smaller molecular size of NaOH and K_2CO_3 than the organic molecules meaning they can diffuse into the porous structure mitigating any pore blockage effects. The alkaline modification of the zeolite reduced the heat of adsorption, thereby suggesting that these would provide weak adsorption sites for CO_2 making regeneration less energy intensive.

Reinik et al. demonstrated that the hydrothermal activation of oil shale FA with NaOH could increase the physical adsorption of CO_2 from 0.06 to 3–4 mass%. The hydrothermal activation technique was used to develop synthetic calcium-silica-aluminium hydrates, mainly 1.1 nm

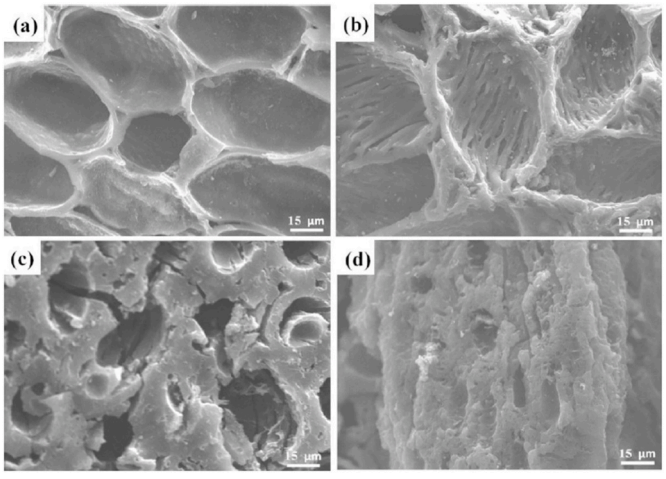

Fig. 6. SEM images of the prepared ACs: (a) KOH physically mixed; (b) KOH impregnated; (c) NaOH physically mixed; (d) NaOH impregnated.

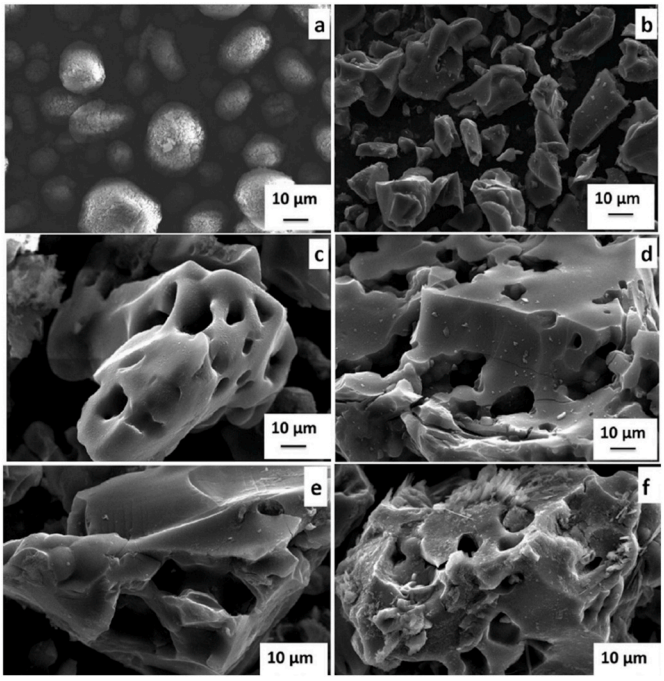

Fig. 7. SEM images of: (a) raw PN; (b) PN-800; (c) PN-3-NaNH2; (d) PN-3-NaOH; and (e)–(f) PN-3-K2CO3 [313].

$$2NaOH + SiO_2 \rightarrow Na_2SiO_3 + H_2O \text{ Quartz} \quad (27)$$

$$4NaOH + SiO_2 \cdot Al_2O_3 \rightarrow 2NaAlO_2 + Na_2SiO_3 + 2H_2O \text{ Mullite} \quad (28)$$

tobermite and katoite. The concentration of NaOH (1–8 M NaOH solution) and reaction temperature (130 °C and 160 °C) were varied whilst maintaining solid/liquid ratio and reaction time. Sodium hydroxide is often employed as a reagent when synthesising zeolitic phases from various precursors such as FA [229,230]. The synthesis of cancrinite-type zeolite *via* hydrothermal fusion in the work of Dindi et al. employed NaOH. Sodium hydroxide was fused with FA in order to breakdown the crystalline phases within the FA (Quartz and Mullite) and convert them into more soluble sodium silicates and aluminates as shown in Eq. (27) and Eq. (28).

Upon treating hydrothermally the sodium silicates and aluminates formed during the fusion reaction dissolve to form monomeric SiO_4^{-4} which undergo a condensation reaction to form polymeric amorphous aluminosilicates after which nucleation and growth of the zeolite crystal begins on the surface of the aluminosilicate particles [229]. A significant body of information regarding the synthesis of zeolites can be found in the work of Belviso [264].

Interestingly, the silicate-rich filtrate by-product obtained after the hydrothermal synthesis of zeolites from FA (20 kg FA, 12 kg NaOH, 90 dm^3 H_2O at 80 °C for 36 h) has been demonstrated as a suitable source to produce MCM-41 [316]. Sodium hydroxide has also found applications as a binder for amine-functionalised mesoporous silica. Klinthong et al. [317] employed a binder solution of polyallylamine (PAA) and NaOH to construct pellets from powdered MCM-41 functionalised with PEI or APTES. The solution that contained 3% PAA and 2% NaOH was identified as the most suitable for pelleting the silica adsorbents whilst maintaining considerable CO_2 capacity compared to the powdered sorbent (~90%) and improving significantly the mechanical strength (>0.45 MPa) and thermal stability. These sorbents then proving to be promising for large-scale applications when applying temperature swing adsorption (TSA).

5.2.3. Ammonium hydroxide – NH_4OH

Ammonium hydroxide (NH_4OH) has been used to functionalise oil FA using wet impregnation techniques [293] by Yaumi et al. The ash sample (100 g) was mixed with NH_4OH (300 ml) and refluxed for 24 h after which half was dried at room temperature and half at 105 °C for 24 h. Large portions of alkali, alkali earth and metal oxides were leached out based on their water solubility, while non-metallic oxides of sulphur remained in the carbon matrix. The low ionisation energy of metal oxides meant that more metal hydroxide ions existed in the reaction mixture. The silicon oxide could then be separated by settling. The XRD analysis confirmed the dominance of crystalline carbon, quartz and mullite phases in the activated sample. An increase in surface area and pore volume was seen in the activated sorbent, 59 m^2/g to 318 m^2/g and 0.0368 cm^3–0.679 cm^3, respectively, with the average pore diameter widening from 133 Å to 147 Å as a result of the ammonium hydroxide molecules diffusing into the pores of the ash permitting further reactions with the carbon. The presence of amino, hydroxyl and amide groups on the adsorbent's surface were confirmed by FTIR analysis. The modification facilitated an equilibrium capacity of 5.45 $mmol_{CO2}/g$. He et al. have shown that hyperbranched polymers can be functionalised to quaternary ammonium hydroxide groups that can reversibly capture CO_2 *via* humidity swing [318] and were able to achieve a 3–4 fold increase in the reaction kinetics compared with the Excellion membrane. Ammonium hydroxide has also been employed to introduce $–NH_2$ functional groups within the pores of mesoporous silicas (SBA-15) [319]. Ullah et al. dissolved the prepared SBA-15 (1 g) in the ammonium hydroxide solution (5 ml, 50 wt%) followed by the addition of deionised water (2 ml), the mixture was then stirred for 3 h. The structure of the modified SBA-15 (MSBA-15) was unchanged but its capacity was more than double the unmodified sample, 1.651 $mmol_{CO2}/g$ vs 0.6462 $mmol_{CO2}/g$ at 25 °C and 1 bar. The authors attributed this improved performance to the sorbents increased affinity to CO_2 as a result of the introduced amine group [320] since the performance of MSBA-15 and SBA-15 were similar at elevated pressures (200 bar) and temperatures (65 °C).

5.2.4. Ammonia – NH_3

High temperature treatments with ammonia will lead to the introduction of nitrogenous SFGs and the removal of acidic oxygen SFGs. It has been shown that the specific method of modification will govern the specific species of nitrogen that are introduced [244,321]. It has been shown by Pietrzak [322] that the order of modification methods can also significantly influence the amount of nitrogen that can be introduced. In this case, (ammoxidation after activation) the doped nitrogen acted to decrease pore volume, surface area and hence capacity due to a pore blockage effect. Interestingly however, the species that were introduced were independent of the methodology as a wide range of species were identified. Geng et al. used a one-step synthesis (activation + modification) technique to produce N-doped monolithic carbons by carbonising corncob under N_2 flow at 400 °C and subsequently activating the carbons using NH_3 at 400 °C–800 °C [323]. Activation temperature and duration were varied to compare their effect on the synthesised adsorbents. With an activation temperature of 400 °C, nitrogen could be easily doped into the carbon; however, pore development was learned to be difficult. At higher temperatures (800 °C) an increase in nitrogen content was found (12 wt%), much higher than other chemical activation methods [323]. This differs from the literature where it is common to see that at over 500 °C the N-content would decrease due to the high volatility of the N-containing species; this implies that for this case the amount of N-doping was higher than the removal of N at these higher temperatures. With activation conditions of 800 °C and 4 h, the pore size distribution is similar to porous carbons prepared by KOH activation. When considering the N-groups on the surface, FTIR analysis found peaks characteristic of pyridine and quinoline. This is corroborated by the XPS spectra that identified pyridine-N, pH-NH_2, pyrrolic-N, quaternary-N and N-oxides. The presence of these groups was shown to be dependent on activation temperature with Ph-NH_2 seen at < 400 °C, pyridine-N and Ph-NH_2 at > 600 °C and all of the groups seen above 750 °C. At this temperature, the volatility of these groups means that above 800 °C only the pyridine-N and Ph-NH_2 groups remain. These groups are often considered the most effective groups for CO_2 capture due to the preferred interactions between CO_2 and the electronegative N-containing groups [172,323]. Thermodynamically, the direct reaction between carbon and NH_3 (Eq. (29)) is only favourable at high temperatures. Geng et al. postulated that the ability to realise high amounts of N-doping at lower temperatures could be attributed to the oxygen-containing functional groups that exist within the precursor (*i.e.* corncob).

$$NH_3(g) + C \rightarrow HCN(g) + H_2(g) \tag{29}$$

These O-containing groups react with the NH_3 to form amine containing sites such as Ph-NH_2 moieties; when increasing the activation temperature the carbon itself reacts with the NH_3 forming pores by transforming carbon into hydrogen cyanide gas (HCN) during which N atoms are doped into the aromatic rings [323]. This was confirmed by comparing the activation with conventional KOH which would remove any O-groups prior to modification with NH_3. Subsequently, ammonia can be simultaneously used to activate and modify the surface of carbonaceous precursors. The highest capacity (2.81$mmol_{CO2}/g$) was associated with an activation temperature of 800 °C and 3 h of reaction time. The sorbent also had a selectivity towards CO_2 over N_2 of 82:1 [323]. Heidari et al. used ammonia modification on eucalyptus derived-AC where instead of utilising pure gaseous ammonia, a nitrogen stream was first blown on an ammonia solution, the mixture was then introduced to the AC and then treated thermally [146]. AC (4 g) was heated to 400 °C in the presence of the aforementioned gas mixture and held for 2 h. The same procedure was conducted at 800 °C. This method of modification facilitated an increase in nitrogen content from 0.52 wt % for the unmodified carbon to 3.14 wt% and 7.76 wt% for the modified carbon at 400 °C and 800 °C, respectively. The ammonia heat treatment here caused decomposition of the ammonia to free radicals such as NH_2, NH and atomic H and N; attractions of these free radicals to carbon surface; and formation of nitrogen containing functional groups. Amides and nitriles are created by the reaction of ammonia with carboxylic acid sites that exist in the carbon (Eq. (30)) [215,296]. Amine functionality can also be created by the substitution of OH groups (Eq. (31)); imine and pyridine can be formed by replacement of ether like oxygen surface groups by –NH– at high temperatures by the reaction of carbon with ammonia and then by a dehydrogenation reaction [215,296]. The decomposition of oxygen functional groups such as CO_2 and CO when treated at 800 °C compared to 400 °C, explains the higher N-content in the two modified sorbents.

$$-COO^- NH_4^+ \xrightarrow{-H_2O} -CO-NH_2 \xrightarrow{-H_2O} C \equiv N \tag{30}$$

$$-OH + NH_3 \rightarrow -NH_2 + H_2O \tag{31}$$

The FTIR spectra of both modified and un-modified samples indicated the presence of phenol, alcohol and carboxylic acid as well as ketones and secondary cyclic alcohol. In the modified samples there existed aromatic bonds and carbonyl. The basicity of the modified samples evaluated using Boehm titration indicated that at higher temperatures (800 °C) a higher content of basic groups could be achieved, 0.315 meg/g vs 0.062 meq/g for the 400 °C treatment. XPS results showed that for all samples seven components were present: graphite, phenols, ethers/alcohols, carbonyls, quinones and carboxylic groups as well as carbonates. The modified samples however, showed four further peaks: pyridine, pyrrole, quaternary nitrogen and N–F - with pyridinic and pyrrolic at higher concentrations in the high temperature modification and quaternary and N–F higher in the low temperature modification. The ammonia treatment was able to increase the presence of nitrogen from 0 wt% to 13.9 wt% and 18.3 wt% for the low and high

temperature modifications, respectively. The greatest CO_2 capacity was exhibited by the 800 °C sample (3.22 $mmol_{CO2}/g$) vs 1.10 $mmol_{CO2}/g$ and 2.98 $mmol_{CO2}/g$ for the 400 °C and unmodified samples, respectively. Interestingly here, the unmodified sample had a higher capacity than the low-temperature modified sorbent. This was identified as a result of the textural properties. The 400 °C sorbent had the lowest micropore volume (80%) and highest pore diameter (2.44 nm). Unequivocally, there seems to exist a synergistic effect between the micropore volume, pore size and nitrogen content on CO_2 capacity.

Ammonia can also be employed in combination with other reagents and activating mediums such as CO_2 [203], HNO_3 [324] or KOH [87]. Zhang et al. [87] employed a three-step procedure (carbonisation at 650 °C, KOH activation at 830 °C and NH_3 modification at 600 °C) where the final treatment acted to both enhance the development of the carbons porosity and modify the surface with nitrogenous SFGs. The pore development arises as a result of the thermal decomposition of oxygen SFGs that either block or occupy the micropores, their removal creates vacant sites [279,325] that the free radicals can then react with to further expand the structure. Aside from reactions detailed in Eq. (30) and Eq. (31), a further reaction has been suggested [87,215,326] in Eq. (32). It was also identified that the free radicals may react within the mesopore walls of the carbon releasing H_2, CH_4, HCN and $(CN)_2$ that can aid the development of porosity [215,326] specifically microporosity. The presence of the introduced groups that included pyrrolic/pyridonic and pyridine species along with amino-type nitrogen facilitated a capacity of 5.05 $mmol_{CO2}/g$ at 25 °C and 1 bar.

$$-C=O+NH_3 \rightarrow -C=NH+H_2O \quad (32)$$

The combination of CO_2 and ammonia treatments was learned to enhance the amount of available free radicals hence, improving the development of porosity [203] but also improving the efficiency of nitrogen doping. At a temperature of 800 °C using a mixture of CO_2 and NH_3, nitrogen contents of up to 6 wt% were realised attributed to the CO_2 gasification reactions with the carbon surface that provides more sites for amination [279].

5.2.5. Hydroxylamine – NH_2OH

The inorganic compound, hydroxylamine, can be used to prepare amidoximes that can be used for CO_2 capture [170]. In this work, four amidoximes were chosen based on their valency, the synthesis follows a facile method of treating the corresponding nitriles with hydroxylamine [327]; for acetamidoxime (AAO-monovalent) acetonitrile (0.02 mol) was mixed with a solution of hydroxylamine (50 wt% in H_2O, 0.022 mol) in ethanol at 70 °C for 7 h. Three other adsorbents were prepared: terephthalamidoxime (TPAO-divalent), tetraquinoamidoxime (TQAO--tetravalent) and polyamidoxime (PAO-polyvalent). The percentage of amidoxime SFGs present was shown to influence the CO_2 adsorption performance. AAO had the highest amidoxime functionality per molecule (79.7% w/w) and showed the greatest capacity of 1.64 $mmol_{CO2}/g$ and 2.71 $mmol_{CO2}/g$ at 43 °C and 70 °C respectively (at 180 bar). The chemical affinity of PAO with CO_2 was assessed per unit surface; 0.53 $mmol_{CO2}/m^2$ and 0.41 $mmol_{CO2}/m^2$ indicating a stronger adsorbate-adsorbent interaction than the other sorbents. Interestingly, AAO was the only material that demonstrated a higher capacity with increasing adsorption temperature. This is likely a result of the dimerization that did not occur in the other materials. In another study, amidoxime SFGs were introduced noninvasively into polymers of intrinsic microporosity (PIM), increasing the capacity up to 17% by Patel and Yavuz [169]. Similarly, the PIM-1 was functionalised by a rapid reaction of the nitrile groups with hydroxylamine under reflux conditions (69 °C for 20 h) achieving complete conversion of the nitrile groups. Alongside this conversion an unprecedented increase in micropore surface area was observed (313 m^2/g to 376 m^2/g) postulated to be a result of the conversion of mesopores to micropores upon replacement of a nitrile group by a bulkier amidoxime group. The presence of amidoxime sites creates a stronger affinity toward CO_2 through its high quadrupole moment; the capacity was shown to be 2.74 $mmol_{CO2}/g$ vs 2.53 $mmol_{CO2}/g$ at 273 K and 1 bar or 1.65 $mmol_{CO2}/g$ vs 1.41 $mmol_{CO2}/g$ at 298 K and 1 bar for the modified PIM vs PIM-1. Amidoxime--grafted carbons have also been produced that demonstrated significantly improved CO_2 selectivity (CO_2/N_2) although the overall capacity decreased (4.97 $mmol_{CO2}/g$ to 4.24$mmol_{CO2}/g$). Mahurin et al. [171] sonochemically grafted ordered mesoporous carbon (OMC) with PAN. The sonochemical polymerisation of PAN was followed by a chemical conversion of the grafted PAN to amidoxime. Ordered mesoporous carbon (0.3 g) was added to 1 g of initiator (benzoyl peroxide, (BPO)) in acetone with subsequent evaporation of the acetone at room temperature. The grafting involved a sonication bath charged with 100 ml of the solvent mixture, BPO-impregnated carbon and 16.6 ml of acrylonitrile. Upon completion of 3 cycles of evacuation and refilling with a nitrogen purge, the polymerisation was performed under N_2 flow and sonication at 60 °C–70 °C for 2 h or 5 h, depending on the sonication method. The product, collected by centrifugation, was washed, dried and then converted to amidoxime using hydroxylamine in a 50/50 solution of H_2O/methanol for 72 h at 80 °C. Two loadings were achieved: 10.6% and 5.4% with maintenance of the pore structure and morphology but at the expense of micropore volume and surface area indicating the deposition of amidoxime primarily occurs in the micropores and small mesopores. The CO_2 loadings of the modified samples were remarkably similar at 2.489 $mmol_{CO2}/g$ and 2.498 $mmol_{CO2}/g$ at 298 K and 1 bar vs 2.871 $mmol_{CO2}/g$ for the unmodified sample. However, upon normalising the capacity to total surface area, the modified samples were realised to perform better. Also, when considering the improvements observed in selectivity over N_2, amidoxime SFGs are a promising group for the selective capture of CO_2 that have not seen as much interest compared to the more common SFGs.

5.3. Salts

5.3.1. Ammonium sulphate – $(NH_4)_2SO_4$

Ammonium sulphate was used by Yadavalli et al. to modify the surface of AC [271]. The impregnation of the prepared AC (100 g) with a saturated solution of ammonium sulphate salt using 5 g, 7.5 g and 10 g, achieved weight fractions (AC/$(NH_4)_2SO_4$) of 4.76%, 6.98% and 9.1%, respectively. An increase in $(NH_4)_2SO_4$ led to an increase in adsorbent exhaustion time from 4.5 min to 7 min, 10 min and 12.5 min for the 3 loadings without changing the 1.5 min breakthrough time. It was also found that through the modification there exists a larger number of active sites for CO_2 adsorption due to the addition of nitrogen-based functional groups [271]. The adsorption of CO_2 was conducted with a gas mixture containing methane. Although all biomass-derived ACs showed higher selectivity (>5) towards CO_2, an increase in ammonium sulphate content did decrease the adsorbents selectivity with regards to methane. Therefore, at higher loadings this must be accounted for.

5.3.2. Sodium amide – $NaNH_2$

Sodium amide has advantages that lie with its strong basicity and nucleophilicity [328,329], enabling $NaNH_2$ to be an effective reagent that can perform activation to develop porosity at lower temperatures *i.e.* 450 °C–550 °C [330,331] whilst simultaneously acting as a nitrogen source that enables N-doping within the porous support. Lower activation temperature is known to be good for both generation of narrow microporosity and preservation of N-containing groups [330].

Liu et al. synthesised a series of N-doped porous carbons with a single-step activation using $NaNH_2$. The activation temperature and weight ratio of $NaNH_2$ was varied between 450 °C–550 °C and 1–3 ($NaNH_2$ to Carbon), respectively [330]. The adsorbents prepared at a weight ratio of 2 ($NaNH_2$:carbon) showed the highest values in porous textural properties regardless of activation temperature. This was postulated to be a result of the complex solid-state and gas erosion reactions, whereby the $NaNH_2$ will attack the oxygen species on the surface of the carbon precursor to create pores and dope nitrogen into the

framework [330]. The content of nitrogen within the adsorbents was found to increase with increasing ratios of $NaNH_2$ during the activation. However, it decreases with an increase in activation temperature due to the decomposition of unstable nitrogen species; all samples were found to have pyridinic and pyrrolic-N but not quaternary or oxidised-N that are typically developed at higher temperatures. Two further peaks were found in the XPS spectra corresponding to carbonyl and hydroxyl groups. The oxygen present in each sample is primarily in the form of hydroxyl groups that are reported to be Lewis basic sites that can bind CO_2 [332]. The maximum capacity of 3.5 $mmol_{CO2}/g$ at 25 °C and atmospheric pressure was found with a ratio of $NaNH_2$:carbon of 1 and an activation temperature of 550 °C. No direct correlation could be found between porous textural characteristic, nitrogen content and CO_2 capture performance. It was understood however that there exists a synergistic effect between all of these parameters. Sodium amide was also employed by Rao et al. [333] in a single step procedure to produce nitrogen-enriched porous carbon from water chestnut shells. The authors carbonised the shells (WSC), mixed the product with $NaNH_2$ (95%) (solid-solid mixing), and heated the mixture to a temperature between 400 °C and 500 °C (5 °C/min) under nitrogen flow (400 ml/min). Samples were categorised as WSC-X-Y where X represents activation temperature and Y represents mass ratio of $NaNH_2$ to WCS, the yield of which varied between 36% (WSC-400-1) and 86% (WSC-500-3). Micropore size was shown to increase with both activation variables and was further verified by PSD plots. The mechanism of pore development follows reactions between 1) $NaNH_2$ and the oxygen SFGs of the carbon, 2) NaOH and/or Na_2O formed during activation which further activates the carbon in a similar fashion to KOH/NaOH activation and 3) physical activation by NH_3 and water vapour which are simultaneously released during the $NaNH_2$ reactions. Nitrogen moieties were present within the structure after modification at higher quantities with greater concentrations of the reagent and a decreasing temperature indicating that high temperatures can decompose more unstable nitrogen species. XPS spectra elucidated to the presence of two peaks indexed to pyridinic-N and pyrrolic/pyridonic-N. High-temperature N-species such as quaternary N and pyridine-N-oxide, were not detected due to the low activation temperatures; a benefit to CO_2 capture performance since the low temperature species are more CO_2-philic [334]. The maximum capacity at 1 bar and 25 °C was demonstrated to be 4.5 $mmol_{CO2}/g$ (WSC-500-1) with a saturation time of around 5 min and high selectivity, cyclic stability and suitable isosteric heat of adsorption. Zhang et al. utilised $NaNH_2$ to synthesis ultra-high surface area and nitrogen-rich porous carbons from oil-tea seed shell (OTSS) [331]. In their work, 1 g of the carbonised OTSS (550 °C for 1 h under nitrogen flow) was mixed and ground with sodium amide at a ratio of 1:1–3 by weight (OTSS/$NaNH_2$) and subsequently heated to between 350 °C–650 °C (10 °C/min) and held for 1 h under nitrogen flow; referred to as OTSS-X-Y where X represents reagent ratio and Y represent activation temperature. The prepared samples exhibited a large proportion of micropores and it was observed that when increasing both OTSS/$NaNH_2$ ratio and activation temperature the BET surface area would increase from 498 m^2/g to 1154.7 m^2/g for OTSS-1-450 and from 778.8 m^2/g to 2965.7 m^2/g for OTSS-3-350; this value is extremely large and the sample showed a larger pore size distribution (PSD). Interestingly, the pore size distribution was shown to be controllable. With an increase in the ratio from 1 to 3, pore sizes increased from 0.7 nm to 2.5 nm (at 650 °C). Also, with an increase in temperature from 350 °C to 650 °C, the pore size increased from 0.55 nm to 1.2 nm (at a ratio of 1). The FTIR spectra showed that in the modified samples, there existed a strong indication of either a nitrile group or C═N from the pyridine and quinoline groups. XPS analysis identified that within the unmodified sample the nitrogen content was small at 2.11 at%; at a weight ratio of 1:1 the nitrogen content was still negligible at 0.38 at% (for OTSS-1-550) however at higher ratios such as OTSS-2-450 and OTSS-3-350 the nitrogen content increased to 4.81 at% and 6.78 at% respectively. In the two aforementioned samples the spectrums corresponded to pyridinic-N and pyrrole/pyridine-N. The campaign to assess the CO_2 capture performance was undertaken with three samples of very similar textural properties (BET surface area, pore volume and PSD) but significantly different N content to better understand the role of N functionalities. The samples termed OTSS-3-350, OTSS-2-450 and OTSS-1-550 had N contents of 6.78 at%, 4.81 at% and 0.38 at%, respectively. Interestingly there was no discernible difference in their performance at temperatures of 273 K, 298 K and 323 K and pressures up to 1 bar thus, elucidating the limited impact of N-groups on adsorption. At 273 K and 1 bar OTS-2-550 with the largest micropore volume 0.63 cm^3/g under 2 nm displayed the highest capacity 5.65 $mmol_{Co2}/g$; at 298 K OTS-1-650 with the largest narrow micropore volume (0.21 cm^3/g under 0.68 nm) displayed the greatest capacity, 3.5 $mmol_{Co2}/g$. Evidently, micropores are imperative to CO_2 capture, at higher temperatures narrow micropores are more beneficial. Thus, microporous structures have a greater influence on CO_2 adsorption rather than N functionalities [331]. The role of nitrogen functionalities, however, was identified to be a great influence on the selectivity of the adsorbent. It was observed that pyrrole/pyridine-N facilitated a CO_2/N_2 selectivity of 126 and 77.9 for OTSS-2-450 at 273 K and 298 K, respectively. The single-step activation of hazelnut-shell using sodium amide [335] by Liu et al. also investigated the effect of temperature (500 °C–600 °C) and $NaNH_2$/carbon ratio (1–3 by mass). A decrease in temperature and an increase $NaNH_2$ dosage was shown to increase the N content of the carbons as expected due to the instability of various nitrogen species. The species present were pyridinic, pyrrolic and quaternary nitrogen with pyrrolic being the predominant; with respect to O-SFGs, the hydroxyl groups were more prevalent. Again, an increase in both activation temperature and agent dosage led to an increase in all textural properties however a smaller dosage was learned to be more beneficial for creating narrow microporosity. At higher dosages the effect of higher temperature becomes more negative for the formation of narrow micropores. The highest capacity achieved was 4.32 $mmol_{CO2}/g$ and 6.23 $mmol_{CO2}/g$ at (1 bar) 25 °C and 0 °C, respectively. The authors identified that aside from nitrogen content and narrow micropore volume, the pore size and pore size distribution also influence the adsorption of CO_2 under ambient conditions. Huang et al. have investigated the effect of sodium amide activation on hydrothermal carbons (HTCs); the HTCs were mixed with $NaNH_2$ and heated to between 400 °C and 600 °C (10 °C/min) under nitrogen for 1 h, the weight ratio of $NaNH_2$/HTC was varied between 2 and 4. Interestingly here, the nitrogen species developed included amine/imine/amide-N and pyrrolic-N in greater proportions than pyridinic-N. The sorbent prepared at 600 °C at a weight ratio of 3 demonstrated a capacity of 5.58 $mmol_{CO2}/g$ and 3.41 $mmol_{CO2}/g$ at (1 bar) 0 °C and 25 °C, respectively; at 0.15 bar, capacities of 1.99 $mmol_{CO2}/g$ and 1.23 $mmol_{CO2}/g$ were achieved (0 °C and 25 °C, respectively) with the carbon prepared at 600 °C and a weight ratio of 2. This was identified a result of the adsorption of CO_2 being dominated by narrow micropores at lower pressures ($P_{CO2} = 0.15$ bar), the same trend does not exist at elevated pressures ($P_{CO2} = 1$ bar).

5.3.3. Sodium dithionite – ($Na_2S_2O_4$)

In the modification of NPOFs by Islamoglu et al. [77] both fuming nitric acid and sodium dithionite were employed. The sodium dithionite ($Na_2S_2O_4$) modification was carried out after the HNO_3 modification and follows charging a round-bottom flask with 80 mg NPOF-1-NO_2 (HNO_3 modified NPOF), 10 ml methanol and 10 ml distilled water under nitrogen flow. The suspension was degassed for 20 min prior to the $Na_2S_2O_4$ (1.2 g, 6.9 mmol) addition which itself was followed by heating at 75 °C for 18 h. Subsequently, the material was filtered and suspended in warm water (25 ml) for 30 min resulting in a polymer that was then suspended in 25 ml 4 M HCl (to ensure complete reduction to amine) and then washed with 2 M NaOH to neutralise the amine. The product was the suspended in warm water, filtered and suspending once more in warm ethanol and THF for two 30-min cycles. The product was termed NPOF-1-NH_2; alongside this the over functionalised NPOF

(NPOF-1-NO_2(xs)) was also reduced in the same way and termed NPOF-1-NH_2(xs). The successful conversion of nitro groups in NPOF-1-NO_2 was confirmed by a lack of NO_2 presence and new bands corresponding to asymmetrical and symmetrical N–H stretching in the FTIR spectra. Micropore volume was shown to increase up to 77% of total pore volume for NPOF-1-NH_2(xs); however, NPOF-1-NH_2 may be more beneficial since micropore volume comprised 71% of its total pore volume. The CO_2 capture capacity of the two amine derivatives was demonstrated to be 2.93 $mmol_{CO2}/g$ and 3.77 $mmol_{CO2}/g$ (at 298 K and 1 bar) for NPOF-1-NH_2(xs) and NPOF-1-NH_2, respectively.

5.3.4. Sodium carbonate – Na_2CO_3

The modification of anthracite by Lillo-Ródenas et al. [299] using a number of reagents also endeavoured to employ sodium carbonate in an attempt to compare the modification against hydroxides. The method involved physically mixing the reagent with the coal precursor in a 4:1 wt ratio (so as to achieve the same quantity of Na as in the sample prepared by NaOH) and then heating the mixture under nitrogen flow (500 ml/min, 5 °C/min) up to 760 °C and holding for 1 h. This method of activation showed poor performance with respect to porosity development when compared to the sample prepared with NaOH under the same conditions due to the fact that the carbonate species do not decompose at 760 °C [312]. At higher temperatures the carbonate would act to simultaneously chemically and physically activate the carbon due to the formation of sodium oxide and CO_2. Caglayan et al. [117] investigated HNO_3 oxidation, air oxidation, alkali impregnation (10 wt% Na_2CO_3) and heat treatment of commercial AC (Norit ROX 0.8). Conversely, the authors were able to achieve mass uptakes of CO_2 8-times (at 1 bar) that of the air oxidised and nitric acid oxidised counterparts. This postulated to be a result of the Na sites acting as active adsorption sites for CO_2; the carboxylic acid sites formed during HNO_3 treatment providing anchor-sites for the Na-precursor thereby enhancing its dispersion.

5.3.5. Potassium carbonate – K_2CO_3

Potassium carbonate has been employed as an alternative reagent to KOH given it's highly caustic nature and thus, potentially serious environmental pollution in the activation of D-glucose derived carbons [253]. Here, the activation was carried out after an initial urea treatment and at different temperatures (600 °C–700 °C) and K_2CO_3/carbon ratios (2–4) although heating time and rate was kept constant at 1 h and 5 °C/min. The activation led to a reduction in nitrogen content from 20.66 wt% (urea-modified carbon) to between 12.27 wt% - 4.69 wt%. A higher activation temperature and reagent ratio may lead to lower nitrogen content as a result of the decomposition of N-containing moieties [253]. XPS spectra demonstrated the presence of pyridinic-N, amine and pyrrole/pyridine-N. Under mild pyrolysis conditions, the unstable amine functionalities are converted to pyridinic or pyrrole/pyridine-N. However, with an increase in temperature to between 650 °C and 700 °C, some of these N-groups are transformed to quaternary nitrogen. When increasing the quantity of K_2CO_3 or the activation temperature, the values of BET surface area, total pore volume and micropore volume increase accordingly as well as the narrow micropore volume. However, at 700 °C the development of narrow micropore is proportionately less. The highest CO_2 uptake of 3.92 $mmol_{CO2}/g$ at 1 bar and 25 °C was observed with the sample prepared at 650 °C and a ratio of 4; again there is no unambiguous correlation between capacity for CO_2 and porous textural characteristics [253] despite the postulation that a synergistic effect between nitrogen content and narrow micropore does, in fact, influence CO_2 capacity. A similar procedure has been employed by Yue et al. [336] in the post K_2CO_3 activation of urea-modified carbonised coconut shell (CN). The CN (2 g) was impregnated with an aqueous solution of K_2SO_3 (6 g) for 6 h at ambient temperature followed by heating to 600 °C followed by heating to 600 °C (5 °C/min) for 1 h under nitrogen flow (400 ml/min). The activation was shown to decrease the nitrogen content of the sorbents from 4.47 wt% to 2.76 wt% - 0.86 wt%; primarily in the form of pyrrole/pyridine-N but with similar amounts of pyridinic and quaternary-N. During the activation K_2CO_3 firstly decomposes into CO_2 and K_2O (Eq. (33)), aside from this, metallic K is formed through a series of redox reactions (Eq. (34) and Eq. (35)) that can then intercalate with the carbon matrix thereby expanding the lattice, this method then is much the same as KOH activation. The highest capacity was found in the sample prepared with a weight ratio of 3, 3.71 $mmol_{CO2}/g$ at 25 °C and 1 bar with Q_{st} values between 21 kJ/mol and 29 kJ/mol typical of physisorption processes.

$$K_2CO_3 \rightarrow K_2O + CO_2 \quad (33)$$

$$K_2CO_3 + C \rightarrow K_2O + 2CO \quad (34)$$

$$K_2O + C \rightarrow 2K + CO \quad (35)$$

Conversely, trace amounts of K_2CO_3 (<2 wt%) have been shown to produce ACs with superior textural properties to those prepared with a weight ratio of K_2CO_3/carbon of 3 *via* an induced catalytic activation strategy in the work of Wang et al. [337]. Sub-bituminous coal was initially washed with HCl (5 M) and HF (20 wt%) and then impregnated with aqueous K_2CO_3 followed by heating to 900 °C (10 °C/min) for 1 h under a mixture of CO_2 and N_2 ($CO_2/N_2 = 0.3$ or 0.4, total flow of 200 ml/min). The weight ratios of K_2CO_3/carbon evaluated were 0.02 and 0.01; the two catalytically activated samples were termed Ca_AC-1 (K_2CO_3/carbon = 0.02; $CO_2/N_2 = 0.3$) and Ca_AC-2 (K_2CO_3/carbon = 0.01; $CO_2/N_2 = 0.4$). Ca_AC-1 presented the highest BET surface area (1773 m^2/g) and pore volume (1.11 cm^3/g), four times that of the CO_2 activated counterpart. CO_2 activation is often limited by diffusion processes. The presence of trace K_2CO_3 promotes pore development through the release of CO from the K_2CO_3 attached to the carbon matrix forming a composite structure containing C–O–K during CO_2 activation; the surface carbon then reduces this complex to form the K–C complex with the release of CO, this new complex will be oxidised to a new C–O–K complex when CO_2 is introduced at high temperature [337]. Under the assistance of a CO_2 atmosphere, the potassium species will be regenerated and continue to catalyse the activation reactions. The capacity of Ca_AC-1 was demonstrated to be 4.36 $mmol_{CO2}/g$ at 273 K and 1 bar, suggesting that this technique is extremely promising without the need for large amounts of K_2CO_3.

Mestre et al. have activated cork powder waste with K_2CO_3 [208]. The researchers mixed cork powder with ground K_2CO_3 in a 1:1 wt ratio and calcined under nitrogen flow (300 ml/min) at 700 °C (10 °C/min) for 1 h. Boehm titration identified the presence of a number of surface oxygen functional groups, including carboxylic acid and R–OCO as well as R–OH and R = O. This revealed the samples to be significantly more acidic compared to the steam-activated sample [208]. Potassium carbonate has been shown by Liu et al. [315] to enhance the performance of zeolites more significantly than both the inorganic (NaOH) and organic (DEA, AMP and MEA + AMP) alternatives assessed in their work despite it having the lowest BET surface area and micropore volume. Bhatta et al. [338] have investigated the applications of K_2CO_3-promoted Mg–Al hydrotalcite-like compounds (HTLcs) supported on coal-derived graphitic material (CGM). A series of K_2CO_3 loadings (10 wt% - 25 wt%) were investigated *via* an incipient wetness method [339], followed by calcination at 400 °C. The K^+ ions interact with Mg–O and/or Al–O centres on the surface of the adsorbent generating more basic sites [338]; K_2CO_3 leads to the formation of defects in the crystal structure. The increase in basic site density can enhance the adsorption capacity; an optimum loading of 15 wt% was identified.

5.3.6. Zinc chloride – $ZnCl_2$

Zinc chloride was employed as the activating reagent for powdered dry fish [340]. Mixtures of dry fish and $ZnCl_2$ were prepared in various concentrations and heated in an inert atmosphere at temperatures between 500 °C–650 °C for 1. Surface area and both total and micropore volume were shown to increase as activation temperature increased

from 500 °C to 550 °C after which an increase in temperature leads to a decrease; the optimum was identified at 550 °C. Varying the $ZnCl_2$:fish powder ratio between 1:1 and 3:1 presented an increase in surface area and total pore volume but a decrease in micropore volume. The N–H peak shift indicated that the nitrogen in the amide group co-ordinates with Zn^{2+} ions through the lone pair of electrons and the C═O indicates back donation of electrons from the completely filled orbitals of Zn^{2+} to the vacant orbitals of the amide carbonyl group leading to an improved thermal stability and thus, retention of carbon and nitrogen at higher temperatures. Without $ZnCl_2$, the nitrogen content was measured to be 12.4 wt% which decreased to 7.9 wt%, 5.8 wt% and 5.2 wt% with an increase of the $ZnCl_2$ ratio from 0 to 3 (at 550 °C). The same trend was observed when increasing temperature from 550 °C–650 °C and maintaining a ratio of 1:1, 7.3 wt% to 5.9 wt%. The nitrogen was present in the form of pyridinic (48.3%), pyrrolic (40.8%) and quaternary (10.9%). The CO_2 capacity of the modified adsorbents prepared at 550 °C was shown to increase from 1.3 $mmol_{CO2}/g$ to 2.4 $mmol_{CO2}/g$ at 25 °C. This however, decreased when increasing the ratio of $ZnCl_2$ (from 1 to 3). Given that the unmodified sample had a much smaller ultramicropore volume but greater nitrogen content, Wilson et al. postulated that the micropore volume coupled with N-content were the governing factors determining capacity. Chang et al. have employed higher temperatures (up to 900 °C) and weight ratios ($ZnCl_2$:carbon up to 8) in the synthesis of N-doped hierarchical porous carbon microtubes from poplar catkin (PC) [341]. The chemical activation of carbonised (400 °C) PC followed removal of organic impurities, the PC aliquots were mixed with $ZnCl_2$ at various weight ratios (2–8) in aqueous solutions (30 ml) and then stirred for 4 h at 110 °C. The dried samples were then calcined at between 700 °C and 900 °C for 2 h under nitrogen. During the activation, hydrogen and oxygen atoms are stoichiometrically removed from the precursor framework producing H_2O with the assistance of the $ZnCl_2$ which causes the formation of pores [341]. It was observed that an increase in temperature would increase the size of pores attributed to an increased $ZnCl_2$ etching effect and therefore release of volatile species. Capacities as high as 6.22 $mmol_{CO2}/g$ and 4.05 $mmol_{CO2}/g$ were achieved at 273 K and 298 K (1 bar), respectively. Zinc chloride activation of Coca Cola ® [342] was able to produce HTC ACs with an adsorption capacity of up to 3.2 $mmol_{CO2}/g$ at 25 °C and 1 atm, attributed to the *in-situ* doping of heteroatoms as a result of the various additives in the beverage and the micropore volume developed. The $ZnCl_2$ activation of triazine-based hyper-cross-linked polymers (600 °C–800 °C) produced carbons with the highest nitrogen contents compared to KOH and $FeCl_3$ activations, 7.55 at% in the form of pyridinic-N (2.44 wt%), pyrrolic-N (1.24 wt%), quaternary-N (2.8 wt%) and oxidised-N (0.78 wt%). It was identified that while KOH etches the soft components and increases BET surface area and pore development [343] it can degrade N-species whereas $ZnCl_2$ acts as a dehydrating agent. This has been identified by Ludwinowicz and Jaroniec [344] as a limiting factor in its applications since it has an insignificant ability to activate already carbonised materials. At 1 bar and 273 K the sorbent demonstrated a capacity of 5.36 $mmol_{CO2}/g$, less than the KOH activated counterpart. Interestingly, at 0.1 bar, the $ZnCl_2$ activated sorbent had the largest uptake which was postulated to be a result of the nitrogen content which also provided the sample with the highest CO_2/N_2 selectivity (IAST: 42.6). The application of $ZnCl_2$ activated biocarbons has been demonstrated by Singh et al. [345] where the samples demonstrated capacities of up to 13.1 $mmol_{CO2}/g$ at 25 °C and 30 bar, and 2.1 $mmol_{CO2}/g$ at 25 °C and 1 bar using an activation temperature of 500 °C and impregnation ratio of 3 ($ZnCl_2$: chitosan). An activation temperature of 500 °C has been found as the optimum for the development of surface area and micropore volume in a number of studies [346,347]. Aside from carbon activation, zinc chloride is often employed in the synthesis of covalent triazine frameworks (CTFs) [348–351] through ionothermal reactions with molten $ZnCl_2$ that acts as both a Lewis acid trimerization catalyst and reaction medium [352].

5.4. Carbamide – urea ($CO(NH_2)_2$)

Rehman and Park [304] tailored the ultra-microporosity of N-doped carbon by varying the concentration of urea and KOH during the synthesis of the adsorbent from a chitosan precursor. High surface areas (368 m^2/g to 2150 m^2/g) and high micropore volumes (0.2255 cm^3/g to 1.3030 cm^3/g) were attained with nitrogen concentrations ranging from 0 wt% to 11 wt%. A one-step synthesis procedure was employed (simultaneous activation and nitrogen doping) whereby carbonised chitosan (1 g) saw additions of urea and KOH, 30 min of grinding in an agar mortar, followed by further carbonisation. Using TG-DTA curves it was deduced that the mechanism for producing nitrogen-doped carbon materials includes i) transformation of chitosan-derived nitrogen-derived carbon to graphene-like sheets followed by the successful nitrogen-doping from urea-derived carbon-nitride structure and ii) the reaction of KOH with graphene-like sheets transformed them into three-dimensional porous carbon-structure [304]. An evaluation of activation temperature showed that at 650 °C, the carbon prepared in the absence of urea but with KOH (1:0:1; carbon:urea:KOH) showed a nitrogen content of 9.3 wt%; this decreased to 0.6 wt% after the second carbonisation at 800 °C demonstrating the evaporation of volatile nitrogen compounds. However, when increasing the urea concentration to 1:3:1 the nitrogen content could be increased to 11 wt%; at higher KOH ratios (1:1:3) the nitrogen content decreased to 0.62 wt% thus, highlighting the importance of optimising both microporosity and N-doping. The N-doping occurs when urea reacts with surface functionalities on the carbon. Upon thermal treatment hydroxyl groups can react with the amino groups of urea, introducing nitrogen moieties into the carbon lattice. These moieties can be located on the edges of the lattices in the form of amine, pyridinic and pyrrolic nitrogen that at high temperature can be transformed into graphitic nitrogen. Within the synthesised adsorbents four forms of nitrogen were observed: pyridinic, pyrrole/pyridine, graphitic and oxidised nitrogen. Pyridine and pyrrolic groups are often considered beneficial for CO_2 uptake as they induce stronger hydrogen-bond interactions between the surrounding C–H bonds and CO_2 molecules [323]. Both of these nitrogen forms exhibit Lewis basic character (Pyridinic-nitrogen donates one electron to aromatic π-system while pyrrolic-nitrogen offers 2 p-electrons), whereas graphitic nitrogen is highly acidic and present at higher urea concentrations. It was concluded that the carbon prepared with a ratio of 1:1:2 would have the most basic nature given it had the largest proportion of pyridinic nitrogen. This was confirmed during the adsorption campaign where the adsorbent (ratio 1:1:2) had a CO_2 uptake of 6.36 $mmol_{CO2}/g$ at 273 K and 1 bar (3.91 mmol and 298 K), owing to the optimal nitrogen-content and narrow micropores (<1 nm) that were shown to be crucial for efficient CO_2 adsorption. The co-hydrothermal treatment of D-glucose and urea followed by KOH activation produced carbons with capacities up to 4.26 $mmol_{CO2}/g$ at 25 °C and 1 bar as a result of its high nitrogen content (6.2–12.17 wt%) and narrow microporosity [353]. The hydrothermal process was conducted at 180 °C for 12 h using 20 g of urea and 20 g D-glucose that were dissolved in 100 ml water. Interestingly, only pyridinic and pyrrolic/pyridonic nitrogen were observed after KOH activation (600 °C–700 °C). Chen et al. [305] employed a combination of urea and KOH in a two stage synthesis protocol, whereby carbonised coconut shell were first mixed with urea in a 1:1 ratio by weight and heated for 2 h at 350 °C and then impregnated with KOH and thermally treated. In this work, the ratio of urea to carbon was kept constant and the activation temperature and KOH ratio were changed. Analyses showed that pyridinic, pyrrolic and quaternary nitrogen were present with pyrrolic-N, the most beneficial for CO_2 capture [247] being the predominant species. The material prepared with activation conditions of 650 °C for 3 h demonstrated a capacity of 4.8 $mmol_{CO2}/g$ at 25 °C and 1 bar, owing to an optimum combination of micropore development and nitrogen content. This phenomenon was confirmed by implementing urea modification after the KOH activation. The sample showed a higher nitrogen content but lacked in the development of porosity and as such

demonstrated a much smaller CO_2 capacity, believed to be the result of pore wall demolition or pore blockage by the abundant nitrogen species during urea modification. Therefore, post-modification with urea is much less advantageous for CO_2 capture than the pre-treatment [305] or simultaneous modification/activation [304]. Examples of urea-modification prior to activation can also be found with alternative reagents such as K_2CO_3 [253,336]; Yue et al. were able to produce carbons with capacities of up to 3.92 $mmol_{CO2}/g$ at 25 °C and 1 bar [253]. It was learned that under relatively mild pyrolysis conditions, unstable amine functionalities would be converted to pyrrole/pyridine and pyridinic-N; above 650 °C or 700 °C part of these would be transformed to quaternary-N. The urea modification *via* post-KOH activation of a carbonaceous precursor (*i.e.* wool) was employed by Li et al. [295]. The authors documented the presence of the four nitrogen-containing groups with pyrrolic being the predominant form. They reported that the introduction of oxygen-containing groups made the material highly reactive for subsequent nitridation with urea, permitting an increase in nitrogen content from 4.14 wt% to 14.48 wt%. SEM analysis showed that although the urea treatment more or less collapsed the structure of the untreated sample, the sponge-like porous structure was maintained. The urea-treated sample was able to capture 2.91 $mmol_{CO2}/g$ at 25 °C and 1 bar, somewhat lower than found in the aforementioned studies [304,305] - perhaps due to the source of carbon or as a result of urea modification after activation. Ma et al. demonstrated the synthesis of N-doped porous carbon with hierarchical porosity *via* the carbonisation of a MOF-5 template (carbon source) and subsequent urea modification [107]. The degassed MOF-5 (1 g) was immersed in 40 mL of a solution that contained urea and ethanol (0.15 mol/L), and then stirred for 3 h at room temperature; the composite was then carbonised at various temperatures (600 °C–900 °C) for 5 h. The temperature of carbonisation determines which type of nitrogen exists in the material, at 600 °C amide; above 700 °C this amide is lost and the species are transformed into protonated graphitic-N, pyridinic-N and oxidised-N species. It was determined that the correlation between micropore surface area, nitrogen content and the SFGs within the carbon and the equilibrium capacity is very much dependant on the adsorption conditions. The highest capacity was seen with the sample prepared at 900 °C (3.71 $mmol_{CO2}/g$ at 0 °C and 1 bar); however, at 25 °C and 1 bar the sample carbonised at 600 °C showed the highest capacity (2.44 $mmol_{CO2}/g$). At lower CO_2 partial pressures, the nitrogen content and the presence of C–OH bonds within the carbon is significant to its performance as demonstrated by the larger presence of N groups in the 600 °C sample when compared to the more porous 900 °C sample.

Zhao et al. have investigated composites of MOFs and animated graphite oxide [354]. The graphite oxide (GO) was produced using Hummers' method which is detailed in the work of Seredych and Bandosz [355]. By dispersing GO (1 g) in a urea solution (0.03 mol/L, 0.15 mol/L and 0.3 mol/L in water) animated GO (GO-U1, GO-U2 and GO-U3, respectively) can be produced. The composites were prepared by simultaneously dispersing/dissolving in the solvent (ethanol) by sonication with a view to introduce 10 wt% GO-U in the composite; the composites were referred to as MOF/GO-U1, MOF/GO-U2 and MOF/GO-U3. The presence of hydroxyl, carbonyl/carboxyl groups were found in GO-U along with epoxy and $–NH_2$ moieties; C–O bonds were shown to be weaker in GO-U supporting the involvement of carboxylic groups in acid-base reactions with urea. The presence of GO-U was not found to prevent the formation of linkages between the copper dimmers and organic bridges (of the Cu-BTC MOF); the d_{002} signal of GO-U was absent and linked to the presence of exfoliated sheets of GO-U in the MOF composites. The MOF-composites exhibited reactions between the carboxylate ligands and amine groups which should leave uncoordinated copper sites that can then coordinate with SFGs from GO-U which can be observed in the imperfect crystals of Fig. 8; alkyl ammonium was present in the FTIR spectra. In Fig. 8 exhibits preferential localisation of copper oxide on the surface of the composites and the deeply embedded graphene phases within the larger crystals along with potentially modified 'micro' MOF units with amine linkages visible as the 'lace--type' structures [354]. The composites demonstrated a 50% increase in porosity *vs* the parent MOF the size of which comparable to the sizes of the acid gas (CO_2) facilitating a capacity of 4.23 $mmol_{CO2}/g$ at ambient temperature. Urea has also been introduced as a seven-membered diazepine ring at the centre of 4,4′-biphenyl-dicarboxylic acid from which four Zn-MOFs can be obtained [356].

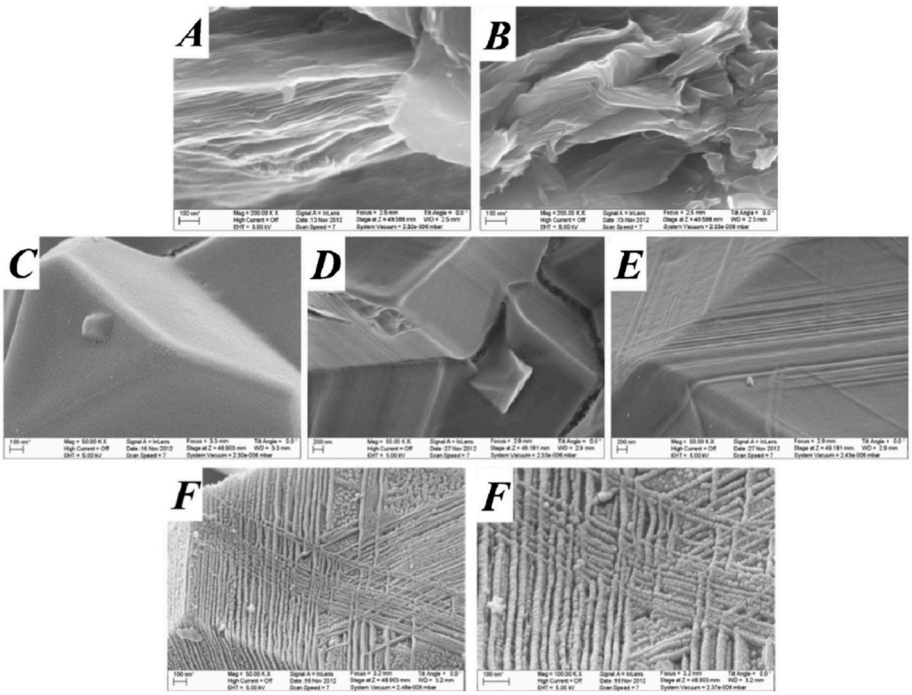

Fig. 8. SEM images of GO-U and their composites with MOF. A) GO; B) GO-U3; C) MOF; D) MOF/GO-U1; E) MOF/GO-U2; F) MOF/GO-U3; D) MOF/GO-U3 [355].

5.5. Iron

A mixture of iron powder and acetic acid was used by Zhang et al. [284] as the second step in a two-step protocol to reduce the nitro groups introduced through nitration of AC with a mixture of H_2SO_4 and HNO_3 to amino groups. Deionised water (250 ml) was mixed with acetic (10 ml) acid followed by the addition of iron powder (5 g). The mixture was refluxed for 15 min to produce ferrous acetate. The nitrated AC (AC-NO_2, 1 g) was added into the system with continuous refluxing for a further hour before cooling to room temperature; superfluous iron was removed using a magnet and aqueous HCl (0.01 N). The two samples were termed AC-NH_2 and AC-NH_2(strong) corresponding to the nitrated samples prepared with 1:1 (acid:water) and just acid in the first step of preparation. FTIR spectra confirmed the conversion of the introduced nitro (NO_2) SFGs into amine (NH_2) groups thus, reinforcing the success of a simple reduction processes. XPS analyses was able to provide more evidence of this whilst also elucidating to the presence of an Fe (2p) peak. Deconvolution of the peaks showed that within the nitrogen SFGs of the aminated samples there existed a strong peak characteristic of amino-type nitrogen associated with the carbon-matrix such as imine, amine and amide without the presence of pyrrolic/pyridonic or pyridine type N found in the nitrated samples suggesting the amino groups are formed primarily from the reduction of nitro groups followed by pyrrolic and pyridonic N. Porous carbon has also been produced from a tannic acid-Fe coordination compound prepared *via* a simple mechanochemical method by Cai et al. [357]. The prepared sorbent (NFePC-10-A) exhibited a capacity of 5.8 $mmol_{CO2}/g$ and 3.4 $mmol_{CO2}/g$ at 0 °C and 25 °C, respectively with an initial Q_{st} of 63.16 kJ/mol. The synthesis followed mixing iron (III) chloride hexahydrate (99 wt%) and tannic acid (TA) at different molar ratios (1:5, 1:10 and 1:15) by grinding; the mixture was then aged for several days at 60 °C. The product was then carbonised (800 °C, 5 °C/min) under nitrogen. The post-activation employed KOH at 800 °C (5°/min) for 1 h. The sorbent possessed sp^2-hybridised graphitic C–C, phenolic/alcoholic groups and carbonyl/quinone groups. The carbons also possessed a narrow PSD primarily between 0.4 nm and 0.7 nm; interestingly, the development of porosity was enhanced by the presence of iron.

5.6. Alkali and alkaline earth metals

The tailoring of electrostatic interaction on the pore surface of porous aromatic frameworks (PAF) by Ma et al. [358] investigated the incorporation of various metal ions in the porous skeleton to tune the electrostatic charge-quadrupole and charge-induced dipole interactions with gas molecules [359]. The POF decorated with carboxylic-rich pores (POF-26-COOH) was synthesised *via* palladium-catalysed Sonogashira-Hagihara cross-coupling reaction and was subsequently modified with various metals. For PAF-26-COOH modified with Li, Na and K, the metal hydroxide (10 mg) was mixed with the PAF (100 mg) in CH_3OH/H_2O (10 ml/10 ml), followed by stirring, filtration, washing and drying. For the Mg modification, 210 μl of magnesium methoxide (7%–8% in methanol) solution was added to a mixture of the PAF (100 mg) and anhydrous methanol (15 ml) followed by stirring, filtration, washing and drying. The magnesium methoxide solution being used to overcome the poor solubility of $Mg(OH)_2$ in CH_3OH or water. PAF-26-COOH was found to be composed of highly conjugated phenyl groups. With the metal-modified samples, –COO groups were found to be linked with metal cations. The protons in carboxyl groups were almost substituted stoichiometrically by the metal ions. The high replacement of these ions (85%) confirms that nearly all of the carboxylic groups in the parent material were available for post-metallisation. The replacement of hydrogen atoms with metal ions leads to a decrease in surface area consistent with an increase in atomic weights of the metals from Li to K. A similar trend was observed for the pore size distribution except for the Mg-modified PAF. The introduction of these metal active centres did improve CO_2 capture performance in terms of both capacity and selectivity. Potassium-based sorbents were prepared by Lee et al. [69] *via* impregnation with K_2CO_3 on various supports such as AC, TiO_2, Al_2O_3, MgO, SiO_2, Al_2O_3, NaX and CsNaX. The method follows adding the support (5 g) into an aqueous solution containing 2.5 g of anhydrous potassium carbonate in 15 ml deionised water followed by mixing drying and calcination at 300 °C (3 °C/min) for 4 h under N_2 flow (100 ml/min). The total CO_2 capacities for the 30 wt% K_2CO_3 impregnated supports were as follows: K_2CO_3/AC = 1.95 $mmol_{CO2}/g$; K_2CO_3/TiO_2 = 1.89 $mmol_{CO2}/g$; K_2CO_3/MgO = 2.7 $mmol_{CO2}/g$; K_2CO_3/Al_2O_3 = 1.93 $mmol_{CO2}/g$. All but the MgO sorbent demonstrated a capacity 90% of the theoretical maximum. The adsorption was carried out with 1 %vol concentration of CO_2 at 60 °C. the four aforementioned sorbents could be regenerated at 150 °C, 150 °C, 350 °C and 400 °C, respectively.

Impregnation of carbons with basic metals and their oxides has been shown to improve their adsorptive performance [7]; both metal oxides and their hydroxides too, have been demonstrated to enhance basicity, surface area and the potential for carbonate formation [360,361]. Creamer et al. [362] investigated a number of composites from hickory wood namely, aluminium hydroxide, magnesium hydroxide and iron hydroxide. The optimum was found with aluminium at a ratio of 4:1 ($AlCl_2$:cotton wood) and exhibited a capacity of 1.61 $mmol_{CO2}/g$. Copper and zinc have been exclusively studied by Hosseini et al. [363] producing sorbents with capacities up to 2.25 $mmol_{CO2}/g$ at 30 °C and 100 kPa. The acid modified carbons (HNO_3) possessed a number oxygen SFGs which aided in the deposition of the metals; the ratio of which were varied between 4% and 20% (Cu/Zn). The metal ions from the impregnated $Cu(NO_3)_2$ and $ZnSO_4$ *via* aqueous ion exchange were found to link with the negatively charge groups thereby forming metal complexes [363], the increased presence of O-SFGs being highly favourable. The deposition of the metals is itself considered an ion exchange reaction whereby hydrogen ions on the surface of the carbon are replaced by copper [364]; the negatively charged SFGs on the carbon surface and the now Cu-loaded surface are then surrounded by Zn^{2+} ions. These Zn^{2+} ions are adsorbed on the surface and can diffuse hence, facilitating the reduction of these ions at more favourable positions [363]. Lahijani et al. investigated the impregnation of biochar with various metal compounds, namely: Mg, Al, Fe, Ni, Ca and Na [365]. The single-step 90 min pyrolysed walnut shell (500 °C–900 °C) were mixed with a solution of each metal's nitrile salt (5 wt%, 80 ml deionised water) and aged for 12 h and subsequently heated to 500° under nitrogen. All bar the sodium impregnated sample demonstrated improved CO_2 capacities in the order of Mg, Al, Fe, Ni, Ca, biochar, Na; the highest capacity observed was 1.82 $mmol_{CO2}/g$ at 25° and 1 bar. It was identified that the formation of basic MgO sites enhances the interactions of CO_2 with the basic oxygen in the O^2–Mg^{2+} bonds thereby forming carbonates (CO_3^{2-}) [366,367]. The MgO sites form from the magnesium nitrate hexahydrate which dehydrates to the anhydrous salt $Mg(NO_3)_2$ between 110 °C and 190 °C; over 400 °C these decompose to MgO. The formation of carbonates is an additional avenue that is seeing increased focus especially in the context of producing adsorbents from waste such as wood ash, biomass ash, coal ash, solid refuse fuel ash and steel slag to name a few [368–372]; the process of carbonation however and the methods to improve such are not within the scope of this review.

5.7. Amines

There are three main classes of amine supported sorbents in the existing literature [108,373]: physically impregnated amines into or onto porous supports *via* mixing the amine with the support using an additional solvent [154,162,374]; covalently bonded amines of the silane group [92,254,375]; and *in-situ* polymerisation of an amine-containing precursor [376,377].

5.7.1. Tetraethylenepentamine – TEPA

TEPA has been shown to be one of the most effective amines for improving the CO_2 capture performance of carbonaceous adsorbents

[155,227,228,378]. Wang et al. [155] modified waste wood ashes with a number of polyamines (TEPA, MEA, DEA, PEI and DETA) to selectively capture CO_2 at 60 °C. The TEPA-modified sorbent demonstrated the longest breakthrough time and a corresponding equilibrium capacity of 1.76 $mmol_{CO2}/g$ with a 92.6% regeneration conversion. It is worth noting that although the TEPA modified sorbent had the largest capacity, the efficiency of the impregnated amine (a function of amine molecular weight, capacity, amine loading and number of nitrogen atoms) was higher for the DEA-modified sorbent. The TEPA loading was varied between 14.66 wt% and 72.04 wt% in an attempt to identify the optimum loading for CO_2 capture. An increase in the content of TEPA was learned to affect the dispersion of the amine and thus, the number of available active sites. The capacity of the adsorbent first increased and then decreased when increasing the amine loading, with the optimum at 45 wt% (2.02 $mmol_{CO2}/g$). The bentonite activation using H_2SO_4 employed by Wang et al. [286] facilitated the development of an MBS, whereby TEPA was introduced into the support *via* wet impregnation. TEPA (3 g) was dissolved in ethanol (30 g) under 30 min of stirring; the sulphuric acid modified bentonite was then added and stirred for 3 h at room temperature. Various TEPA loadings were evaluated (10 wt% - 60 wt%) to identify an optimum. It was deduced that the maximum TEPA loading capacity was 50 wt% which also corresponds to the largest CO_2 capacity of 3.07 $mmol_{CO2}/g$ and highest amine efficiency of 0.23 mol_{CO2}/mol_{amine} at 75 °C adsorption temperature; this could have been further improved when considering the maximum theoretical amine efficiency of 0.5 by facilitating more effective CO_2 diffusion [286]. At 30 °C, both capacity and amine efficiency are reduced due to the decrease in CO_2 diffusion, reducing the ability of CO_2 to be retained *via* chemisorption. Increasing adsorption temperature can aid in the adsorbate overcoming the kinetic barrier and reduce diffusional resistance but there is an obvious trade-off in that, at elevated temperatures the effect of steric hindrance is slim and the thermodynamics of adsorption take precedence [379]. Interestingly, in the presence of moisture (up to 18 vol%), both capacity and amine efficiency increased to 3.84 $mmol_{CO2}/g$ and 0.29 mol_{CO2}/mol_{amine}, respectively - indicating the formation of not only carbamate but bicarbonate [286]. The TEPA modification of an ACF was carried out alongside KOH modification by Chiang et al. [307]. In this work, ACF was soaked with a liquor of TEPA solution (10 wt% in alcohol with a ratio of 0.07 g/ml). The mixture was sonicated for 90 min at 60 °C and then dried after which is was treated at 500 °C (10 °C/min) for 1 h under N_2 and named nACF. TEPA modification was shown to decrease the BET surface area and both total and micropore volumes as a result of total or partial blinding of micropores by N-functionalities [380]. Amine groups that do not possess a silanol anchoring group such as TEPA are believed to react with surface hydroxyl groups to form hydrogen bonds [381]. The grafted TEPA possesses a long-chain structure and as such can hinder the gas molecules access to pores; if the TEPA is attached within the pores then it would act to reduce the available adsorption sites; based on characterisation data TEPA modification would block half of the macropores and close a quarter of the micropores. XPS spectra confirmed a negligible increase in nitrogen content after modification. This could be a result of the high temperature treatment (500 °C). Deconvolution of the XPS spectra highlighted the presence of 5 nitrogen SFGs namely: pyrrolic/pyridonic-N > pyridine-type N > quaternary-N > pyridine-N-oxides > nitro groups. The CO_2 capture capacity was demonstrated to be 1.61 $mmol_{CO2}/g$ - lower than that of both the unmodified AC and KOH modified AC. TEPA has also been grafted onto MOFs. In the work of Cao et al. [382], 0.8 g of Mg_2(dobc) was dispersed in 30 ml anhydrous toluene which saw the addition of TEPA in ratios of 30 wt%, 40 wt% and 50 wt% (TEPA/Mg_2(dobc)) and reacted under reflux for 12 h. The MOF structure was maintained throughout the modification; however, an increase in pore filling was seen as the TEPA concentration increased. The observed capacities were 4.49 $mmol_{CO2}/g$ and 6.06 $mmol_{CO2}/g$ for the 30 wt% and 40 wt% samples, respectively. The capacity decreased to 3.48 $mmol_{CO2}/g$ at 50 wt% as a result of pore blockage. Conversely, the rapid synthesis of Al fumarate MOFs impregnated with TEPA [379] demonstrated an optimum capacity (4.1 $mmol_{CO2}/g$ at 75 °C and 1 bar) with a TEPA loading of 60 wt% and the loss of just 2.81% of the capacity after 10 cycles. A study by Wang et al. was able to demonstrate enhancements in the adsorption of CO_2 in TEPA-functionalised sorbents, specifically MCM-41 when co-functionalised with polyetheramine [383]. The co-dispersion of polyetheramine and TEPA within the support provided the sorbent with good physisorption performance at low temperatures and effective chemisorption at 60 °C. The breakthrough time and equilibrium adsorption capacity were 14 min and 3.58 $mmol_{CO2}/g$ at 30 °C, and 12 min and 3.09 $mmol_{CO2}/g$ at 60 °C, all significantly increased with respect to TEPA individually functionalised MCM-41.

5.7.2. Triethylenetetramine – TETA

The triethylenetetramine (TETA) and TEPA modification of bagasse sourced AC by Wei et al. [384] employed either $ZnCl_2$ or KOH for activation evaluated CO_2 adsorption at 60 °C and 0.15 bar. The modification follows mixing the AC (500 mg) with pure water (50 ml) and the desired amount of amine. The mixture was then stirred at 150 rpm and 30 °C for 6 h to produce sorbents with amine mass fractions of between 5 wt% and 50 wt%. An optimum capacity of 3.49 $mmol_{CO2}/g$ was achieved with 5 wt% TETA modification, less than the TEPA modified counterpart (3.62 $mmol_{CO2}/g$). Both TETA and TEPA have also been impregnated in pore-expanded mesoporous silica KIT-6 [385]. Similarly, TETA modification underperformed when compared (1.87 $mmol_{CO2}/g$ vs 2.9 $mmol_{CO2}/g$) to TEPA attributed to the availability of amine groups, TEPA possesses one more than that of TETA [385]. Mei et al. studied the effect of mixed amine functionalisation namely, 3-[2-(2-Aminoethylamino)ethylamino]propyl-trimethoxysilane (*via* grafting) and TETA (*via* impregnation) on KIT-6. An optimum loading of 30 wt% TETA and 1:1 ratio of the grafted amine:KIT-6 facilitated a capacity of 2.063 $mmol_{CO2}/g$ losing only 3.54% of this after 5 cycles. SBA-15 and expanded SBA-15 (SBA-15 k) have also been modified with TETA [386]. A peak capacity was reached with a 30 wt% loading for both SBA-15 and SBA-15 k – 0.97 $mmol_{CO2}/g$ and 1.53 $mmol_{CO2}/g$ respectively (60 °C and 0.15 bar).

5.7.3. (3-Aminopropyl)triethoxysilane – APTES

Dindi et al. [229] functionalised coal FA-derived cancrinite-type zeolite with DEA and MEA *via* impregnation and APTES *via* grafting. The morphology of the acicular particles was mostly unchanged after functionalisation, although properties such as surface area, pore size and pore volume saw significant change as a result of pore blockage. The CO_2 capacity of the APTES grafted sample was shown to be 0.15 $mmol_{CO2}/g$ at 25 °C - only 0.02 mmol greater than the unmodified sample. This rose to a maximum of 0.55 $mmol_{CO2}/g$ at 80 °C. The observed increase is due to the kinetically diffusion-controlled process of CO_2 adsorption that at high temperatures, facilitates the transport of CO_2 into the porous network where it can react with the amino group. The pore blockage effect was further reinforced when Dindi et al. studied the effect of amine loading on the APTES sorbents capacity: from 20 wt% – 30 wt%, the capacity increased but beyond 30 wt%, the capacity dropped, owing to the blockage of pores within the cancrinite thus, stopping the exposure of CO_2 molecules to NH groups [229]. The capacity of the impregnated samples was significantly higher than APTES grafting due to the higher density of amine present within the porous structure. The APTES molecules, however, only join the Si–O–Si groups on the pore walls thus, lowering the amino group density. A combination of APTES grafting and TEPA impregnation has also been employed by Zhang et al. [387] when functionalising mesoporous silica molecular sieves with a view to overcome the amine agglomeration phenomenon. Capacities up to 5.7 $mmol_{CO2}/g$ were achieved which decreased to 5.2 $mmol_{CO2}/g$ after 15 cycles. The grafted APTES and residual P123 in the support provided spatial partition structures and hydrogen bonding functional groups for the dispersion and fixation of TEPA [387]. Mesocellular foams derived from mesoporous silicas have also been functionalised

with APTES [388]. Vilarrasa-García et al. prepared four adsorbents based on SBA-15 prepared from tetraethyl orthosilicate (TEOS) with and without trimethyl-benzene (TMB) and *n*-heptane as swelling agents and adding ammonium fluoride as a solubility enhancer in some cases. The grafting of APTES followed mixing the support (0.7 g) with a solution of APTES (20 vol% – 60 vol%) in dry toluene (35 ml) and refluxing under He (110 °C) for 12 h. An abundance of silanol groups was found, essentially lining the interior surface of the mesoporous channels which ensures an optimal anchoring of the amino groups [388]. When increasing APTES content, an increase in aminopropyl groups was observed; the Si–OH stretching disappears in the functionalised silicas suggesting the majority of the isolated terminal silanol groups had reacted with the ethoxy groups of APTES. Immobilised APTES on zeolite-β facilitated a capacity of 4.7 $mmol_{CO2}/g$ at 60 °C *via* both carbamate and bicarbonate mechanisms [83]. Aminosilanes (*e.g.* APTES) can react with surface hydroxyl groups and form stable Si–O–Si bonds where the functional amine catalyses the reaction [389]. The silicon anchoring group of APTES was learned to form stable covalent bonds on the surface of the support promoting good stability over nine cycles and various process conditions (up to 150 °C). The amine was dissolved in anhydrous toluene (15 ml) to produce loadings of between 10 wt% and 80 wt% with the optimum at 40 wt%. APTES, polyethyleneimine (PEI) and ethylenediamine (EDA) functionalisation of ZIF-8, GO and their composites (ZIF-8/GO) has been evaluated by Pokhrel et al. [390]. The APTES modification of GO followed dispersing GO (200 mg) in deionised water (200 ml) with sonication followed by adding APTES (2 ml) with sonication for 1 h and stirring for 24 h. The ZIF-8 functionalisation required mixing the ZIF-8 (200 mg) with toluene (30 ml) to which APTES (0.25 ml) was added, stirred and refluxed (70 °C) for 5 h. The composites (ZIF-8/GO) were first activated and then post-functionalised in either toluene as with the ZIF-8 functionalisation or water as with the GO functionalisation. An alternative method was also employed by synthesising the composites through *in-situ* MOF growth on pre-functionalised GO (ZIF-8/(*f*-GO)).

5.7.4. (3-aminopropyl)trimethoxysilane – APTMS

A series of primary, secondary and tertiary aminosilica sorbents were prepared by Ko et al. [266] by immobilising APTMS, [3-(methylamino) propyl] trimethoxysilane (MAPTMS) and 3-(diethylamino) propyl] trimethoxysilane (DEAPTMS) on SBA-15. The amine immobilisation followed mixing the amine (25 mmol) with SBA-15 (2 g) in anhydrous toluene (150 ml) and then aging for 24 h at 25 °C, the procedure was repeated three times with rinsing (ethanol and/or toluene) each time. It has been suggested that the nitrogen in APTMS may be predominantly hydrogen bonded to surface silanol groups, in a protonated form or acting as a five-coordinate species with the surface silicon atoms [266]. Capacities of 0.95 $mmol_{CO2}/g$, 0.75 $mmol_{CO2}/g$ and 0.17 $mmol_{CO2}/g$ were achieved with the 1°, 2°, and 3° amines, respectively. Energy consumption for desorption was in the order of 3°, 2° and 1° whereas adsorption amount and bonding affinity was in the reverse order. Porous silica gels have also been functionalised with APTMS although the maximum capacity here was 0.67 $mmol_{CO2}/g$ [391]. The effect of APTMS functionalisation on mesoporous ceria nanoparticles (MCNs) was investigated by Azmi et al. [106]. The MCNs were prepared by the sol-gel method using cetrimonium bromide, water, cerium chloride and aqueous ammonia solution. The amine functionalisation was carried out *via* impregnation using APTMS (0.467 g) dissolved in distilled water (250 ml). MCN (4 g) was added to the solution under continuous stirring for 3 h at 343 K and then dried over night at 383 K and ground into a powder. FTIR spectra elucidated to the presence of hydroxyl groups along with the stretching of various bands such as H–O–H, Si–O and $–NH_2$. Pyrrole adsorbed FTIR spectroscopy was employed to assess the O^{2-} basicity of the samples. The modified sample demonstrated a less intense spectra, possibly due to the decrease in basicity after impregnation but also perhaps due to the hindrance of adsorption as a result of APTMS being present within the structure. CO_2-adsorbed FTIR was able to indicate the reactions that take place between CO_2 and oxygen basic, oxygen vacant and hydroxyl sites on the MCNs. The products of these reactions are various carbonates such as bidentate, monodentate, polydentate and hydrogen carbonate as well as carbamates formed from the interaction of NH groups and CO_2. The APTMS modified sample showed a 10-fold increase in CO_2 capture performance, 0.04 $mmol_{CO2}/g$ to 0.44 $mmol_{CO2}/g$ at 1 atm and 298 K which equates to 10.08 $\mu mol_{CO2}/m$. Grafting APTMS onto hierarchical Linde Type A (LTA) zeolite has been demonstrated by Nguyen et al. to produce more highly performing sorbents than aminosilicas such as SBA-15 and MCM-41 [392]. Silicas (mesoporous) tend to have thick pore walls that have no influence on the adsorption of CO_2, zeolites however can actively participate in the adsorption of CO_2. The implication is that LTA zeolite containing alkylamine-functionalised mesopore domains can outperform conventional aminosilicas since both the zeolite active sites and the amine groups can capture the CO_2 [392]. The amines (APTMS or N-[3-(trimethoxysilyl)propyl]ethylenediamine (TMPED)) were grafted post-synthetically after ion-exchange with Ca^{2+} ions: LTA zeolite (1 g) was dispersed in toluene (100 ml), the amine (5 ml) was then added and stirred for 24 h at room temperature. Capacities up to 2.3 $mmol_{CO2}/g$ at 60 °C and 0.15 bar were achieved with successful regeneration at 150 °C losing just 0.1 mmol capacity over 10 cycles.

5.7.5. Piperazine – PZ

Fashi et al. [373] modified 13× zeolite with piperazine (PZ) *via* wet impregnation. These researchers mixed the dried zeolite with 1 wt% - 4 wt% PZ concentrations. The impregnation solutions were composed of PZ and methanol (i.e. 1 wt% PZ was produced with 1 g PZ and 99 g methanol). The solution was added to the zeolite (5 g) and mixed for 2 h at 35 °C and then filtered, washed, and dried. The CO_2 capture performance was evaluated over a range of operating conditions such as pressure, temperature, particle size and PZ concentration, where one parameter was varied whilst the others maintained (*i.e.* linear optimisation). The greatest adsorbent capacity was demonstrated at 25 °C, 8 bar, 1 g of adsorbent at a size of 200 μm and a PZ concentration of 2 wt%: 5.5 $mmol_{CO2}/g$. A nanocomposite of multi-walled carbon nanotubes (MWCNTs) and MOF-199 denoted as CNT@MOF-99 has also been impregnated with PZ at various amounts (10 wt% to 30 wt%) [393]. In spite of a decrease in surface area, pore size and pore volume, the functionalised composite exhibited a higher adsorption capacity and selectivity than the unmodified counterpart due to an improved affinity between CO_2 and the amine sites. Wet impregnation of PZ was employed whereby PZ (*i.e.* 0.05 g for the 10 wt% sample) was dissolved in ethanol (5 ml) under 15 min of stirring after which the CNT@MOF-199 (0.5 g) was added and mixed at 500 rpm for 2 h. The obtained sorbents were termed CNT@MOF-199/10PZ, CNT@MOF-199/20PZ, and CNT@MOF-199/30PZ for 10 wt%, 20 wt%, and 30 wt% PZ, respectively. Fig. 9 exhibits the SEM images of the MOF-199 products; Fig. 9(b) and (c) exhibit the tubular MWCNTs on the MOF surface. Fig. 9(d), (e) and (f) clearly show that very little PZ can be observed on the external surface, the majority must be deposited or dispersed within the pores without destroying the MOF structure. Increasing PZ content increased CO_2 uptake and reduced CH_4 uptake. The PZ was incorporated on the Cu^{2+} cation sites exposed in the framework, the shorter length of the PZ molecule compared to the distance between two adjacent metal sites led the authors to assume that one amine from each PZ molecule was bound to a single metal site – the other amine was free to interact with the gas molecules [393].

5.7.6. Methyl-diethyl-amine – MDEA

In the work of Xue and Liu [394] mesoporous silica (SBA-15) was modified with methyl-diethyl-amine (MDEA) and piperazine (PZ). SBA-15 was synthesised by a direct hydrothermal method [395], using tetraethyl orthosilicate (TEOS) as the silica source and Pluronic P123 as a template. The modification was carried out *via* impregnation. The amines were dissolved in acetone and then dried. SBA-15 was added into

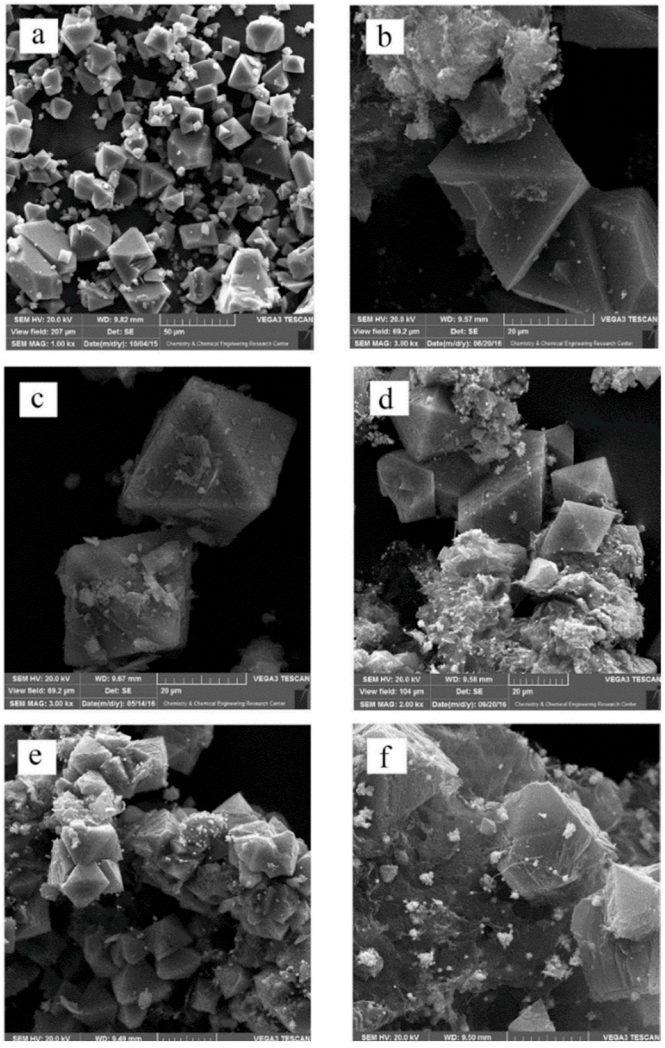

Fig. 9. SEM images of (a) MOF-199; (b and c) CNT@MOF-199; (d) CNT@MOF-199/10PZ; (e) CNT@MOF-199/10PZ; and (f) CNT@MOF-199/30PZ [393].

the solution, stirred and refluxed for 6 h. With an increase in amine concentration a reduction of pore size was observed (6.8 nm–4.8 nm) whilst maintaining a narrow pore size distribution. At a loading ratio of 0.8 (wt.% of loaded amine) the separation factor reached a maximum. This was seen to increase dramatically when a combination of MDEA and PZ were impregnated, possibly a consequence of the faster rate of reaction with PZ acting as an activator. The sample modified with MDEA and PZ demonstrated a capacity of 1.36 $mmol_{CO2}/g$ at 25 °C and could be regenerated at the same temperature with a relatively good cyclic stability. More recently, de Ávila et al. [396] have introduced MDEA, MEA and DEA into SBA-15. The sorbent was prepared by adding MDEA to an acetone suspension of SBA-15 at either a 1:1 or 1:2 wt proportion and stirring. MDEA was the amine that presented the best optimisation of the support for CO_2 capture with efficiencies up to 99.1% with a 1:2 wt ratio.

5.7.7. *Monoethanolamine – MEA*

Monoethanolamine (MEA), the benchmark solvent used in the process of chemical absorption for CO_2 capture [397], has naturally found itself used for the purpose of adsorbent modification. Mercedes Maroto-Valer et al. [231] employed both steam activation (850 °C) and impregnation with different amine compounds (MEA, MDEA, and DEA) on FA-derived carbons. It was deemed that an activation temperature of 850 °C and a hold time of 90 min were most effective at enhancing the pore development. When coupled with the impregnation of MEA, the sample demonstrated an adsorption capacity of 1.56 $mmol_{CO2}/g$ at 30 °C. When compared to the purely activated sample which had a capacity of 0.95 $mmol_{CO2}/g$, the reduction in pore volume and surface area is compensated by the nature of MEA. A primary alkanol amine that is demonstrated to have higher absorption rates in aqueous systems than secondary and tertiary amines. MEA-modified attapulgite based amorphous silica sorbents were prepared *via* the wet impregnation method by Li et al. [398]. Here MEA (3 g) was dissolved in 30 ml methanol, followed by the addition of 10 g a-SiO_2 powder. Different MEA loadings were evaluated: 9.1 wt%, 23.1 wt%, 33.3 wt% and 37.5 wt%. The highest capacity was observed for the sample prepared with 33.3 wt%, 2.14 $mmol_{CO2}/g$ at 60 °C. MEA along with benzylamine (BZA – primary cyclic amine) and N-(2-aminoethyl) ethanolamine (AEEA – secondary diamine) have been impregnated on a MCM-41 in the work of Mukherjee et al. [399]. The functionalisation was such that 20 wt% - 60 wt% loadings were achieved by adding an amount of amine to methanol (12 ml) followed by aging and drying. At 25 °C and 1.07 bar the MEA modified sample (50 wt%) demonstrated a capacity of 1.47 $mmol_{CO2}/g$, less than the 2.34 $mmol_{CO2}/g$ demonstrated by the 40 wt% AEEA-modified sample. Kongnoo et al. were able to demonstrate MEA and DEA impregnation of palm shell AC [400]. Micropore volume dropped by 52% when impregnated with MEA; at atmospheric pressure and 70 °C the capacity for the MEA sample was 1.48 $mmol_{CO2}/g$, less than the DEA sample due to pore blockage. The difference in capacity (between MEA and DEA modified sorbents) was 16.2% at 150 kPa, at 500 kPa it reduced to 6.4% as steric hindrance is less significant. The blockage of pores however, resulted in mass transfer hindrance and longer desorption times. Capacities up to 2.07 $mmol_{CO2}/g$ have been achieved by Kamarudin et al. on an agro-based kenaf adsorbent (*Hibiscus cannabinus* L.) [401]. Several amines were investigated (MEA, DEA, MDEA, AMP, PEI, DETA, TETA, TEPA, diisopropylamine (DIPA), pentaethylenehexamine (PEHA), triethanolamine (TEA) and diglycolamine (DGA)) *via* an incipient wetness impregnation technique reported by Chatti et al. [402] where dried kenaf leaf was mixed in methanol in a solid to liquid ratio of 1:20 (by weight); the amine was mixed with methanol and stirred for 20 min after which the kenaf solution was added and stirred for 15 min. The initial amine concentration was 50 wt %, the combined solutions were agitated for 5 h at 600 rpm. Fig. 10 exhibits the surfaces of the impregnated support, some of which are full of cavities and some demonstrate serrated ad uneven ridge surfaces that lead to partially blocked pores [401]. The combination of primary ($-NH_2$) and secondary (-NH) amines gives more advantages for CO_2 adsorption than a single class as shown with the TEPA modification which possess two primary classes and three secondary. The four methyl groups ($-CH_3$) in DIPA was also learned to enhance the supports basicity and therefore capacity. Primary amines such as MEA and DGA showed higher capacities than AMP due to the steric character of AMP that reduced the stability of the carbamates and hence capacity [401], the same is true for MDEA and TEA.

The capacities of each functionalised sorbent can be seen in Fig. 11. When increasing the amine loading to a ratio of MEA:kenaf to 1:1 capacity can be improved to 2.07 $mmol_{CO2}/g$ dropping to 1.72 $mmol_{CO2}/g$ after the 10th cycle. A rapid reduction in capacity was observed after the first three cycles due to the chemisorption mechanism; the energy required to break the covalent bond is higher than for the raw kenaf leaf.

The proposed mechanism can be seen in Fig. 12; the authors identified a decrease in regeneration values when adsorbate-adsorbent interaction strength increased. The basic active sites on the sorbent depends on the relative content of nitrogen, TEPA has more attached to the main ligand than MEA causing a higher pH value. The energy needed to break the covalent bond is hence larger for TEPA than for MEA [401] which explains the regeneration efficiency of TEPA (75.62%) being lower than for MEA (82.15%).

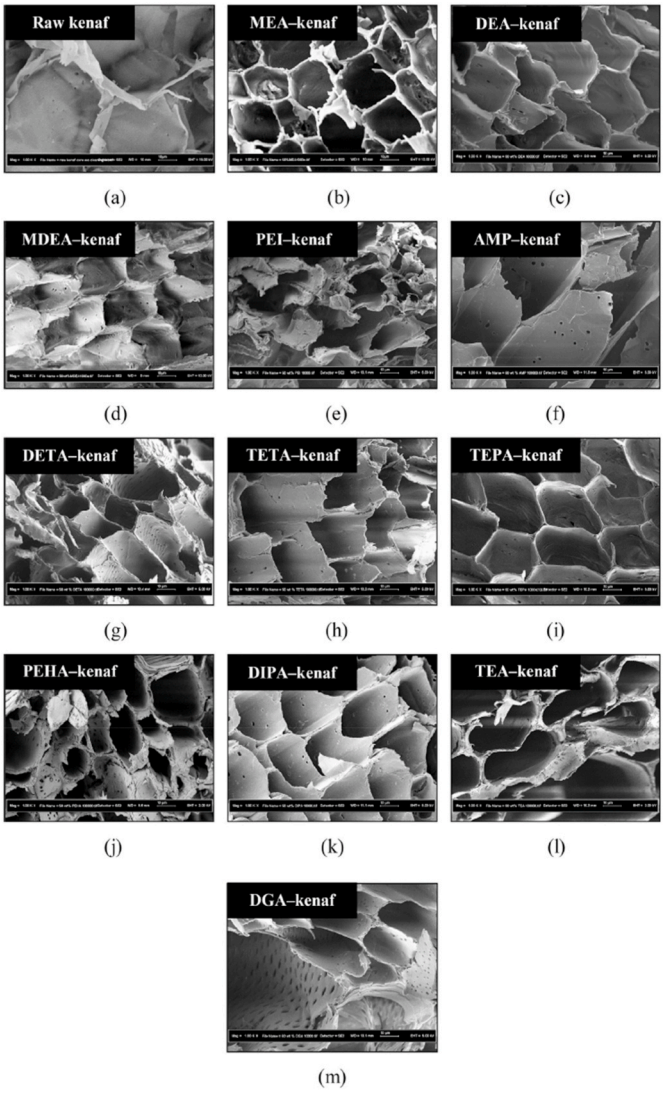

Fig. 10. FESEM microscopy of the amine-functionalised kenaf [401].

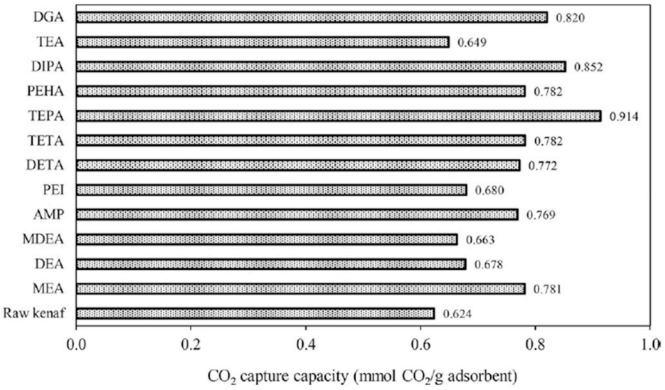

Fig. 11. CO2 adsorption capacity of raw kenaf and amine-functionalised derivatives (50 wt% loading) [401].

5.7.8. *Diethanolamine – DEA*

Diethanolamine (DEA) has been introduced into porous silica in the work of Franchi et al. [403]. Pore-expanded MCM-41 silica (PE-MCM-41) was synthesised using Cab-O-Sil M5 fumed silica *via* a two-step procedure and impregnated with DEA. The DEA was added in various amounts to distilled, deionised water followed by the addition of various amounts of the support. The largest amount of DEA that could be retained by the support is achieved by pore saturation. A capacity of 2.65 $mmol_{CO2}/g$ was achieved with a DEA loading of 7.26 $mmol_{DEA}/g_{adsorbent}$ (5% CO_2 in N_2). At higher DEA concentrations, film diffusional resistance became a limiting factor for the CO_2 uptake kinetics although the performance of these sorbents was higher than that of zeolite 13×. In a study by Ahmed et al. [404], siliceous mesoporous silica MCM-41 was impregnated with MEA, DEA and TEA. The functionalisation followed a procedure reported by Ramli et al. [405], whereby the amines were mixed with methanol (10 g), stirred and added to the MCM-41 (2 g). The concentration of the amines was chosen to be 50 wt% based on the optimum loading of MEA which corresponds to near total pore filling. At 25 °C and 1 bar the capacity was demonstrated to be 0.89 $mmol_{CO2}/g$ for the MEA-MCM-41 and 0.80 $mmol_{CO2}/g$ and 0.63 $mmol_{CO2}/g$ for DEA and TEA MCM-41, respectively. The DEA molecule has a larger structure compared to MEA since two alkyl groups are linked to the central nitrogen atom thus, highlighting that steric hindrance plays a significant role in determining the CO_2 capacity. Conversely, in the case of carbons, Kongnoo et al. [400] demonstrated that DEA impregnated palm shell derived AC could outperform the MEA counterpart. The DEA sorbent demonstrated a capacity of 5.3 $mmol_{CO2}/g$ at 400 kPa and 70 °C or 2.81 $mmol_{CO2}/g$ at atmospheric pressure. The amine impregnation reduced micropore surface areas by 52% for the MEA AC but only 11% in the DEA AC resulting in more hindered mass transfer. The functionalisation of mesoporous γ-alumina with DEA by Castellazzi et al. [406] achieved capacities in the range of 0.27 $mmol_{CO2}/g$ to 0.63 $mmol_{CO2}/g$. It was learned that an increase in DEA loading would increase CO_2 capacity, but the correlation was far from linear. This was concluded to be a result of: 1) strong interactions between the support and DEA limited the amount of 'free' amine sites for CO_2 adsorption; and 2) the formation of urea linkage which hindered the accessibility of chemisorption active sites particularly in dry conditions and samples with high DEA content [406].

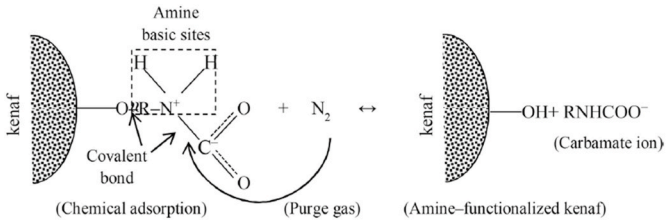

Fig. 12. Proposed desorption mechanism of amine-functionalised kenaf [401].

5.7.9. *Diethylenetriamine – DETA*

MCM-41 has seen the introduction of DETA alongside TETA and AMP in the work of Wei et al. [407]. The modification followed a method of impregnation adapted from Liu et al. [408], where the amine (2 ml) was dissolved in ethanol (20 ml) followed by the addition of the MCM-41 (2 g) and subsequent removal of the ethanol. The DETA modified sample demonstrated the highest pore volume (0.012 ml/g) and surface area of the impregnated sorbents (8.1 m^2/g) and the second highest nitrogen content (10.6 wt%) compared to the TETA sample (14.8 wt%). All impregnated samples showed stability up to 110 °C. The capacities and breakthrough times followed the order of TETA > DETA > AMP. TETA demonstrated a capacity of 2.22 $mmol_{CO2}/g$ at 60 °C followed by 1.87 $mmol_{CO2}/g$ and 1.14 $mmol_{CO2}/g$ for the DETA and AMP modified samples, respectively. This observation was deemed a direct result of the quantity of amino groups present in the impregnated samples and highlights that impregnation is a good tool for the introduction of amino groups without the need for secondary pollution associated with toluene that is used when grafting. Similarly, Zhao et al. [409] evaluated various amines for the amination of graphite oxide (GO) based on the intercalation reaction of GO with amines including EDA, DETA and TETA. The

GO was synthesised following a method detailed by Kovtyukhova [410] using graphite powder, H_2SO_4, $K_2S_2O_8$, P_2O_5, $KMnO_4$ and H_2O_2. The introduction of the amine was achieved by adding 20 ml EDA, DETA or TETA into an aqueous solution of GO under vigorous stirring and refluxing for 24 h at 80 °C. The oxidation of graphite creates oxygen containing SFGs which includes carboxyl, hydroxyl, epoxy groups and *etc.* The insertion of amine moieties to the internal space of GO is attributed to the interaction between amines and oxygen SFGs such as hydrogen-bonding interactions, protonation of the amine by weakly acidic sites of the GO layers and chemical grafting of the amine to GO *via* nucleophilic substitution reactions of the epoxy group [411]. It was identified that given the excess of amines relative to epoxy groups, it would be unlikely there would exist more unreacted sites for intercalation of a monofunctional amine vs polyfunctional [412]. However, the elemental analysis showed that GO/EDA had the highest nitrogen content. This arises from the respective chain length of each amine. Shorter chain amines will intercalate the layers of GO more readily and react with oxygen SFGs, whereas longer chains may cause blockage and hinder further intercalation. Chain length order follows EDA < DETA < TETA and thus, nitrogen content follows EDA > DETA > TETA. With amine modification, a number of primary and secondary amines are present. These are readily able to react with CO_2 *i.e.* the more of these sites that are present the higher the capacity as demonstrated by the capacities which followed GO/EDA > GO/DETA > GO/TETA or 1.22 $mmol_{CO2}/g$ > 1.10 $mmol_{CO2}/g$ > 0.99 $mmol_{CO2}/g$ at 30 °C and 0.15 mol % CO_2 in N_2. DETA impregnated mesoporous silicas were shown to capture 2.89 $mmol_{CO2}/g$ by Jiao et al. [413] although this was less than the TEPA modified equivalent; postulated to be a result of the increasing strength of interaction between amine and Si–OH bonds as the amine molecular weight increases [407]. Post-synthesis modification of POPs by Li et al. [414] produced DETA-modified sorbents with capacities up to 4.5 $mmol_{CO2}/g$ at 1 bar and 273 K (3.4 $mmol_{CO2}/g$ at 298 K) and an IAST selectivity of 194. The low-cost silica gel impregnation with DETA by Martín et al. [415] followed dissolving the amine in methanol (7 g) and adding the silica gel (3.5 g), stirring for 30 min and then drying for 17 h. Although the capacities were unremarkable the authors were able to demonstrate fast kinetics and relatively stable cyclic performance. Regeneration could be achieved completely at 60 °C which may be a limiting factor if this sorbent were to be used in the post-combustion context. Similar cyclic stability was found by Liu et al. in the DETA impregnation of acid-activated sepiolite [237]. The amine (DETA) was dissolved in methanol (20 g) after which the support (4 g) was added.

Fig. 13 illustrates the pore structure when increasing DETA loading, initially (0 g–0.2 g DETA per 1 g sepiolite) capacity decreases due to a decline in physisorption as the micropores and their necks are blocked as shown in Scheme I and II of Fig. 13. Increasing the loading to 0.8 capacity reaches a maximum of 1.65 $mmol_{CO2}/g$ (35 °C) indicating the predominance of chemisorption mechanisms due to the multiple layers of DETA (scheme III). Further increases to amine loading (1 g:1 g) result in capacity reductions (scheme IV) as when the pores and external surface are saturated with DETA CO_2 diffusivity is restrained.

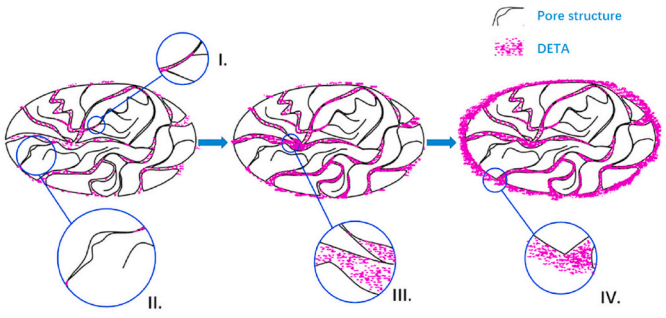

Fig. 13. Schematic diagram of the pore blocking process in sepiolite particles by DETA: I) Surface area reduction due to micropore blockage; II) Surface area reduction due to pore neck blockage; III) Multiple-layer DETA films; IV) Sepiolite particle covered by DETA [237].

5.7.10. 3-Chloropropylamine hydrochloride (CPAHCl)

An amine salt, 3-Chloropropylamine hydrochloride, was used in the chemical treatment of carbon-enriched FA concentrates to increase the nitrogen content of the FA, specifically for CO_2 capture performance enhancements [416]. The FA (10 g, 9.5% unburned carbon) was treated with 500 ml 1×10^{-3} M3-CPAHCL salt solution with and without 1×10^{-2} M KOH for 1 h at 25 °C. it was proposed that the oxidised surface of the ash/carbon when mixed with a halogenated amine would see its acidic carboxyl groups and alcohol groups replaced with amine ester and ether groups as shown in Fig. 14.

The presence of KOH was found to have little to no effect on the amount of nitrogen introduced. The carbon containing the highest nitrogen content was shown to capture 0.174 $mmol_{CO2}/g$ - much less than commercially available sorbents (1.8 $mmol_{CO2}/g$ – 2 $mmol_{CO2}/g$) but the difference in surface area which was 27 m^2/g compared to 1000 m^2/g – 1700 m^2/g may account for this smaller capacity.

5.7.11. Ethylenediamine – (EDA)

Ngoy et al. synthesised a functionalised MCWNT with a polyaspartamide (PAA) surfactant [30]. In this study, ethylenediamine (EDA) was chosen as the diamine and incorporated into polysuccinimide (PSI) to produce PAA which was then noncovalently bound to the MCWNT. The synthesis followed homogenizing a mixture of aspartic acid (50 g) and H_3PO_4 (25 g) and heating to 190 °C–250 °C, after drying the product it was mixed with dicyclohexylcarbodiimide (DCC) in an ice bath for 24 h. Centrifugation and precipitation left PSI as long chain. This PSI was then mixed with an excess of EDA for 24 h after which, it was precipitated with the aid of diethyl ether followed by washing with hot toluene and hot acetone to give PAA. The PAA can then be mixed with MCWNT at a ratio of 1:0.03 at room temperature for 72 h followed by washing with acetone to give MCWNT-PAA. This method of incorporation was able to maintain the primary amine groups and amide groups present in the PAA and introduce them into the MCWNT. The MCWNT-PAA demonstrated the largest CO_2 capacity vs MCWNT, PSI and PAA of 1.59 $mmol_{CO2}/g$, highlighting the importance of both textural properties and nitrogen containing SFGs such as amine and amides especially when considering that the MCWNT had a capacity of 0.28 $mmol_{CO2}/g$. The MCWNT-PAA sorbent did however, require regeneration at 100 °C due to the predominance of chemisorption; however, the stability of the sorbent was evaluated up to 200 °C. A series of nitrogen-containing polymer and carbon spheres prepared by a sol-gel method [417] with varying concentrations of EDA were shown to capture up to 6.2 $mmol_{CO2}/g$ at 273 K and 4.1 $mmol_{CO2}/g$ at 298 K (1 bar). The one-pot hydrothermal method required the mixing of ethanol (16 ml) and distilled water (40 ml) to which various amounts of EDA were added (0.2 ml–0.8 ml) after which resorcinol was added (0.4 g). Formaldehyde was then added (0.6 ml of 37 wt%) and stirred for 24 h at 30 °C. The dried spheres were then treated at 350 °C (2 °C/min) under

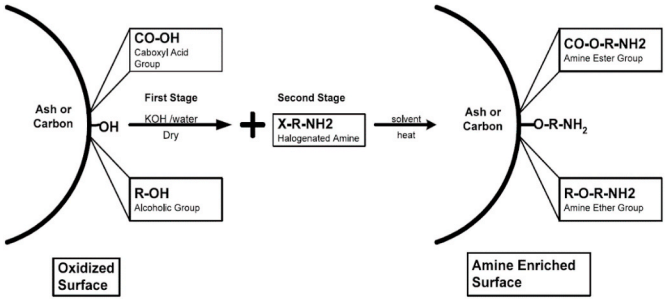

Fig. 14. Proposed reactions for preparation of the amine-enriched fly ash sorbent [416].

nitrogen for 2 h and then 600 °C (5 °C/min) for 2 h. The possible reactions for resorcinol-formaldehyde-EDA polymerisation are shown in Fig. 15 the success of which was shown by XPS and FTIR analyses. Alongside the nitrogen containing moieties a number of oxygen SFGs were also present namely, phenol and/or ether type and negligible carboxylic type. The intermediate and excess formaldehyde react with resorcinol to form polymer framework with pyrrolic and pyridinic-type rings [417].

The post-synthetic modification by Puthiaraj et al. [418] sought to functionalise two porous aromatic polymers incorporated with carbonyl-functionalities with EDA. The polymers were produced *via* a Friedel-Crafts benzoylation and the EDA modification *via* dissolution in methanol, stirring and refluxing. Interestingly, the EDA functionalised derivates demonstrated lower CO_2 capacities than their porous parents but significantly enhanced selectivities (CO_2/N_2).

5.7.12. Polymeric amines

A comprehensive review on the functionalisation of adsorbents by amine-bearing polymers has been published by Varghese and Karanikolos [42]. The authors have reviewed the literature on polymeric amine-functionalised solid sorbents for CO_2 capture, including polyethyleneimine, polypropylenimine, polyallylamine, polyaniline, amino dendrimers and hyperbranched polyamines. Polyethyleneimine (PEI), also named polyaziridine, is one of the most highly investigated aliphatic polymeric amines for CO_2 capture due to its availability, high capture capability, increased amine density, primary amine chain ends and stability as it can maintain its sorption capability up to 90 °C [42]. To date, all sorbents prepared by loading PEI on the carbon materials, have shown a much lower CO_2 capacity in comparison to those by loading PEI on the mesoporous silica molecular sieves [108]. Capacities for PEI modified sorbents can be as large as 3.01 $mmol_{CO2}/g$ at 0.15 bar and 75 °C [419] or 6 $mmol_{CO2}/g$ at 1 atm, 95% CO_2 and 85 °C [420], with the supports being precipitated silica and silica foam, respectively.

5.7.13. Halogenated amines

One alternative method to grafting amino groups onto the surface of adsorbents among nitration/reduction, silylation with aminosilane, amination, grafting diamenes and polyamines, is grafting halogenated amines as demonstrated in the work of Houshmand et al. [421]. Here, 2-chloroethylamine hydrochloric acid (CEA) was grafted onto the surface of an oxidised AC. The AC samples underwent a two-stage modification: oxidation by nitric acid and CEA grafting. The oxidation increases the density of oxygen SFGs which can act as a coupling or linking agent for the grafting of other SFGs. For halogenated amines, the OH bond of a carboxylic group as well as phenolic and alcoholic OH bonds may act as sites for this anchoring. It was found that at 2.17 h the production of NO_2 stopped thus, elucidating to the end of the oxidation with 8 N nitric acid, whereas with concentrated acid, this occurred at 6 h. The grafting which was carried out by mixing the oxidised AC with NaOH (1 M) which were then treated with CEA (1 M) solution, permitted

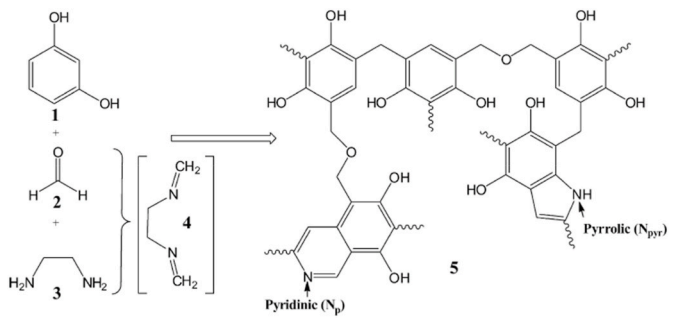

Fig. 15. Representation of possible resorcinol-formaldehyde-ethylenediamine polymerisation [417].

a 45% increase in CO_2 capacity at 100 °C vs the oxidised sample or a two-to-six fold increase vs the parent at 30° - 115 °C.

6. Conclusion

The urgency that is associated with the necessity for the mitigation of climate change and abatement of greenhouse gas emissions has facilitated unprecedented amounts of research to improve the efficiency and cost-effectiveness of the array of PCC technologies, yet the effort to actually implement and utilise this work is insignificant compared to what is required. If the current trend in global response continues, the effects will be far reaching and irreversible. Without significant change in the legislation, the myriad technologies that can be used to capture CO_2 need to become significantly more viable. This paper has comprehensively reviewed, in detail, the various surface functional groups that can positively influence the selective separation of CO_2. It has endeavoured to report and critically discuss the applied methods for their introduction and the efficacy of such for enhanced CO_2 capture within the domain of post-combustion capture.

In this critical review of the literature data has been compiled using Scopus as the primary search engine by surveying the research in the context of surface modification for enhancing the selective adsorption of CO_2. A total of 421 works published between the years of 1964 and 2020 have been embodied in this review. Of the 421 reference that this critical review is founded upon, 43 are review articles, 7 are conference proceedings and 370 are original research papers.

In the context of adsorption there exists a wide range of possible sorbents; carbons, zeolites, MOFs, ZIFs, silicates, porous polymers, alkali metals and their carbonates as well as solid amine-based materials. The advantages and disadvantages for each become more prevalent when considering large-scale deployment. The cost and complexity of synthesis for materials such as MOFs, MOPs, ZIFs *etc.* can all but entirely remove their large-scale viability. Zeolites can possess vast surface areas and stabilities yet often require excessive energies for desorption and are hydrophilic. Carbons can suffer from unsatisfactory selectivity as well as a high sensitivity to temperature due to the weak van der Waals forces that underpin the physical adsorption of CO_2, yet they are abundant, cheap, easily regenerated and stable. The volume of small pores and especially ultra-micropore volume has often been a primary factor in determining the performance of adsorbents for CO_2 capture yet the chemistry that exists within the surface functional groups on adsorbents can often be just as critical for the adsorption energies and affinities towards the adsorbate; something which is just as important as capacity when considering the applicability of these developed materials for use in various industrial settings. The introduction of various SFGs permits a selective separation and enhanced interaction with CO_2; if the sorbent were to only possess a narrow microporosity then the impact that this would have on the adsorption of gas molecules such as N_2 or CH_4 would be significantly disadvantageous for the selective separation of CO_2.

Surface modifications can lead to an increase in the prevalence of oxygen containing SFGs which can aid in enhancing sorption characteristics by increasing surface polarity (*e.g.* –C═O), binding energy (*e.g.* –COOH), selectivity over N_2 (*e.g.* phenol) and capturing the CO_2 *via* hydrogen bonds (*e.g.* –OH) and *etc*. However, attention has to be paid when undertaking modifications to avoid pore blockage that would hinder the diffusion of CO_2 through the porous structure and thus, reduce the availability of active sites for adsorption. Careful control of the treatments is paramount to ensure that those SFGs that are introduced are beneficial for the purpose of CO_2 capture given that not all can actually have a positive effect. Regarding nitrogen-containing groups, the general idea still persists: adding basic polar sites should benefit the capture of CO_2. Undoubtedly, the influence of pyridinic, pyrrolic and pyridonic nitrogen on the selective capture of CO_2 is far more significant than of the groups such as quaternary or oxidised nitrogen. A surface nitro group should yield weaker results when compared to $–NH_2$ due to the inherent lower polarity, higher acidity and larger size of the former.

The amino group is largely considered the starting point in surface functionalisation for the majority of adsorbents. The positive effects of $–NH_2$ incorporation have been widely demonstrated for myriad materials, such as MOFs, zeolites, ACs *etc.* In the case of mesoporous silica, CO_2 uptake is vastly improved by the incorporation of $–NH_2$ groups; in their absence, the CO_2 sorption characteristics are poor and the material has little-to-no application in the PCC context. Bearing in mind that chemical absorption with amine solvents is the conventional CCS process, the introduction of such moieties on the surface of solid supports would be the logical step. Generally, amino-functionalised materials will complement CO_2 capture with further amine efficiency enhancements realised in the presence of moisture. Amines however, are not without limitations. Pore blockage becomes a major issue for long-chain amines and/or at high amine concentrations. Moreover, care has to be taken when regenerating the modified-adsorbent with regards to concerns surrounding both toxicity and downstream equipment corrosion. The degradation of amines is also of significance given there may be the need for subsequent modifications which could impede the viability of large-scale deployment of such modified, and often costly, materials.

Even with the vast volume of research that exists it is still difficult to confirm that the surface modification of adsorbents will act to facilitate the separation of CO_2 from the hugely diverse mixtures that present themselves within our industries. There is a lack of data that elucidates to the complex phenomena that occurs during the selective capture of CO_2. Data for the adsorption of competing gases, breakthrough points, selectivities and for larger scale demonstrations is almost always lacking in some respect. There is an extensive gap to bridge between adsorption of pure CO_2 in the laboratory (1 bar, 273 K) and the adsorption of CO_2 under the conditions present in the post-combustion environment, especially with adsorbents of physical nature. This information is invaluable when considering the viability of these adsorbents; capacity is one in a long list of requirements for the optimal sorbent. Optimisation of the modifications must come simultaneously with the optimisation of the process for which the sorbent is designed. Comprehensive studies on the materials long-term stability, resistance to impurities as well as the cost, complexity and secondary pollution associated with their synthesis have to be considered before a modification can be considered successful and the adsorbent practical.

By focussing on the surface functional groups as opposed to a specific material, this review has provided an invaluable and vastly relevant resource that will inform and enlighten future research in the development of optimum materials with the wherewithal to efficiently and effectively capture CO_2. There will be no single material that can decarbonise every aspect of our civilisation; the solution lies in developing highly specialised materials for each case. This is no small feat but, collations of work such as this act to significantly advance and progress the response required to curtail and mitigate the effects of anthropomorphic-induced climate change.

Declaration of competing interest

The authors declare that they have no known competing financial interests or personal relationships that could have appeared to influence the work reported in this paper.

Acknowledgments

This work has been funded by the UK Carbon Capture and Storage Research Centre (EP/P026214/1) through the flexible funded research programme “Biomass Combustion Ash in Carbon Capture”. The UKCCSRC is supported by the Engineering and Physical Sciences Research Council (EPSRC), UK, as part of the UKRI Energy Programme. The authors are grateful to the Research Centre for providing this funding. The authors would also like to acknowledge Brunel Research Initiative and Enterprise Fund (BRIEF) to support this work.

References

[1] Committe on Climate Change, Change C on C. Net Zero: the UK’s contribution to stopping global warming, Committe on Climate Change, 2019.
[2] Commission E, European Commission. Paris Agreement | Climate Action, European Commission Climate Action, 2015. Available from: https://ec.europa.eu/clima/policies/international/negotiations/paris_en.
[3] M. Bui, C.S. Adjiman, A. Bardow, E.J. Anthony, A. Boston, S.F. Brown, et al., Carbon capture and storage (CCS): the way forward, Energy Environ. Sci. 11 (5) (2018) 1062–1176. Available from: http://eprints.whiterose.ac.uk/126186/.
[4] Y. Liu, Q. Ye, M. Shen, J. Shi, J. Chen, H. Pan, et al., Carbon dioxide capture by functionalized solid amine sorbents with simulated flue gas conditions, Environ. Sci. Technol. 45 (13) (2011) 5710–5716.
[5] J.R. Li, Y. Ma, M.C. McCarthy, J. Sculley, J. Yu, H.K. Jeong, et al., Carbon dioxide capture-related gas adsorption and separation in metal-organic frameworks, Coord. Chem. Rev. 255 (2011) 1791–1823.
[6] A. Al-Mamoori, A. Krishnamurthy, A.A. Rownaghi, F. Rezaei, Carbon capture and utilization update, Energy Technol. 5 (6) (2017 Jun) 834–849. Available from: https://onlinelibrary.wiley.com/doi/abs/10.1002/ente.201600747.
[7] Y.C. Chiang, R.S. Juang, Surface modifications of carbonaceous materials for carbon dioxide adsorption: a review, J. Taiwan Inst. Chem. Eng. 71 (2017) 214–234, https://doi.org/10.1016/j.jtice.2016.12.014. Available from:.
[8] A.A. Adelodun, K.H. Kim, J.C. Ngila, J. Szulejko, A review on the effect of amination pretreatment for the selective separation of CO2, Appl Energy 158 (2015) 631–642, https://doi.org/10.1016/j.apenergy.2015.08.107. Available from:.
[9] F. Vega, F.M. Baena-Moreno, L.M. Gallego Fernández, E. Portillo, B. Navarrete, Z. Zhang, Current status of CO2 chemical absorption research applied to CCS: towards full deployment at industrial scale, Appl. Energy (2020) 260.
[10] Z. Yong, V. Mata, A.E. Rodrigues, Adsorption of carbon dioxide at high temperature - a review, Separ. Purif. Technol. 26 (2–3) (2002) 195–205.
[11] M. Sevilla, A.B. Fuertes, Sustainable porous carbons with a superior performance for CO2 capture, Energy Environ. Sci. 4 (5) (2011) 1765–1771.
[12] M. Sevilla, C. Falco, M.M. Titirici, A.B. Fuertes, High-performance CO2 sorbents from algae, RSC Adv. 2 (33) (2012) 12792–12797.
[13] R. Wang, P. Wang, X. Yan, J. Lang, C. Peng, Q. Xue, Promising porous carbon derived from celtuce leaves with outstanding supercapacitance and CO2 capture performance, ACS Appl. Mater. Interfaces 4 (11) (2012) 5800–5806.
[14] M. Sevilla, J.B. Parra, A.B. Fuertes, Assessment of the role of micropore size and N-doping in CO2 capture by porous carbons, ACS Appl. Mater. Interfaces 5 (13) (2013) 6360–6368.
[15] H. Wei, S. Deng, B. Hu, Z. Chen, B. Wang, J. Huang, et al., Granular bamboo-derived activated carbon for high CO2 adsorption: the dominant role of narrow micropores, ChemSusChem 5 (12) (2012) 2354–2360.
[16] M.K. Al Mesfer, M. Danish, Y.M. Fahmy, M.M. Rashid, Post-combustion CO2 capture with activated carbons using fixed bed adsorption, Heat Mass Transf und Stoffuebertragung 54 (9) (2018) 2715–2724.
[17] B.S. Girgis, A.A. Attia, N.A. Fathy, Modification in adsorption characteristics of activated carbon produced by H3PO4 under flowing gases, Colloids Surfaces A Physicochem Eng Asp 299 (1–3) (2007) 79–87.
[18] R. Ahmed, G. Liu, B. Yousaf, Q. Abbas, H. Ullah, M.U. Ali, Recent advances in carbon-based renewable adsorbent for selective carbon dioxide capture and separation-A review, J. Clean Prod. 242 (2020) 118409, https://doi.org/10.1016/j.jclepro.2019.118409. Available from:.
[19] M. Al Bahri, L. Calvo, M.A. Gilarranz, J.J. Rodriguez, Activated carbon from grape seeds upon chemical activation with phosphoric acid: application to the adsorption of diuron from water, Chem. Eng. J. 203 (2012) 348–356.
[20] W.H. Chan, M.N. Mazlee, Z.A. Ahmad, M.A.M. Ishak, J.B. Shamsul, The development of low cost adsorbents from clay and waste materials: a review, J. Mater. Cycles Waste Manag. 19 (1) (2017) 1–14.
[21] W. Shen, S. Zhang, Y. He, J. Li, W. Fan, Hierarchical porous polyacrylonitrile-based activated carbon fibers for CO2 capture, J. Mater. Chem. 21 (36) (2011) 14036–14040.
[22] H. An, B. Feng, S. Su, CO2 capture by electrothermal swing adsorption with activated carbon fibre materials, Int. J. Greenh Gas Control 5 (1) (2011) 16–25.
[23] H. An, B. Feng, S. Su, CO2 capture capacities of activated carbon fibre-phenolic resin composites, Carbon N Y 47 (10) (2009) 2396–2405.
[24] C. Lu, H. Bai, B. Wu, F. Su, J.F. Hwang, Comparative study of CO2 capture by carbon nanotubes, activated carbons, and zeolites, Energy Fuels 22 (5) (2008) 3050–3056.
[25] S.Y. Sawant, R.S. Somani, H.C. Bajaj, S.S. Sharma, A dechlorination pathway for synthesis of horn shaped carbon nanotubes and its adsorption properties for CO 2, CH 4, CO and N 2 [Internet]. Vols. 227–228, J. Hazard Mater. (2012) 317–326. Available from: http://www.sciencedirect.com/science/article/pii/S0304389412005651.
[26] D.J. Babu, M. Lange, G. Cherkashinin, A. Issanin, R. Staudt, J.J. Schneider, Gas Adsorption Studies of CO2 and N2 in Spatially Aligned Double-Walled Carbon Nanotube Arrays, Carbon 61 (2013) 616–623. Available from: http://www.sciencedirect.com/science/article/pii/S0008622313004818.
[27] M.A. Atieh, O.Y. Bakather, B. Al-Tawbini, A.A. Bukhari, F.A. Abuilaiwi, M. B. Fettouhi, Effect of carboxylic functional group functionalized on carbon nanotubes surface on the removal of lead from water, Bioinorgan. Chem. Appl. 2010 (2010).
[28] A. Douglas, R. Carter, M. Li, C.L. Pint, Toward small-diameter carbon nanotubes synthesized from captured carbon dioxide: critical role of catalyst coarsening,

ACS Appl Mater Interfaces 10 (22) (2018), 19010–8. Available from: https://www.ncbi.nlm.nih.gov/pubmed/29715008.
[29] E. Raymundo-Piñero, D. Cazorla-Amorós, A. Linares-Solano, S. Delpeux, E. Frackowiak, K. Szostak, et al., High surface area carbon nanotubes prepared by chemical activation [7], Carbon N Y 40 (9) (2002) 1614–1617.
[30] J.M. Ngoy, N. Wagner, L. Riboldi, O. Bolland, A CO2 capture technology using multi-walled carbon nanotubes with polyaspartamide surfactant, Energy Procedia 63 (2014) 2230–2248. Available from: https://www.sciencedirect.com/science/article/pii/S1876610214020578.
[31] G.P. Lithoxoos, A. Labropoulos, L.D. Peristeras, N. Kanellopoulos, J. Samios, I. G. Economou, Adsorption of N2, CH4, CO and CO2 gases in single walled carbon nanotubes: a combined experimental and Monte Carlo molecular simulation study, J. Supercrit. Fluids 55 (2010) 510–523. Available from: http://www.sciencedirect.com/science/article/pii/S0896844610003074.
[32] S. Gadipelli, Z.X. Guo, Graphene-based materials: synthesis and gas sorption, storage and separation, Prog. Mater. Sci. 69 (2015) 1–60.
[33] T.H. Liou, P.Y. Wang, Utilization of rice husk wastes in synthesis of graphene oxide-based carbonaceous nanocomposites, Waste Manag 108 (2020) 51–61, https://doi.org/10.1016/j.wasman.2020.04.029. Available from:.
[34] B. Szczęśniak, J. Choma, M. Jaroniec, Gas adsorption properties of graphene-based materials, Adv. Colloid Interface Sci. 243 (2017) 46–59.
[35] J. Zhang, Q. Xin, X. Li, M. Yun, R. Xu, S. Wang, et al., Mixed matrix membranes comprising aminosilane-functionalized graphene oxide for enhanced CO2 separation, J. Membr. Sci. (2019), 570–571(October 2018):343–54.
[36] V. Chandra, S.U. Yu, S.H. Kim, Y.S. Yoon, D.Y. Kim, A.H. Kwon, et al., Highly selective CO2 capture on N-doped carbon produced by chemical activation of polypyrrole functionalized graphene sheets, Chem. Commun. 48 (5) (2012) 735–737.
[37] S. Yang, L. Zhan, X. Xu, Y. Wang, L. Ling, X. Feng, Graphene-based porous silica sheets impregnated with polyethyleneimine for superior CO2 capture, Adv. Mater. 25 (15) (2013) 2130–2134.
[38] S. Wang, Y. Wu, N. Zhang, G. He, Q. Xin, X. Wu, et al., A highly permeable graphene oxide membrane with fast and selective transport nanochannels for efficient carbon capture, Energy Environ. Sci. 9 (10) (2016) 3107–3112.
[39] N. Politakos, I. Barbarin, L.S. Cantador, J.A. Cecilia, E. Mehravar, R. Tomovska, Graphene-based monolithic nanostructures for CO2 capture, Ind. Eng. Chem. Res. 59 (18) (2020) 8612–8621.
[40] R. Dawson, D.J. Adams, A.I. Cooper, Chemical tuning of CO2 sorption in robust nanoporous organic polymers, Chem. Sci. 2 (6) (2011) 1173–1177.
[41] Y. He, X. Zhu, Y. Li, C. Peng, J. Hu, H. Liu, Efficient CO2 capture by triptycene-based microporous organic polymer with functionalized modification, Microporous Mesoporous Mater. 214 (2015) 181–187.
[42] A.M. Varghese, G.N. Karanikolos, CO2 capture adsorbents functionalized by amine – bearing polymers: a review, Int. J. Greenh Gas Control 2020 (96) (September 2019) 103005, https://doi.org/10.1016/j.ijggc.2020.103005. Available from.
[43] R. Dawson, A.I. Cooper, D.J. Adams, Chemical functionalization strategies for carbon dioxide capture in microporous organic polymers, Polym. Int. 62 (2013) 345–352.
[44] S. Cho, H.R. Yu, K.D. Kim, K.B. Yi, Y.S. Lee, Surface characteristics and carbon dioxide capture characteristics of oxyfluorinated carbon molecular sieves, Chem. Eng. J. 211–212 (2012) 89–96.
[45] X. Xu, C. Song, J.M. Andresen, B.G. Miller, A.W. Scaroni, Novel polyethylenimine-modified mesoporous molecular sieve of MCM-41 type as high-capacity adsorbent for CO2 capture, Energy Fuels 16 (6) (2002) 1463–1469.
[46] V. Zeleňák, M. Badaničová, D. Halamová, J. Čejka, A. Zukal, N. Murafa, et al., Amine-modified ordered mesoporous silica: effect of pore size on carbon dioxide capture, Chem. Eng. J. 144 (2) (2008) 336–342.
[47] J. Alcañiz-Monge, J.P. Marco-Lozar, M.Á. Lillo-Ródenas, CO2 separation by carbon molecular sieve monoliths prepared from nitrated coal tar pitch, Fuel Process. Technol. 92 (5) (2011) 915–919.
[48] G. Li, P. Xiao, P. Webley, J. Zhang, R. Singh, M. Marshall, Capture of CO2 from high humidity flue gas by vacuum swing adsorption with zeolite 13X, Adsorption 14 (2–3) (2008) 415–422.
[49] Y. Kalvachev, D. Zgureva, S. Boycheva, B. Barbov, N. Petrova, Synthesis of carbon dioxide adsorbents by zeolitization of fly ash, J. Therm. Anal. Calorim. 124 (1) (2016) 101–106.
[50] L. Liu, R. Singh, P. Xiao, P.A. Webley, Y. Zhai, Zeolite synthesis from waste fly ash and its application in CO2 capture from flue gas streams, Adsorption 17 (5) (2011) 795–800.
[51] Y. Wang, H. Jia, P. Chen, X. Fang, T. Du, Synthesis of La and Ce modified X zeolite from rice husk ash for carbon dioxide capture, J. Mater. Res. Technol. (2020), https://doi.org/10.1016/j.jmrt.2020.02.061 (x x). Available from:.
[52] T.H. Bae, M.R. Hudson, J.A. Mason, W.L. Queen, J.J. Dutton, K. Sumida, et al., Evaluation of cation-exchanged zeolite adsorbents for post-combustion carbon dioxide capture, Energy Environ. Sci. 6 (1) (2013) 128–138.
[53] J. Merel, M. Clausse, F. Meunier, Experimental investigation on CO2 post-combustion capture by indirect thermal swing adsorption using 13X and 5A zeolites, Ind. Eng. Chem. Res. 47 (1) (2008) 209–215.
[54] J. Zhang, R. Singh, P.A. Webley, Alkali and alkaline-earth cation exchanged chabazite zeolites for adsorption based CO2 capture, Microporous Mesoporous Mater. 111 (1–3) (2008) 478–487.
[55] T.F. de Aquino, S.T. Estevam, V.O. Viola, C.R.M.M. Marques, F.L. Zancan, L. B. Vasconcelos, et al., CO2 adsorption capacity of zeolites synthesized from coal fly ashes, Fuel 276 (May) (2020) 118143, https://doi.org/10.1016/j.fuel.2020.118143. Available from:.
[56] S. Boycheva, D. Zgureva, K. Lazarova, T. Babeva, C. Popov, H. Lazarova, et al., Progress in the utilization of coal fly ash by conversion to zeolites with green energy applications, Materials 13 (9) (2020) 2014.
[57] C.A. Trickett, A. Helal, B.A. Al-Maythalony, Z.H. Yamani, K.E. Cordova, O. M. Yaghi, The chemistry of metal-organic frameworks for CO2 capture, regeneration and conversion, Nat Rev Mater 2 (8) (2017).
[58] D.A. Yang, H.Y. Cho, J. Kim, S.T. Yang, W.S. Ahn, CO2 capture and conversion using Mg-MOF-74 prepared by a sonochemical method, Energy Environ. Sci. 5 (4) (2012) 6465–6473.
[59] L. Du, Z. Lu, K. Zheng, J. Wang, X. Zheng, Y. Pan, et al., Fine-tuning pore size by shifting coordination sites of ligands and surface polarization of metal-organic frameworks to sharply enhance the selectivity for CO2, J. Am. Chem. Soc. 135 (2) (2013) 562–565.
[60] J.J. Gassensmith, H. Furukawa, R.A. Smaldone, R.S. Forgan, Y.Y. Botros, O. M. Yaghi, et al., Strong and reversible binding of carbon dioxide in a green metal-organic framework, J. Am. Chem. Soc. 133 (39) (2011) 15312–15315.
[61] S. Chaemchuen, N.A. Kabir, K. Zhou, F. Verpoort, Metal-organic frameworks for upgrading biogas via CO2 adsorption to biogas green Energy, Chemical Society Reviews 42 (2013) 9304–9332.
[62] A. Torrisi, R.G. Bell, C. Mellot-Draznieks, Functionalized MOFs for enhanced CO2 capture, Cryst. Growth Des. 10 (7) (2010) 2839–2841.
[63] R. Banerjee, A. Phan, B. Wang, C. Knobler, H. Furukawa, M. O'Keeffe, et al., High-throughput synthesis of zeolitic imidazolate frameworks and application to CO2 capture, Science (80) 319 (5865) (2008) 939–943.
[64] A. Phan, C.J. Doonan, F.J. Uribe-Romo, C.B. Knobler, M. Okeeffe, O.M. Yaghi, Synthesis, structure, and carbon dioxide capture properties of zeolitic imidazolate frameworks, Acc. Chem. Res. 43 (1) (2010) 58–67.
[65] V. Nafisi, M.B. Hägg, Development of dual layer of ZIF-8/PEBAX-2533 mixed matrix membrane for CO2 capture, J. Membr. Sci. 459 (2014) 244–255.
[66] W. Morris, B. Leung, H. Furukawa, O.K. Yaghi, N. He, H. Hayashi, et al., A combined experimental-computational investigation of carbon dioxide capture in a series of isoreticular zeolitic imidazolate frameworks, J. Am. Chem. Soc. 132 (32) (2010) 11006–11008.
[67] S. Wang, X. Wang, Imidazolium ionic liquids, imidazolylidene heterocyclic carbenes, and zeolitic imidazolate frameworks for CO2 capture and photochemical reduction, Angew. Chem. Int. Ed. 55 (2016) 2308–2320.
[68] Y. Duan, D.C. Sorescu, CO2 capture properties of alkaline earth metal oxides and hydroxides: a combined density functional theory and lattice phonon dynamics study, J. Chem. Phys. 133 (7) (2010) 1–11.
[69] S.C. Lee, B.Y. Choi, T.J. Lee, C.K. Ryu, Y.S. Ahn, J.C. Kim, CO2 absorption and regeneration of alkali metal-based solid sorbents, Catal. Today 111 (3–4) (2006) 385–390.
[70] A.A. Azmi, M.A.A.A. Aziz, Mesoporous adsorbent for CO 2 capture application under mild condition: a review, J Environ Chem Eng 7 (2) (2019) 103022, https://doi.org/10.1016/j.jece.2019.103022. Available from:.
[71] D. Bonenfant, M. Kharoune, P. Niquette, M. Mimeault, R. Hausler, Advances in principal factors influencing carbon dioxide adsorption on zeolites, in: Science and Technology of Advanced Materials, 2008.
[72] N.P. Wickramaratne, M. Jaroniec, Activated carbon spheres for CO2 adsorption, ACS Appl. Mater. Interfaces 5 (5) (2013) 1849–1855.
[73] M. Suzuki, Adsorption Engineering, Chemical Engineering Monographs, Elsevier Science 25 (1991) 278.
[74] S. Choi, J.H. Drese, C.W. Jones, Adsorbent materials for carbon dioxide capture from large anthropogenic point sources, ChemSusChem 2 (9) (2009) 796–854.
[75] K.S. Walton, M.B. Abney, M.D. LeVan, CO2 adsorption in y and X zeolites modified by alkali metal cation exchange, Microporous Mesoporous Mater. 91 (1–3) (2006) 78–84.
[76] J.A. Menéndez, J. Phillips, B. Xia, L.R. Radovic, On the modification and characterization of chemical surface properties of activated carbon: in the search of carbons with stable basic properties, Langmuir 12 (18) (1996) 4404–4410.
[77] T. Islamoglu, T. Kim, Z. Kahveci, O.M. El-Kadri, H.M. El-Kaderi, Systematic postsynthetic modification of nanoporous organic frameworks for enhanced CO2 capture from flue gas and landfill gas, J. Phys. Chem. C 120 (5) (2016) 2592–2599.
[78] K.K. Tanabe, S.M. Cohen, Postsynthetic modification of metal–organic frameworks—a progress report, Chem. Soc. Rev. 40 (2) (2011) 498–519.
[79] Z. Wang, S.M. Cohen, Postsynthetic modification of metal–organic frameworks, Chem. Soc. Rev. 38 (5) (2009) 1315–1329.
[80] C. Shen, Z. Wang, Tetraphenyladamantane-based microporous polyimide and its nitro-functionalization for highly efficient CO2 capture, J. Phys. Chem. C 118 (31) (2014) 17585–17593.
[81] S. Masoudi Soltani, S.K. Yazdi, S. Hosseini, Effects of pyrolysis conditions on the porous structure construction of mesoporous charred carbon from used cigarette filters, Appl. Nanosci. 4 (5) (2014) 551–569.
[82] M.S. Salman, S.K. Yazdi, S. Hosseini, M.K. Gargari, Effect of nitric acid modification on porous characteristics of mesoporous char synthesized from the pyrolysis of used cigarette filters, J. Environ. Chem. Eng. 2 (3) (2014) 1301–1308.
[83] D. Madden, T. Curtin, Carbon dioxide capture with amino-functionalised zeolite-β: a temperature programmed desorption study under dry and humid conditions, Microporous Mesoporous Mater [Internet 228 (2016) 310–317, https://doi.org/10.1016/j.micromeso.2016.03.041. Available from:.
[84] A.P. Beltrao-Nunes, R. Sennour, V.A. Arus, S. Anoma, M. Pires, N. Bouazizi, et al., CO2 capture by coal ash-derived zeolites- roles of the intrinsic basicity and hydrophilic character, J. Alloys Compd. 778 (2019) 866–877.
[85] M.A. Wójtowicz, J.R. Pels, J.A. Moulijn, The fate of nitrogen functionalities in coal during pyrolysis and combustion, Fuel 74 (4) (1995) 507–516.

[86] T. Chen, S. Deng, B. Wang, J. Huang, Y. Wang, G. Yu, CO2 adsorption on crab shell derived activated carbons: contribution of micropores and nitrogen-containing groups, RSC Adv. 5 (60) (2015) 48323–48330.

[87] C. Zhang, W. Song, Q. Ma, L. Xie, X. Zhang, H. Guo, Enhancement of CO2 capture on biomass-based carbon from black locust by KOH activation and ammonia modification, Energy Fuels 30 (5) (2016) 4181–4190.

[88] J. Jiang, L. Zhang, X. Wang, N. Holm, K. Rajagopalan, F. Chen, et al., Highly ordered macroporous woody biochar with ultra-high carbon content as supercapacitor electrodes, Electrochim. Acta 113 (2013) 481–489.

[89] J. Wang, R. Krishna, J. Yang, S. Deng, Hydroquinone and quinone-grafted porous carbons for highly selective CO2 capture from flue gases and natural gas upgrading, Environ. Sci. Technol. 49 (15) (2015) 9364–9373.

[90] O. Boujibar, A. Souikny, F. Ghamouss, O. Achak, M. Dahbi, T. Chafik, CO2 capture using N-containing nanoporous activated carbon obtained from argan fruit shells, J. Environ. Chem. Eng. 6 (2) (2018) 1995–2002.

[91] X. Cao, K.S. Ro, M. Chappell, Y. Li, J. Mao, Chemical structures of swine-manure chars produced under different carbonization conditions investigated by advanced solid-state 13C nuclear magnetic resonance (NMR) spectroscopy, Energy Fuels 25 (1) (2011) 388–397.

[92] A. Sayari, A. Heydari-Gorji, Y. Yang, CO 2-induced degradation of amine-containing adsorbents: reaction products and pathways, J. Am. Chem. Soc. 134 (33) (2012) 13834–13842.

[93] K.A. Wepasnick, B.A. Smith, J.L. Bitter, D. Howard Fairbrother, Chemical and structural characterization of carbon nanotube surfaces, Anal. Bioanal. Chem. 396 (3) (2010) 1003–1014.

[94] P. González-García, Activated carbon from lignocellulosics precursors: a review of the synthesis methods, characterization techniques and applications, Renew Sustain Energy Rev [Internet]. 2018 82 (August 2017), https://doi.org/10.1016/j.rser.2017.04.117, 1393–414. Available from:.

[95] A.D. Igalavithana, S. Mandal, N.K. Niazi, M. Vithanage, S.J. Parikh, F.N. D. Mukome, et al., Advances and future directions of biochar characterization methods and applications, Crit. Rev. Environ. Sci. Technol. 47 (23) (2017) 2275–2330, https://doi.org/10.1080/10643389.2017.1421844. Available from:.

[96] M.V. Lopez-Ramon, F. Stoeckli, C. Moreno-Castilla, F. Carrasco-Marin, On the characterization of acidic and basic surface sites on carbons by various techniques, Carbon N Y 37 (8) (1999) 1215–1221.

[97] J.H. Zhou, Z.J. Sui, J. Zhu, P. Li, D. Chen, Y.C. Dai, et al., Characterization of surface oxygen complexes on carbon nanofibers by TPD, XPS and FT-IR, Carbon N Y (2007).

[98] C.J. Geankoplis, J.C. Geankoplis, Transport Processes and Separation Process Principles (Includes Unit Operations). Transport Processes and Separation Process Principles, 2003, pp. 559–625.

[99] M.L. McGlashan, Manual of symbols and terminology for physicochemical quantities and units, Pure Appl. Chem. 21 (1) (1970) 1–44.

[100] D.D. Do, Adsorption Analysis: Equilibria and Kinetics, vol. 2, Chemical Engineering, 1998, p. 913. Available from: http://ebooks.worldscinet.com/ISBN/9781860943829/9781860943829.html.

[101] W. Kast, Principles of adsorption and adsorption processes, Chem Eng Process Process Intensif 19 (2) (1985) 118.

[102] R.B. Bird, W.E. Stewart, E.N. Lightfoot, Transport Phenomena, John Wiley and Sons, Inc., New York, 1960.

[103] S. Ghanbari, G. Kamath, Dynamic simulation and mass transfer study of carbon dioxide capture using biochar and mgo-impregnated activated carbon in a swing adsorption process, Energy Fuels 33 (6) (2019) 5452–5463.

[104] T.M. McDonald, D.M. D'Alessandro, R. Krishna, J.R. Long, Enhanced carbon dioxide capture upon incorporation of N,N′- dimethylethylenediamine in the metal-organic framework CuBTTri, Chem. Sci. 2 (10) (2011) 2022–2028.

[105] T. Ratvijitvech, R. Dawson, A. Laybourn, Y.Z. Khimyak, D.J. Adams, A.I. Cooper, Post-synthetic modification of conjugated microporous polymers, Polymer 55 (1) (2014) 321–325.

[106] A.A. Azmi, A.H. Ruhaimi, M.A.A. Aziz, Efficient 3-aminopropyltrimethoxysilane functionalised mesoporous ceria nanoparticles for CO2 capture, Mater. Today Chem. 16 (2020) 100273, https://doi.org/10.1016/j.mtchem.2020.100273. Available from:.

[107] X. Ma, L. Li, R. Chen, C. Wang, H. Li, S. Wang, Heteroatom-doped nanoporous carbon derived from MOF-5 for CO 2 capture, Appl Surf Sci 435 (2018) 494–502, https://doi.org/10.1016/j.apsusc.2017.11.069. Available from:.

[108] M. Sarmah, B.P. Baruah, P. Khare, A comparison between CO2 capturing capacities of fly ash based composites of MEA/DMA and DEA/DMA, Fuel Process Technol. 106 (2013) 490–497, https://doi.org/10.1016/j.fuproc.2012.09.017. Available from:.

[109] Z. Wu, P.A. Webley, D. Zhao, Comprehensive study of pore evolution, mesostructural stability, and simultaneous surface functionalization of ordered mesoporous carbon (FDU-15) by wet oxidation as a promising adsorbent, Langmuir 26 (12) (2010) 10277–10286.

[110] D. Saha, M.J. Kienbaum, Role of oxygen, nitrogen and sulfur functionalities on the surface of nanoporous carbons in CO2 adsorption: a critical review, Microporous Mesoporous Mater 287 (April) (2019) 29–55, https://doi.org/10.1016/j.micromeso.2019.05.051. Available from:.

[111] M.G. Plaza, K.J. Thurecht, C. Pevida, F. Rubiera, J.J. Pis, C.E. Snape, et al., Influence of oxidation upon the CO2 capture performance of a phenolic-resin-derived carbon, Fuel Process Technol. 110 (2013) 53–60, https://doi.org/10.1016/j.fuproc.2013.01.011. Available from:.

[112] J.A. Mason, K. Sumida, Z.R. Herm, R. Krishna, J.R. Long, Evaluating metal-organic frameworks for post-combustion carbon dioxide capture via temperature swing adsorption, Energy Environ. Sci. 4 (8) (2011) 3030–3040.

[113] H. Wu, K. Yao, Y. Zhu, B. Li, Z. Shi, R. Krishna, et al., Cu-TDPAT, an rht -type dual-functional metal-organic framework offering significant potential for use in H 2 and natural gas purification processes operating at high pressures, J. Phys. Chem. C 116 (31) (2012) 16609–16618.

[114] K.V. Kumar, K. Preuss, L. Lu, Z.X. Guo, M.M. Titirici, Effect of nitrogen doping on the CO2 adsorption behavior in nanoporous carbon structures: a molecular simulation study, J. Phys. Chem. C 119 (39) (2015) 22310–22321.

[115] S. Biswas, J. Zhang, Z. Li, Y.Y. Liu, M. Grzywa, L. Sun, et al., Enhanced selectivity of CO2 over CH4 in sulphonate-, carboxylate- and iodo-functionalized UiO-66 frameworks, Dalton Trans. 42 (13) (2013) 4730–4737.

[116] A. Torrisi, C. Mellot-Draznieks, R.G. Bell, Impact of ligands on CO2 adsorption in metal-organic frameworks: first principles study of the interaction of CO2 with functionalized benzenes. II. Effect of polar and acidic substituents, J. Chem. Phys. 132 (4) (2010).

[117] B.S. Caglayan, A.E. Aksoylu, CO2 adsorption on chemically modified activated carbon, J. Hazard Mater. 252–253 (2013) 19–28.

[118] M.A. Montes-Morán, D. Suárez, J.A. Menéndez, E. Fuente, On the nature of basic sites on carbon surfaces: an overview, Carbon N Y 42 (7) (2004) 1219–1225.

[119] B.C. Bai, E.A. Kim, C.W. Lee, Y.S. Lee, J.S. Im, Effects of surface chemical properties of activated carbon fibers modified by liquid oxidation for CO 2 adsorption, Appl. Surf. Sci. 353 (2015) 158–164.

[120] K.J. Lee, S.J. Kim, Theoretical investigation of CO2 adsorption on graphene, Bull. Kor. Chem. Soc. 34 (10) (2013) 3022–3026.

[121] B. Sajjadi, W.Y. Chen, N.O. Egiebor, A comprehensive review on physical activation of biochar for energy and environmental applications, Rev. Chem. Eng. 35 (6) (2019) 735–776.

[122] H.M. Lee, I.S. Youn, M. Saleh, J.W. Lee, K.S. Kim, Interactions of CO2 with various functional molecules, Phys. Chem. Chem. Phys. 17 (16) (2015) 10925–10933.

[123] J.R. Pels, F. Kapteijn, J.A. Moulijn, Q. Zhu, K.M. Thomas, Evolution of nitrogen functionalities in carbonaceous materials during pyrolysis, Carbon N Y 33 (11) (1995) 1641–1653.

[124] M.R. Nelson, R.F. Borkman, Ab initio calculations on CO2 binding to carbonyl groups, J. Phys. Chem. 102 (40) (1998) 7860–7863.

[125] H. Kim, Y. Kim, M. Yoon, S. Lim, S.M. Park, G. Seo, et al., Highly selective carbon dioxide sorption in an organic molecular porous material, J. Am. Chem. Soc. 132 (35) (2010) 12200–12202.

[126] G. Chang, Y. Xu, L. Zhang, L. Yang, Enhanced carbon dioxide capture in an indole-based microporous organic polymer via synergistic effects of indoles and their adjacent carbonyl groups, Polym. Chem. 9 (35) (2018) 4455–4459.

[127] L. Yang, G. Chang, D. Wang, High and selective carbon dioxide capture in nitrogen-containing aerogels via synergistic effects of electrostatic in-plane and dispersive π-π-Stacking interactions, ACS Appl. Mater. Interfaces 9 (18) (2017) 15213–15218.

[128] Y. Zeng, R. Zou, Y. Zhao, Covalent organic frameworks for CO2 Capture, Adv. Mater. 28 (2016) 2855–2873.

[129] G.E. Cmarik, M. Kim, S.M. Cohen, K.S. Walton, Tuning the adsorption properties of uio-66 via ligand functionalization, Langmuir 28 (44) (2012) 15606–15613.

[130] A. Kronast, S. Eckstein, P.T. Altenbuchner, K. Hindelang, S.I. Vagin, B. Rieger, Gated channels and selectivity tuning of CO2over N2Sorption by post-synthetic modification of a UiO-66-type metal–organic framework, Chem. Eur J. 22 (36) (2016) 12800–12807.

[131] H. Molavi, A. Eskandari, A. Shojaei, S.A. Mousavi, Enhancing CO2/N2 adsorption selectivity via post-synthetic modification of NH2-UiO-66(Zr), Microporous Mesoporous Mater 257 (2018) 193–201, https://doi.org/10.1016/j.micromeso.2017.08.043. Available from:.

[132] B. Liu, H. Li, X. Ma, R. Chen, S. Wang, L. Li, The synergistic effect of oxygen-containing functional groups on CO2 adsorption by the glucose-potassium citrate-derived activated carbon, RSC Adv. 8 (68) (2018) 38965–38973.

[133] E. Stavitski, E.A. Pidko, S. Couck, T. Remy, E.J.M. Hensen, B.M. Weckhuysen, et al., Complexity behind CO2 capture on NH2-MIL-53(Al), Langmuir 27 (7) (2011) 3970–3976.

[134] H.R. Abid, Z.H. Rada, J. Shang, S. Wang, Synthesis, characterization, and CO2adsorption of three metal-organic frameworks (MOFs): MIL-53, MIL-96, and amino-MIL-53, Polyhedron 120 (2016) 103–111.

[135] N. Ravi, S.A. Anuar, N.Y.M. Yusuf, W.N.R.W. Isahak, M.S. Masdar, Amine-mixed oxide hybrid materials for carbon dioxide adsorption from CO2/H2 mixture, Mater. Res. Express 5 (5) (2018).

[136] K.Y.A. Lin, A.H.A. Park, Effects of bonding types and functional groups on CO 2 capture using novel multiphase systems of liquid-like nanoparticle organic hybrid materials, Environ. Sci. Technol. 45 (15) (2011) 6633–6639.

[137] V.R. Deitz, F.G. Carpenter, R.G. Arnold, Interaction of carbon dioxide with carbon adsorbents below 400°C, Carbon N Y 1 (3) (1964) 245–254.

[138] M. Mastalerz, M.W. Schneider, I.M. Oppel, O. Presly, A salicylbisimine cage compound with high surface area and selective CO2/CH4 adsorption, Angew. Chem. Int. Ed. 50 (2011) 1046–1051.

[139] Y. Zhao, X. Liu, K.X. Yao, L. Zhao, Y. Han, Superior capture of CO2 achieved by introducing extra-framework cations into N-doped microporous carbon, Chem. Mater. 24 (24) (2012) 4725–4734.

[140] L. Wang, R.T. Yang, Significantly increased CO 2 adsorption performance of nanostructured templated carbon by tuning surface area and nitrogen doping, J. Phys. Chem. C 116 (1) (2012) 1099–1106.

[141] T. Horikawa, N. Sakao, T. Sekida, J. Hayashi, D.D. Do, M. Katoh, Preparation of nitrogen-doped porous carbon by ammonia gas treatment and the effects of N-doping on water adsorption, Carbon N Y 50 (5) (2012) 1833–1842.

[142] G.P. Hao, G. Mondin, Z. Zheng, T. Biemelt, S. Klosz, R. Schubel, et al., Unusual ultra-hydrophilic, porous carbon cuboids for atmospheric-water capture, Angew. Chem. Int. Ed. 54 (6) (2015) 1941–1945.
[143] J.C. Liu, P.A. Monson, Does water condense in carbon pores? Langmuir 21 (22) (2005) 10219–10225.
[144] G. Lim, K.B. Lee, H.C. Ham, Effect of N-containing functional groups on CO2 adsorption of carbonaceous materials: a density functional theory approach, J. Phys. Chem. C 120 (15) (2016) 8087–8095.
[145] D. Saha, R. Thorpe, S.E. Van Bramer, N. Alexander, D.K. Hensley, G. Orkoulas, et al., Synthesis of Nitrogen and Sulfur Codoped Nanoporous Carbons from Algae: Role in CO2 Separation, ACS Omega 3 (2018), 18592–602.
[146] A. Heidari, H. Younesi, A. Rashidi, A.A. Ghoreyshi, Evaluation of CO2 adsorption with eucalyptus wood based activated carbon modified by ammonia solution through heat treatment, Chem Eng J 254 (2014) 503–513, https://doi.org/10.1016/j.cej.2014.06.004. Available from:.
[147] L. Nie, Y. Mu, J. Jin, J. Chen, J. Mi, Recent developments and consideration issues in solid adsorbents for CO2 capture from flue gas, Chinese J. Chem. Eng. 26 (11) (2018) 2303–2317, https://doi.org/10.1016/j.cjche.2018.07.012. Available from:.
[148] F. Su, C. Lu, S.C. Kuo, W. Zeng, Adsorption of CO2 on amine-functionalized y-type zeolites, Energy Fuels 24 (2) (2010) 1441–1448.
[149] V. Zelenak, D. Halamova, L. Gaberova, E. Bloch, P. Llewellyn, Amine-modified SBA-12 mesoporous silica for carbon dioxide capture: effect of amine basicity on sorption properties, Microporous Mesoporous Mater. 116 (1–3) (2008) 358–364.
[150] S. Nakao, K. Yogo, K. Goto, T. Kai, H. Yamada, Advanced CO2 Capture Technologies: Absorption, Adsorption, and Membrane Separation Methods [Internet]. Book, Springer International Publishing, Cham, 2019, pp. 1–90. Available from: http://link.springer.com/10.1007/978-3-030-18858-0.
[151] P.J. Milner, R.L. Siegelman, A.C. Forse, M.I. Gonzalez, T. Runčevski, J.D. Martell, et al., A diaminopropane-appended metal-organic framework enabling efficient CO2 capture from coal flue gas via a mixed adsorption mechanism, J. Am. Chem. Soc. 139 (38) (2017) 13541–13553.
[152] M.G. Plaza, C. Pevida, A. Arenillas, F. Rubiera, J.J. Pis, CO2 capture by adsorption with nitrogen enriched carbons, Fuel 86 (14 SPEC. ISS) (2007) 2204–2212.
[153] B. Arstad, H. Fjellvåg, K.O. Kongshaug, O. Swang, R. Blom, Amine functionalised metal organic frameworks (MOFs) as adsorbents for carbon dioxide, Adsorption 14 (6) (2008) 755–762.
[154] S.H. Khalil, M.K. Aroua, W.M.A.W. Daud, Study on the improvement of the capacity of amine-impregnated commercial activated carbon beds for Co 2 adsorbing, Chem. Eng. J. 183 (2012) (2012) 15–20.
[155] P. Wang, Y. Guo, C. Zhao, J. Yan, P. Lu, Biomass derived wood ash with amine modification for post-combustion CO2 capture, Appl Energy 201 (2) (2017 Sep) 34–44. Available from: https://search.proquest.com/docview/2297045587.
[156] A. Shahtalebi, M. Mar, K. Guérin, S.K. Bhatia, Effect of fluorine doping on structure and CO2 adsorption in silicon carbide-derived carbon, Carbon N Y 96 (2016) 565–577.
[157] G.P. Khokhlova, O.S. Efimova, Surface modification of carbon sorbents with polycarbosilane, Solid Fuel Chem. 46 (4) (2012) 255–260.
[158] M.L. Gray, Y. Soong, K.J. Champagne, H. Pennline, J.P. Baltrus, R.W. Stevens, et al., Improved immobilized carbon dioxide capture sorbents, ACS Div Fuel Chem Prepr 49 (1) (2004) 1449–1455.
[159] D.W. Kim, D.W. Jung, A.A. Adelodun, Y.M. Jo, Evaluation of CO2 adsorption capacity of electrospun carbon fibers with thermal and chemical activation, J. Appl. Polym. Sci. 134 (47) (2017).
[160] A.A. Adelodun, Y.H. Lim, Y.M. Jo, Stabilization of potassium-doped activated carbon by amination for improved CO2 selective capture, J. Anal. Appl. Pyrolysis 108 (2014) 151–159.
[161] A.A. Adelodun, Y.M. Jo, Integrated basic treatment of activated carbon for enhanced CO 2 selectivity, Appl. Surf. Sci. 286 (2013) 306–313.
[162] X. Liu, F. Gao, J. Xu, L. Zhou, H. Liu, J. Hu, Zeolite@Mesoporous silica-supported-amine hybrids for the capture of CO2 in the presence of water, Microporous Mesoporous Mater. 222 (2016) 113–119.
[163] H. Huang, W. Zhang, F. Yang, B. Wang, Q. Yang, Y. Xie, et al., Enhancing CO2 adsorption and separation ability of Zr(IV)-based metal-organic frameworks through ligand functionalization under the guidance of the quantitative structure-property relationship model, Chem. Eng. J. 289 (2016) 247–253.
[164] W. Zhang, H. Huang, C. Zhong, D. Liu, Cooperative effect of temperature and linker functionality on CO 2 capture from industrial gas mixtures in metal-organic frameworks: a combined experimental and molecular simulation study, Phys. Chem. Chem. Phys. 14 (7) (2012) 2317–2325.
[165] D.K. Maity, A. Halder, B. Bhattacharya, A. Das, D. Ghoshal, Selective CO2 adsorption by nitro functionalized metal organic frameworks, Cryst. Growth Des. 16 (3) (2016) 1162–1167.
[166] V. Safarifard, S. Rodríguez-Hermida, V. Guillerm, I. Imaz, M. Bigdeli, A. A. Tehrani, et al., Influence of the amide groups in the CO2/N2 selectivity of a series of isoreticular, interpenetrated metal-organic frameworks, Cryst. Growth Des. 16 (10) (2016) 6016–6023.
[167] R.K. Gajula, R. Kishor, M.J. Prakash, Imine-linked covalent organic cage porous crystals for CO2 adsorption, ChemistrySelect 4 (43) (2019) 12547–12555.
[168] D.H. Jo, H. Jung, D.K. Shin, C.H. Lee, S.H. Kim, Effect of amine structure on CO2 adsorption over tetraethylenepentamine impregnated poly methyl methacrylate supports, Separ. Purif. Technol. 125 (2014) 187–193.
[169] H.A. Patel, C.T. Yavuz, Noninvasive functionalization of polymers of intrinsic microporosity for enhanced CO2capture, Chem. Commun. 48 (80) (2012) 9989–9991.
[170] S. Zulfiqar, F. Karadas, J. Park, E. Deniz, G.D. Stucky, Y. Jung, et al., Amidoximes: promising candidates for CO 2 capture, Energy Environ. Sci. 4 (11) (2011) 4528–4531.
[171] S.M. Mahurin, J. Górka, K.M. Nelson, R.T. Mayes, S. Dai, Enhanced CO2/N2 selectivity in amidoxime-modified porous carbon, Carbon N Y 67 (2014) 457–464.
[172] G.P. Hao, W.C. Li, D. Qian, A.H. Lu, Rapid synthesis of nitrogen-doped porous carbon monolith for CO2 capture, Adv. Mater. 22 (7) (2010) 853–857.
[173] T.J. Bandosz, M. Seredych, E. Rodríguez-Castellón, Y. Cheng, L.L. Daemen, A. J. Ramírez-Cuesta, Evidence for CO2 reactive adsorption on nanoporous S- and N-doped carbon at ambient conditions, Carbon N Y 96 (2016) 856–863.
[174] Y.S. Bae, J. Liu, C.E. Wilmer, H. Sun, A.N. Dickey, M.B. Kim, et al., The effect of pyridine modification of Ni-DOBDC on CO2 capture under humid conditions, Chem. Commun. 50 (25) (2014) 3296–3298.
[175] M. Wang, X. Fan, L. Zhang, J. Liu, B. Wang, R. Cheng, et al., Probing the role of O-containing groups in CO2 adsorption of N-doped porous activated carbon, Nanoscale 9 (44) (2017) 17593–17600.
[176] M. Sevilla, P. Valle-Vigōn, A.B. Fuertes, N-doped polypyrrole-based porous carbons for CO2 capture, Adv. Funct. Mater. 21 (14) (2011) 2781–2787.
[177] G. Zhao, B. Aziz, N. Hedin, Carbon dioxide adsorption on mesoporous silica surfaces containing amine-like motifs, Appl Energy [Internet] 87 (9) (2010) 2907–2913, https://doi.org/10.1016/j.apenergy.2009.06.008. Available from:.
[178] A.D. Igalavithana, S.W. Choi, P.D. Dissanayake, J. Shang, C.H. Wang, X. Yang, et al., Gasification biochar from biowaste (food waste and wood waste) for effective CO2 adsorption, J. Hazard Mater. 2020 (391) (May 2019) 121147, https://doi.org/10.1016/j.jhazmat.2019.121147. Available from:.
[179] W. Kiciński, M. Szala, M. Bystrzejewski, Sulfur-doped porous carbons: synthesis and applications, Carbon N Y 68 (2014) 1–32.
[180] S.A. Wohlgemuth, R.J. White, M.G. Willinger, M.M. Titirici, M. Antonietti, A one-pot hydrothermal synthesis of sulfur and nitrogen doped carbon aerogels with enhanced electrocatalytic activity in the oxygen reduction reaction, Green Chem. 14 (5) (2012) 1515–1523.
[181] A. Torrisi, C. Mellot-Draznieks, R.G. Bell, Impact of ligands on CO2 adsorption in metal-organic frameworks: first principles study of the interaction of CO2 with functionalized benzenes. I. Inductive effects on the aromatic ring, J. Chem. Phys. 130 (19) (2009).
[182] N. Hagemann, K. Spokas, H.P. Schmidt, R. Kägi, M.A. Böhler, T.D. Bucheli, Activated carbon, biochar and charcoal: linkages and synergies across pyrogenic carbon's ABCs, Water (Switzerland) 10 (2) (2018) 1–19.
[183] W.M.A.W. Daud, A.H. Houshamnd, Textural characteristics, surface chemistry and oxidation of activated carbon, J. Nat. Gas Chem. 19 (2010) 267–279.
[184] G. Singh, K.S. Lakhi, S. Sil, S.V. Bhosale, I.Y. Kim, K. Albahily, et al., Biomass derived porous carbon for CO 2 capture, Carbon N Y 148 (2019) 164–186, https://doi.org/10.1016/j.carbon.2019.03.050. Available from:.
[185] F.O. Ochedi, Y. Liu, Y.G. Adewuyi, State-of-the-art review on capture of CO2 using adsorbents prepared from waste materials, Process Saf Environ Prot 139 (2020) 1–25, https://doi.org/10.1016/j.psep.2020.03.036. Available from:.
[186] G. Xu, Y. Lv, J. Sun, H. Shao, L. Wei, Recent advances in biochar applications in agricultural soils: benefits and environmental implications, Clean 40 (10) (2012) 1093–1098.
[187] K.A. Spokas, K.B. Cantrell, J.M. Novak, D.W. Archer, J.A. Ippolito, H.P. Collins, et al., Biochar: a synthesis of its agronomic impact beyond carbon sequestration, J. Environ. Qual. 41 (4) (2012) 973–989.
[188] T. Pröll, F. Zerobin, Biomass-based negative emission technology options with combined heat and power generation, Mitig. Adapt Strateg. Glob Chang. 24 (7) (2019) 1307–1324. Available from: https://search.proquest.com/docview/2175712512.
[189] S.H. Jung, J.S. Kim, Production of biochars by intermediate pyrolysis and activated carbons from oak by three activation methods using CO2, J. Anal. Appl. Pyrolysis 107 (2014) 116–122, https://doi.org/10.1016/j.jaap.2014.02.011. Available from:.
[190] M. Fan, W. Marshall, D. Daugaard, R.C. Brown, Steam activation of chars produced from oat hulls and corn stover, Bioresour. Technol. 93 (1) (2004) 103–107.
[191] A.K. Dalai, R. Azargohar, Production of activated carbon from biochar using chemical and physical activation: mechanism and modeling, ACS (Am. Chem. Soc.) Symp. Ser. (2007) 463–476.
[192] J.L. Figueiredo, M.F.R. Pereira, M.M.A. Freitas, J.J.M. Órfão, Modification of the surface chemistry of activated carbons, Carbon N Y 37 (9) (1999) 1379–1389.
[193] C.L. Mangun, K.R. Benak, M.A. Daley, J. Economy, Oxidation of activated carbon fibers: effect on pore size, surface chemistry, and adsorption properties, Chem. Mater. 11 (12) (1999) 3476–3483.
[194] S.M. Hong, S.W. Choi, S.H. Kim, K.B. Lee, Porous carbon based on polyvinylidene fluoride: enhancement of co2 adsorption by physical activation, Carbon N Y 99 (2016) 354–360, https://doi.org/10.1016/j.carbon.2015.12.012. Available from: .
[195] S. Guo, J. Peng, W. Li, K. Yang, L. Zhang, S. Zhang, et al., Effects of CO 2 activation on porous structures of coconut shell-based activated carbons, Appl. Surf. Sci. 255 (20) (2009) 8443–8449.
[196] J.J. Manyà, B. González, M. Azuara, G. Arner, Ultra-microporous adsorbents prepared from vine shoots-derived biochar with high CO2 uptake and CO2/N2 selectivity, Chem Eng J 345 (November 2017) (2018) 631–639, https://doi.org/10.1016/j.cej.2018.01.092. Available from:.
[197] M.S. Tam, M.J. Antal, Preparation of activated carbons from macadamia nut shell and coconut shell by air activation, Ind. Eng. Chem. Res. 38 (11) (1999) 4268–4276.

[198] M.G. Plaza, A.S. González, J.J. Pis, F. Rubiera, C. Pevida, Production of microporous biochars by single-step oxidation: effect of activation conditions on CO2 capture, Appl Energy 114 (2014) (2014) 551–562, https://doi.org/10.1016/j.apenergy.2013.09.058. Available from:.
[199] L. Xiong, X.F. Wang, L. Li, L. Jin, Y.G. Zhang, S.L. Song, et al., Nitrogen-enriched porous carbon fiber as a CO2 adsorbent with superior CO2 selectivity by air activation, Energy Fuels 33 (12) (2019) 12558–12567.
[200] Y. Guo, C. Tan, J. Sun, W. Li, J. Zhang, C. Zhao, Porous activated carbons derived from waste sugarcane bagasse for CO2 adsorption, Chem Eng J 381 (July 2019) (2020) 122736, https://doi.org/10.1016/j.cej.2019.122736. Available from:.
[201] A. Aworn, P. Thiravetyan, W. Nakbanpote, Preparation and characteristics of agricultural waste activated carbon by physical activation having micro- and mesopores, J. Anal. Appl. Pyrolysis 82 (2) (2008) 279–285.
[202] J.W. Patrick, Porosity in Carbons : Characterization and Applications. Porosity in Carbons, Edward Arnold, London, 1995, p. 253.
[203] X. Zhang, J. Wu, H. Yang, J. Shao, X. Wang, Y. Chen, et al., Preparation of nitrogen-doped microporous modified biochar by high temperature CO2-NH3 treatment for CO2 adsorption: effects of temperature, RSC Adv. 6 (100) (2016) 98157–98166.
[204] D. Zabiegaj, M. Caccia, M.E. Casco, F. Ravera, J. Narciso, Synthesis of carbon monoliths with a tailored hierarchical pore structure for selective CO2 capture, J CO2 Util. 26 (March) (2018) 36–44.
[205] M.K. Al Mesfer, Synthesis and characterization of high-performance activated carbon from walnut shell biomass for CO2 capture, Environ. Sci. Pollut. Res. 27 (13) (2020) 15020–15028.
[206] M.B. Ahmed, J.L. Zhou, H.H. Ngo, W. Guo, M. Chen, Progress in the preparation and application of modified biochar for improved contaminant removal from water and wastewater, Bioresour Technol 214 (2016) 836–851, https://doi.org/10.1016/j.biortech.2016.05.057. Available from:.
[207] T. Budinova, E. Ekinci, F. Yardim, A. Grimm, E. Björnbom, V. Minkova, et al., Characterization and application of activated carbon produced by H3PO4 and water vapor activation, Fuel Process. Technol. 87 (10) (2006) 899–905.
[208] A.S. Mestre, J. Pires, J.M.F. Nogueira, A.P. Carvalho, Activated carbons for the adsorption of ibuprofen, Carbon N Y 45 (10) (2007) 1979–1988.
[209] M.M. Maroto-Valer, D.J. Fauth, M.E. Kuchta, Y. Zhang, J.M. Andrésen, Activation of magnesium rich minerals as carbonation feedstock materials for CO2 sequestration, Fuel Process. Technol. 86 (14–15) (2005) 1627–1645.
[210] M.G. Lussier, Z. Zhang, D.J. Miller, Characterizing rate inhibition in steam/hydrogen gasification via analysis of adsorbed hydrogen, Carbon N Y 36 (9) (1998) 1361–1369.
[211] D. Feng, Y. Zhang, Y. Zhao, S. Sun, J. Gao, Improvement and maintenance of biochar catalytic activity for in-situ biomass tar reforming during pyrolysis and H2O/CO2 gasification, Fuel Process. Technol. 172 (2018) 106–114.
[212] F. Rodríguez-Reinoso, M. Molina-Sabio, M.T. González, The use of steam and CO2 as activating agents in the preparation of activated carbons, Carbon N Y 33 (1) (1995) 15–23.
[213] M.S. Lee, M. Park, H.Y. Kim, S.J. Park, Effects of microporosity and surface chemistry on separation performances of N-containing pitch-based activated carbons for CO2/N2 binary mixture, Sci. Rep. 6 (March) (2016) 1–11, https://doi.org/10.1038/srep23224. Available from:.
[214] E. Raymundo-Piñero, D. Cazorla-Amorós, A. Linares-Solano, J. Find, U. Wild, R. Schlögl, Structural characterization of N-containing activated carbon fibers prepared from a low softening point petroleum pitch and a melamine resin, Carbon N Y 40 (4) (2002) 597–608.
[215] M.S. Shafeeyan, W.M.A.W. Daud, A. Houshmand, A. Shamiri, A review on surface modification of activated carbon for carbon dioxide adsorption, J. Anal. Appl. Pyrolysis 89 (2) (2010) 143–151, https://doi.org/10.1016/j.jaap.2010.07.006. Available from:.
[216] Y. Otake, R.G. Jenkins, Characterization of oxygen-containing surface complexes created on a microporous carbon by air and nitric acid treatment, Carbon N Y 31 (1) (1993) 109–121.
[217] S.S. Barton, M.J.B. Evans, E. Halliop, J.A.F. MacDonald, Acidic and basic sites on the surface of porous carbon, Carbon N Y 35 (9) (1997) 1361–1366.
[218] C.O. Ania, J.B. Parra, J.J. Pis, Oxygen-induced decrease in the equilibrium adsorptive capacities of activated carbons, Adsorpt. Sci. Technol. 22 (4) (2004) 337–352.
[219] E. Papirer, S. Li, J.B. Donnet, Contribution to the study of basic surface groups on carbons, Carbon N Y 25 (2) (1987) 243–247.
[220] A. Dandekar, R.T.K. Baker, M.A. Vannice, Characterization of activated carbon, graphitized carbon fibers and synthetic diamond powder using TPD and DRIFTS, Carbon N Y 36 (12) (1998) 1821–1831.
[221] F. Akhtar, L. Bergström, Colloidal processing and thermal treatment of binderless hierarchically porous zeolite 13X monoliths for CO2 capture, J. Am. Ceram. Soc. 94 (1) (2011) 92–98.
[222] S. Chowdhury, R. Balasubramanian, Highly efficient, rapid and selective CO2 capture by thermally treated graphene nanosheets, J CO2 Util 13 (2016) 50–60, https://doi.org/10.1016/j.jcou.2015.12.001. Available from:.
[223] M. Almarri, X. Ma, C. Song, Role of surface oxygen-containing functional groups in liquid-phase adsorption of nitrogen compounds on carbon-basedadsorbents, Energy Fuels 23 (8) (2009) 3940–3947.
[224] M. Fan, F. Gai, Y. Cao, Z. Zhao, Y. Ao, Y. Liu, et al., Structuring ZIF-8-based hybrid material with hierarchical pores by in situ synthesis and thermal treatment for enhancement of CO2 uptake, J. Solid State Chem. 269 (August 2018) (2019) 507–512, https://doi.org/10.1016/j.jssc.2018.10.027. Available from:.
[225] N.A. Rashidi, S. Yusup, An overview of activated carbons utilization for the post-combustion carbon dioxide capture, J CO2 Util 13 (2016) 1–16, https://doi.org/10.1016/j.jcou.2015.11.002. Available from:.
[226] Y.A. Alhamed, S.U. Rather, A.H. El-Shazly, S.F. Zaman, M.A. Daous, A.A. Al-Zahrani, Preparation of activated carbon from fly ash and its application for CO2 capture, Kor. J. Chem. Eng. 32 (4) (2015 Apr) 723–730.
[227] C. Zhao, Y. Guo, J. Yan, J. Sun, W. Li, P. Lu, Enhanced CO2 sorption capacity of amine-tethered fly ash residues derived from co-firing of coal and biomass blends, Appl Energy 242 (March) (2019) 453–461. Available from: https://www.sciencedirect.com/science/article/pii/S0306261919305525.
[228] Y. Guo, C. Tan, P. Wang, J. Sun, J. Yan, W. Li, et al., Kinetic study on CO 2 adsorption behaviors of amine-modified co-firing fly ash, J Taiwan Inst Chem Eng 96 (xxxx) (2019) 374–381, https://doi.org/10.1016/j.jtice.2018.12.003. Available from:.
[229] A. Dindi, D. Viet Quang, M.R.M. Abu-Zahra, CO2 adsorption testing on fly ash derived cancrinite-type zeolite and its amine-functionalized derivatives, Environ. Prog. Sustain. Energy 38 (1) (2019) 77–88.
[230] A. Dindi, D.V. Quang, E. Nashef, M.R.M.A. Zahra, Effect of PEI impregnation on the CO2 capture performance of activated fly ash, Energy Procedia 114 (November 2016) (2017) 2243–2251, https://doi.org/10.1016/j.egypro.2017.03.1361. Available from:.
[231] M. Mercedes Maroto-Valer, Z. Lu, Y. Zhang, Z. Tang, Sorbents for CO2 capture from high carbon fly ashes, Waste Manag. 28 (11) (2008) 2320–2328.
[232] A. Arenillas, K.M. Smith, T.C. Drage, C.E. Snape, CO2 capture using some fly ash-derived carbon materials, Fuel 84 (17) (2005) 2204–2210.
[233] C. Chen, J. Kim, W.S. Ahn, CO2capture by amine-functionalized nanoporous materials: a review, Kor. J. Chem. Eng. 31 (11) (2014) 1919–1934.
[234] A. Houshmand, W.M.A.W. Daud, M.S. Shafeeyan, Exploring potential methods for anchoring amine groups on the surface of activated carbon for CO2 adsorption, Sep. Sci. Technol. 46 (7) (2011 Apr 28) 1098–1112. Available from: https://www.tandfonline.com/doi/abs/10.1080/01496395.2010.546383.
[235] J. Reinik, I. Heinmaa, U. Kirso, T. Kallaste, J. Ritamäki, D. Boström, et al., Alkaline modified oil shale fly ash: optimal synthesis conditions and preliminary tests on CO 2 adsorption, J. Hazard Mater. 196 (2011) 180–186, https://doi.org/10.1016/j.jhazmat.2011.09.006. Available from:.
[236] N. Rao, M. Wang, Z. Shang, Y. Hou, G. Fan, J. Li, CO2 adsorption by amine-functionalized MCM-41: a comparison between impregnation and grafting modification methods, Energy Fuels 32 (1) (2018) 670–677.
[237] L. Liu, H. Chen, E. Shiko, X. Fan, Y. Zhou, G. Zhang, et al., Low-cost DETA impregnation of acid-activated sepiolite for CO2 capture, Chem Eng J 353 (August) (2018) 940–948, https://doi.org/10.1016/j.cej.2018.07.086. Available from:.
[238] N. Hiyoshi, K. Yogo, T. Yashima, Adsorption characteristics of carbon dioxide on organically functionalized SBA-15, Microporous Mesoporous Mater. 84 (1–3) (2005) 357–365.
[239] Y. Chen, M. Huang, W. Chen, B. Huang, Adsorption of CU(II) from aqueous solution using activated carbon derived from mangosteen peel, BioResources 7 (4) (2012) 4965–4975.
[240] A. Ros, M.A. Lillo-Ródenas, E. Fuente, M.A. Montes-Morán, M.J. Martín, A. Linares-Solano, High surface area materials prepared from sewage sludge-based precursors, Chemosphere 65 (1) (2006) 132–140.
[241] S.M. Cohen, Postsynthetic methods for the functionalization of metal-organic frameworks, Chem. Rev. 112 (2) (2012) 970–1000.
[242] B. Wang, H. Huang, X.L. Lv, Y. Xie, M. Li, J.R. Li, Tuning CO2 selective adsorption over N2 and CH 4 in UiO-67 analogues through ligand functionalization, Inorg. Chem. 53 (17) (2014) 9254–9259.
[243] M.G. Plaza, C. Pevida, B. Arias, J. Fermoso, M.D. Casal, C.F. Martín, et al., Development of low-cost biomass-based adsorbents for postcombustion CO2 capture, Fuel 88 (12) (2009) 2442–2447.
[244] R.J.J. Jansen, H. van Bekkum, Amination and ammoxidation of activated carbons, Carbon N Y 32 (8) (1994) 1507–1516.
[245] M. Yang, L. Guo, G. Hu, X. Hu, L. Xu, J. Chen, et al., Highly cost-effective nitrogen-doped porous coconut shell-based CO2 sorbent synthesized by combining ammoxidation with KOH activation, Environ. Sci. Technol. 49 (11) (2015) 7063–7070.
[246] L. Guo, J. Yang, G. Hu, X. Hu, L. Wang, Y. Dong, et al., Role of hydrogen peroxide preoxidizing on CO2 adsorption of nitrogen-doped carbons produced from coconut shell, ACS Sustain. Chem. Eng. 4 (5) (2016) 2806–2813.
[247] M. Yang, L. Guo, G. Hu, X. Hu, J. Chen, S. Shen, et al., Adsorption of CO2 by petroleum coke nitrogen-doped porous carbons synthesized by combining ammoxidation with KOH activation, Ind. Eng. Chem. Res. 55 (3) (2016) 757–765.
[248] R. Pietrzak, H. Wachowska, P. Nowicki, K. Babeł, Preparation of modified active carbon from brown coal by ammoxidation, Fuel Process. Technol. 88 (4) (2007) 409–415.
[249] P. Nowicki, J. Kazmierczak, R. Pietrzak, Comparison of physicochemical and sorption properties of activated carbons prepared by physical and chemical activation of cherry stones, Powder Technol. 269 (2015) 312–319.
[250] S.H. Liu, Y.Y. Huang, Valorization of coffee grounds to biochar-derived adsorbents for CO2 adsorption, J. Clean. Prod. 175 (2018) 354–360.
[251] S. Meyer, B. Glaser, P. Quicker, Technical, economical, and climate-related aspects of biochar production technologies: a literature Review, Environ. Sci. Technol. 45 (2011) 9473–9483.
[252] S.E. Elaigwu, V. Rocher, G. Kyriakou, G.M. Greenway, Removal of Pb2+ and Cd2 + from aqueous solution using chars from pyrolysis and microwave-assisted hydrothermal carbonization of Prosopis africana shell, J. Ind. Eng. Chem. 20 (5) (2014) 3467–3473.

[253] L. Yue, L. Rao, L. Wang, L. An, C. Hou, C. Ma, et al., Efficient CO2 adsorption on nitrogen-doped porous carbons derived from d -glucose, Energy Fuels 32 (2018) 6955–6963.
[254] H. Yang, Y. Yuan, S.C.E. Tsang, Nitrogen-enriched carbonaceous materials with hierarchical micro-mesopore structures for efficient CO 2 capture, Chem Eng J 185–186 (2012) 374–379, https://doi.org/10.1016/j.cej.2012.01.083. Available from:.
[255] S. Kang, X. Li, J. Fan, J. Chang, Characterization of hydrochars produced by hydrothermal carbonization of lignin, cellulose, d-xylose, and wood meal, in: Industrial and Engineering Chemistry Research, 2012, pp. 9023–9031.
[256] X. Chen, Q. Lin, R. He, X. Zhao, G. Li, Hydrochar production from watermelon peel by hydrothermal carbonization, Bioresour. Technol. 241 (2017) 236–243.
[257] R. Becker, U. Dorgerloh, E. Paulke, J. Mumme, I. Nehls, Hydrothermal carbonization of biomass: major organic components of the aqueous phase, Chem. Eng. Technol. 37 (3) (2014) 511–518.
[258] K.M. Lee, Y.M. Jo, Synthesis of zeolite from waste fly ash for adsorption of CO2, J. Mater. Cycles Waste Manag. 12 (3) (2010) 212–219.
[259] M.G. Nyambura, G.W. Mugera, P.L. Felicia, N.P. Gathura, Carbonation of brine impacted fractionated coal fly ash: Implications for CO2 sequestration, J. Environ. Manag. 92 (3) (2011) 655–664.
[260] N.M. Musyoka, L. Petrik, E. Hums, Synthesis of zeolite A, X and P from a South African coal fly ash, in: Advanced Materials Research, 2012, pp. 1757–1762.
[261] V.K. Jha, M. Nagae, M. Matsuda, M. Miyake, Zeolite formation from coal fly ash and heavy metal ion removal characteristics of thus-obtained Zeolite X in multi-metal systems, J. Environ. Manag. 90 (8) (2009) 2507–2514.
[262] I. Majchrzak-Kucęba, W. Nowak, A thermogravimetric study of the adsorption of CO2 on zeolites synthesized from fly ash, Thermochim. Acta 437 (1–2) (2005) 67–74.
[263] G.N. Muriithi, L.F. Petrik, F.J. Doucet, Synthesis, characterisation and CO2 adsorption potential of NaA and NaX zeolites and hydrotalcite obtained from the same coal fly ash, J CO2 Util. 36 (August 2019) (2020) 220–230.
[264] C. Belviso, State-of-the-art applications of fly ash from coal and biomass: a focus on zeolite synthesis processes and issues, Prog. Energy Combust Sci. 65 (2018) 109–135, https://doi.org/10.1016/j.pecs.2017.10.004. Available from:.
[265] X. Zhang, S. Zhang, H. Yang, Y. Feng, Y. Chen, X. Wang, et al., Nitrogen enriched biochar modified by high temperature CO2-ammonia treatment: characterization and adsorption of CO2, Chem Eng J 257 (2014) 20–27, https://doi.org/10.1016/j.cej.2014.07.024. Available from:.
[266] Y.G. Ko, S.S. Shin, U.S. Choi, Primary, secondary, and tertiary amines for CO2 capture: designing for mesoporous CO2 adsorbents, J Colloid Interface Sci 361 (2) (2011) 594–602, https://doi.org/10.1016/j.jcis.2011.03.045. Available from:.
[267] P.N. Sutar, A. Jha, P.D. Vaidya, E.Y. Kenig, Secondary amines for CO 2 capture: a kinetic investigation using N-ethylmonoethanolamine, Chem. Eng. J. 207–208 (2012) 718–724.
[268] W. Shen, Z. Li, Y. Liu, Surface chemical functional groups modification of porous carbon, Recent Pat. Chem. Eng. 1 (1) (2012) 27–40.
[269] M. Issa, R. Shawabkeh, M. Ar, M.I. Kandah, R. Shawabkeh, Al-Zboon Ma ef, et al., Synthesis and characterization of activated carbon from asphalt, Appl. Surf. Sci. 253 (2) (2006) 821–826.
[270] A. Rehman, M. Park, S.J. Park, Current progress on the surface chemical modification of carbonaceous materials, Coatings 9 (2) (2019) 1–22.
[271] G. Yadavalli, H. Lei, Y. Wei, L. Zhu, X. Zhang, Y. Liu, et al., Carbon dioxide capture using ammonium sulfate surface modified activated biomass carbon, Biomass Bioenergy 98 (2017) 53–60.
[272] S. Khalili, B. Khoshandam, M. Jahanshahi, A comparative study of CO2 and CH4 adsorption using activated carbon prepared from pine cone by phosphoric acid activation, Kor. J. Chem. Eng. 33 (10) (2016) 2943–2952.
[273] A.L. Yaumi, M.Z.A. Bakar, B.H. Hameed, Melamine-nitrogenated mesoporous activated carbon derived from rice husk for carbon dioxide adsorption in fixed-bed, Energy 155 (2018) 46–55, https://doi.org/10.1016/j.energy.2018.04.183. Available from:.
[274] S.M. Yakout, G. Sharaf El-Deen, Characterization of activated carbon prepared by phosphoric acid activation of olive stones, Arab J Chem 9 (2016) S1155–S1162.
[275] A. Dindi, D.V. Quang, L.F. Vega, E. Nashef, M.R.M. Abu-Zahra, Applications of fly ash for CO2 capture, utilization, and storage, J CO2 Util. 29 (2019) 82–102.
[276] I.A.W. Tan, A.L. Ahmad, B.H. Hameed, Adsorption of basic dye on high-surface-area activated carbon prepared from coconut husk: equilibrium, kinetic and thermodynamic studies, J. Hazard Mater. 154 (1–3) (2008) 337–346.
[277] G.G. Stavropoulos, A.A. Zabaniotou, Production and characterization of activated carbons from olive-seed waste residue, Microporous Mesoporous Mater. 82 (1–2) (2005) 79–85.
[278] S.O. Bada, S. Potgieter-Vermaak, Evaluation and treatment of coal fly ash for adsorption application, Leonardo Electron. J. Pract. Technol. 7 (12) (2008) 37–48.
[279] M.S. Shafeeyan, W.M.A.W. Daud, A. Houshmand, A. Arami-Niya, Ammonia modification of activated carbon to enhance carbon dioxide adsorption: effect of pre-oxidation, Appl. Surf. Sci. 257 (9) (2011) 3936–3942.
[280] L. Hadjittofi, M. Prodromou, I. Pashalidis, Activated biochar derived from cactus fibres - preparation, characterization and application on Cu(II) removal from aqueous solutions, Bioresour. Technol. 159 (2014) 460–464.
[281] Y. Xue, B. Gao, Y. Yao, M. Inyang, M. Zhang, A.R. Zimmerman, et al., Hydrogen peroxide modification enhances the ability of biochar (hydrochar) produced from hydrothermal carbonization of peanut hull to remove aqueous heavy metals: batch and column tests, Chem. Eng. J. 200–202 (2012) 673–680.
[282] Y. Li, J. Shao, X. Wang, Y. Deng, H. Yang, H. Chen, Characterization of modified biochars derived from bamboo pyrolysis and their utilization for target component (furfural) adsorption, Energy Fuels 28 (8) (2014) 5119–5127.
[283] R. Shawabkeh, M.J. Khan, A.A. Al-Juhani, H.I. Al-Abdul Wahhab, I.A. Hussein, Enhancement of surface properties of oil fly ash by chemical treatment, Appl Surf Sci 258 (5) (2011) 1643–1650, https://doi.org/10.1016/j.apsusc.2011.07.136. Available from:.
[284] C. Zhang, W. Song, G. Sun, L. Xie, J. Wang, K. Li, et al., CO2 capture with activated carbon grafted by nitrogenous functional groups, Energy Fuels 27 (8) (2013) 4818–4823.
[285] H. Tamai, H. Nagoya, T. Shiono, Adsorption of methyl mercaptan on surface modified activated carbon, J. Colloid Interface Sci. 300 (2) (2006) 814–817.
[286] W. Wang, X. Wang, C. Song, X. Wei, J. Ding, J. Xiao, Sulfuric acid modified bentonite as the support of tetraethylenepentamine for CO2 capture, Energy Fuels 27 (3) (2013) 1538–1546.
[287] K. Legrouri, E. Khouya, M. Ezzine, H. Hannache, R. Denoyel, R. Pallier, et al., Production of activated carbon from a new precursor molasses by activation with sulphuric acid, J. Hazard Mater. 118 (1–3) (2005) 259–263.
[288] Y.H. Chen, D.L. Lu, CO2 capture by kaolinite and its adsorption mechanism, Appl. Clay Sci. 104 (2015) 221–228, https://doi.org/10.1016/j.clay.2014.11.036. Available from:.
[289] D. Li, W.B. Li, J.S. Shi, F.W. Xin, Influence of doping nitrogen, sulfur, and phosphorus on activated carbons for gas adsorption of H2, CH4 and CO2, RSC Adv. 6 (55) (2016) 50138–50143.
[290] Y. Sun, K. Li, J. Zhao, J. Wang, N. Tang, D. Zhang, et al., Nitrogen and sulfur Co-doped microporous activated carbon macro-spheres for CO2 capture, J Colloid Interface Sci 526 (2018) 174–183, https://doi.org/10.1016/j.jcis.2018.04.101. Available from:.
[291] Y. Sun, J. Zhao, J. Wang, N. Tang, R. Zhao, D. Zhang, et al., Sulfur-doped millimeter-sized microporous activated carbon spheres derived from sulfonated poly(styrene-divinylbenzene) for CO2 capture, J. Phys. Chem. C 121 (18) (2017) 10000–10009.
[292] A.E. Creamer, B. Gao, Carbon-based adsorbents for postcombustion CO2 capture: a critical review, Environ. Sci. Technol. 50 (14) (2016) 7276–7289, https://doi.org/10.1021/acs.est.6b00627. Available from:.
[293] A.L. Yaumi, I.A. Hussien, R.A. Shawabkeh, Surface modification of oil fly ash and its application in selective capturing of carbon dioxide, Appl Surf Sci 266 (2013) 118–125, https://doi.org/10.1016/j.apsusc.2012.11.109. Available from:.
[294] A. Fernández-Jiménez, A. Palomo, Mid-infrared spectroscopic studies of alkali-activated fly ash structure, Microporous Mesoporous Mater. 86 (1–3) (2005) 207–214.
[295] Y. Li, R. Xu, B. Wang, J. Wei, L. Wang, M. Shen, et al., Enhanced n-doped porous carbon derived from koh-activated waste wool: a promising material for selective adsorption of CO2/CH4 and CH4/N2, Nanomaterials 9 (2) (2019).
[296] S. Hosseini, E. Marahel, I. Bayesti, A. Abbasi, L. Chuah Abdullah, T.S.Y. Choong, CO 2 adsorption on modified carbon coated monolith: effect of surface modification by using alkaline solutions, Appl Surf Sci 324 (2015) 569–575, https://doi.org/10.1016/j.apsusc.2014.10.054. Available from:.
[297] T. Otowa, R. Tanibata, M. Itoh, Production and adsorption characteristics of MAXSORB: high-surface-area active carbon, Gas Separ. Purif. 7 (4) (1993) 241–245.
[298] J. Wang, S. Kaskel, KOH activation of carbon-based materials for energy storage, J. Mater. Chem. 22 (45) (2012) 23710–23725.
[299] M.A. Lillo-Ródenas, D. Cazorla-Amorós, A. Linares-Solano, Understanding chemical reactions between carbons and NaOH and KOH: an insight into the chemical activation mechanism, Carbon N Y 41 (2) (2003) 267–275.
[300] J. Serafin, U. Narkiewicz, A.W. Morawski, R.J. Wróbel, B. Michalkiewicz, Highly microporous activated carbons from biomass for CO2 capture and effective micropores at different conditions, J CO2 Util. 18 (2017) 73–79.
[301] Y. Sudaryanto, S.B. Hartono, W. Irawaty, H. Hindarso, S. Ismadji, High surface area activated carbon prepared from cassava peel by chemical activation, Bioresour. Technol. 97 (5) (2006) 734–739.
[302] R.L. Tseng, S.K. Tseng, F.C. Wu, Preparation of high surface area carbons from Corncob with KOH etching plus CO2 gasification for the adsorption of dyes and phenols from water, Colloids Surfaces A Physicochem Eng Asp 279 (1–3) (2006) 69–78.
[303] R.L. Tseng, S.K. Tseng, Pore structure and adsorption performance of the KOH-activated carbons prepared from corncob, J. Colloid Interface Sci. 287 (2) (2005) 428–437.
[304] A. Rehman, S.J. Park, From chitosan to urea-modified carbons: tailoring the ultra-microporosity for enhanced CO2 adsorption, Carbon N Y 159 (2020) 625–637.
[305] J. Chen, J. Yang, G. Hu, X. Hu, Z. Li, S. Shen, et al., Enhanced CO2 capture capacity of nitrogen-doped biomass-derived porous carbons, ACS Sustain. Chem. Eng. 4 (3) (2016) 1439–1445.
[306] L. An, S. Liu, L. Wang, J. Wu, Z. Wu, C. Ma, et al., Novel nitrogen-doped porous carbons derived from graphene for effective CO 2 capture, Ind. Eng. Chem. Res. 58 (8) (2019) 3349–3358.
[307] Y.C. Chiang, C.Y. Yeh, C.H. Weng, Carbon dioxide adsorption on porous and functionalized activated carbon fibers, Appl Sci 9 (10) (2019) 1977. Available from: https://search.proquest.com/docview/2297045587.
[308] W. Xing, C. Liu, Z. Zhou, L. Zhang, J. Zhou, S. Zhuo, et al., Superior CO2 uptake of N-doped activated carbon through hydrogen-bonding interaction, Energy Environ. Sci. 5 (6) (2012) 7323–7327.
[309] J. Wang, I. Senkovska, M. Oschatz, M.R. Lohe, L. Borchardt, A. Heerwig, et al., Highly porous nitrogen-doped polyimine-based carbons with adjustable microstructures for CO2 capture, J. Mater. Chem. 1 (36) (2013) 10951–10961.

[310] P. Pandey, A.P. Katsoulidis, I. Eryazici, Y. Wu, M.G. Kanatzidis, S.T. Nguyen, Imine-linked microporous polymer organic frameworks, Chem. Mater. 22 (17) (2010) 4974–4979.
[311] P. Zhang, Y. Zhong, J. Ding, J. Wang, M. Xu, Q. Deng, et al., A new choice of polymer precursor for solvent-free method: preparation of N-enriched porous carbons for highly selective CO2 capture, Chem Eng J 355 (July 2018) (2019) 963–973, https://doi.org/10.1016/j.cej.2018.08.219. Available from:.
[312] M.A. Lillo-Ródenas, J. Juan-Juan, D. Cazorla-Amorós, A. Linares-Solano, About reactions occurring during chemical activation with hydroxides, Carbon N Y 42 (7) (2004) 1371–1375.
[313] J. Singh, S. Basu, H. Bhunia, CO2 capture by modified porous carbon adsorbents: effect of various activating agents, J. Taiwan Inst. Chem. Eng. 102 (2019) 438–447, https://doi.org/10.1016/j.jtice.2019.06.011. Available from:.
[314] A.F. Hassan, A.M. Youssef, Preparation and characterization of microporous NaOH-activated carbons from hydrofluoric acid leached rice husk and its application for lead(II) adsorption, Carbon Lett 15 (1) (2014) 57–66.
[315] Z.S. Liu, Y.H. Peng, C.Y. Huang, M.J. Hung, Application of thermogravimetry and differential scanning calorimetry for the evaluation of CO2 adsorption on chemically modified adsorbents, Thermochim Acta 602 (2015) 8–14, https://doi.org/10.1016/j.tca.2015.01.002. Available from:.
[316] R. Panek, M. Wdowin, W. Franus, D. Czarna, L.A. Stevens, H. Deng, et al., Fly ash-derived MCM-41 as a low-cost silica support for polyethyleneimine in post-combustion CO2 capture, J CO2 Util 22 (September) (2017) 81–90, https://doi.org/10.1016/j.jcou.2017.09.015. Available from:.
[317] W. Klinthong, C.H. Huang, C.S. Tan, Polyallylamine and NaOH as a novel binder to pelletize amine-functionalized mesoporous silicas for CO2 capture, Microporous Mesoporous Mater 197 (2014) 278–287, https://doi.org/10.1016/j.micromeso.2014.06.030. Available from:.
[318] H. He, M. Zhong, D. Konkolewicz, K. Yacatto, T. Rappold, G. Sugar, et al., Carbon black functionalized with hyperbranched polymers: synthesis, characterization, and application in reversible CO2 capture, J. Mater. Chem. 1 (23) (2013) 6810–6821.
[319] R. Ullah, M. Atilhan, S. Aparicio, A. Canlier, C.T. Yavuz, Insights of CO2 adsorption performance of amine impregnated mesoporous silica (SBA-15) at wide range pressure and temperature conditions, Int J Greenh Gas Control 43 (2015) 22–32, https://doi.org/10.1016/j.ijggc.2015.09.013. Available from:.
[320] Y. Belmabkhout, A. Sayari, Effect of pore expansion and amine functionalization of mesoporous silica on CO2 adsorption over a wide range of conditions, Adsorption 15 (3) (2009) 318–328.
[321] R.J.J. Jansen, H. van Bekkum, XPS of nitrogen-containing functional groups on activated carbon, Carbon N Y 33 (8) (1995) 1021–1027.
[322] R. Pietrzak, XPS study and physico-chemical properties of nitrogen-enriched microporous activated carbon from high volatile bituminous coal, Fuel 88 (10) (2009) 1871–1877.
[323] Z. Geng, Q. Xiao, H. Lv, B. Li, H. Wu, Y. Lu, et al., One-step synthesis of microporous carbon monoliths derived from biomass with high nitrogen doping content for highly selective CO2 capture, Sci Rep 6 (August) (2016) 4–11, https://doi.org/10.1038/srep30049. Available from:.
[324] M.V. Nguyen, B.K. Lee, A novel removal of CO2 using nitrogen doped biochar beads as a green adsorbent, Process Saf Environ Prot 104 (2016) 490–498, https://doi.org/10.1016/j.psep.2016.04.007. Available from:.
[325] C. Pevida, M.G. Plaza, B. Arias, J. Fermoso, F. Rubiera, J.J. Pis, Surface modification of activated carbons for CO 2 capture, Appl. Surf. Sci. 254 (22) (2008) 7165–7172.
[326] A. Laheäär, S. Delpeux-Ouldriane, E. Lust, F. Béguin, Ammonia treatment of activated carbon powders for supercapacitor electrode application, J. Electrochem. Soc. 161 (4) (2014) A568–A575.
[327] E.A. Bruton, L. Brammer, F.C. Pigge, C.B. Aakeröy, D.S. Leinen, Hydrogen bond patterns in aromatic and aliphatic dioximes, New J. Chem. 27 (7) (2003) 1084–1094.
[328] L. Rao, S. Liu, J. Chen, L. Wang, L. An, P. Yang, et al., Single-step synthesis of nitrogen-doped porous carbons for CO 2 capture by low-temperature sodium amide activation of petroleum coke, Energy Fuels 32 (12) (2018) 12787–12794.
[329] L. Wang, L. Rao, B. Xia, L. Wang, L. Yue, Y. Liang, et al., Highly efficient CO2 adsorption by nitrogen-doped porous carbons synthesized with low-temperature sodium amide activation, Carbon N Y 130 (2018) 31–40.
[330] S. Liu, P. Yang, L. Wang, Y. Li, Z. Wu, R. Ma, et al., Nitrogen-doped porous carbons from lotus leaf for CO2 capture and supercapacitor electrodes, Energy Fuels 33 (7) (2019) 6568–6576.
[331] Y. Zhang, L. Liu, P. Zhang, J. Wang, M. Xu, Q. Deng, et al., Ultra-high surface area and nitrogen-rich porous carbons prepared by a low-temperature activation method with superior gas selective adsorption and outstanding supercapacitance performance, Chem Eng J 355 (July 2018) (2019) 309–319, https://doi.org/10.1016/j.cej.2018.08.169. Available from:.
[332] D. Tiwari, C. Goel, H. Bhunia, P.K. Bajpai, Melamine-formaldehyde derived porous carbons for adsorption of CO2 capture, J. Environ. Manag. 197 (2017) 415–427.
[333] L. Rao, S. Liu, L. Wang, C. Ma, J. Wu, L. An, et al., N-doped porous carbons from low-temperature and single-step sodium amide activation of carbonized water chestnut shell with excellent CO2 capture performance, Chem Eng J 359 (November 2018) (2019) 428–435, https://doi.org/10.1016/j.cej.2018.11.065. Available from:.
[334] Á. Sánchez-Sánchez, F. Suárez-García, A. Martínez-Alonso, J.M.D. Tascón, Influence of porous texture and surface chemistry on the CO2 adsorption capacity of porous carbons: acidic and basic site interactions, ACS Appl. Mater. Interfaces 6 (23) (2014) 21237–21247.
[335] S. Liu, R. Ma, X. Hu, L. Wang, X. Wang, M. Radosz, et al., CO2 adsorption on hazelnut-shell-derived nitrogen-doped porous carbons synthesized by single-step sodium amide activation, Ind. Eng. Chem. Res. 59 (15) (2019) 7046–7053.
[336] L. Yue, Q. Xia, L.L.L.L.L. Wang, L.L.L.L.L. Wang, H. DaCosta, J. Yang, et al., CO2 adsorption at nitrogen-doped carbons prepared by K2CO3 activation of urea-modified coconut shell, J Colloid Interface Sci 511 (2018) 259–267, https://doi.org/10.1016/j.jcis.2017.09.040. Available from:.
[337] L. Wang, F. Sun, F. Hao, Z. Qu, J. Gao, M. Liu, et al., A green trace K2CO3 induced catalytic activation strategy for developing coal-converted activated carbon as advanced candidate for CO2 adsorption and supercapacitors, Chem Eng J 383 (September 2019) (2020) 123205, https://doi.org/10.1016/j.cej.2019.123205. Available from:.
[338] L.K.G. Bhatta, S. Subramanyam, M.D. Chengala, U.M. Bhatta, K. Venkatesh, Enhancement in CO2 adsorption on hydrotalcite-based material by novel carbon support combined with K2CO3 impregnation, Ind. Eng. Chem. Res. 54 (43) (2015) 10876–10884.
[339] J. Raymond, S. Gerard, T. Richard, J. Richard, B. Thomas, N. Shankar, Materials selectively adsorbing CO2 from CO2 containing streams, EP Pat 7 (19) (2000) 1–8.
[340] P. Wilson, S. Vijayan, K. Prabhakaran, Nitrogen doped microporous carbon by ZnCl2 activation of protein, Mater. Res. Express 4 (9) (2017).
[341] B. Chang, W. Shi, H. Yin, S. Zhang, B. Yang, Poplar catkin-derived self-templated synthesis of N-doped hierarchical porous carbon microtubes for effective CO2 capture, Chem Eng J 358 (September 2018) (2019) 1507–1518, https://doi.org/10.1016/j.cej.2018.10.142. Available from:.
[342] Y. Boyjoo, Y. Cheng, H. Zhong, H. Tian, J. Pan, V.K. Pareek, et al., From waste Coca Cola® to activated carbons with impressive capabilities for CO2 adsorption and supercapacitors, Carbon N Y 116 (2017) 490–499, https://doi.org/10.1016/j.carbon.2017.02.030. Available from.
[343] A. Heidari, H. Younesi, A. Rashidi, A.A. Ghoreyshi, Adsorptive removal of CO2 on highly microporous activated carbons prepared from Eucalyptus camaldulensis wood: effect of chemical activation, J Taiwan Inst Chem Eng 45 (2) (2014) 579–588.
[344] J. Ludwinowicz, M. Jaroniec, Effect of activating agents on the development of microporosity in polymeric-based carbon for CO2 adsorption, Carbon N Y 94 (2015) 673–679.
[345] G. Singh, I.Y. Kim, K.S. Lakhi, S. Joseph, P. Srivastava, R. Naidu, et al., Heteroatom functionalized activated porous biocarbons and their excellent performance for CO2 capture at high pressure, J. Mater. Chem. 5 (40) (2017) 21196–21204.
[346] B. Ashourirad, P. Arab, A. Verlander, H.M. El-Kaderi, From azo-linked polymers to microporous heteroatom-doped carbons: tailored chemical and textural properties for gas separation, ACS Appl. Mater. Interfaces 8 (13) (2016) 8491–8501.
[347] M. Olivares-Marín, C. Fernández-González, A. Macías-García, V. Gómez-Serrano, Preparation of activated carbon from cherry stones by chemical activation with ZnCl 2, Appl. Surf. Sci. 252 (17) (2006) 5967–5971.
[348] S. Dey, A. Bhunia, I. Boldog, C. Janiak, A mixed-linker approach towards improving covalent triazine-based frameworks for CO2 capture and separation, Microporous Mesoporous Mater 241 (2017) 303–315, https://doi.org/10.1016/j.micromeso.2016.11.033. Available from:.
[349] S. Dey, A. Bhunia, H. Breitzke, P.B. Groszewicz, G. Buntkowsky, C. Janiak, Two linkers are better than one: enhancing CO2 capture and separation with porous covalent triazine-based frameworks from mixed nitrile linkers, J. Mater. Chem. 5 (7) (2017) 3609–3620.
[350] G. Wang, K. Leus, S. Zhao, P. Van Der Voort, Newly designed covalent triazine framework based on novel N-heteroaromatic building blocks for efficient CO2 and H2 capture and storage, ACS Appl. Mater. Interfaces 10 (1) (2018) 1244–1249.
[351] A. Bhunia, D. Esquivel, S. Dey, R. Fernández-Terán, Y. Goto, S. Inagaki, et al., A photoluminescent covalent triazine framework: CO2 adsorption, light-driven hydrogen evolution and sensing of nitroaromatics, J. Mater. Chem. 4 (35) (2016) 13450–13457.
[352] P. Kuhn, M. Antonietti, A. Thomas, Porous, covalent triazine-based frameworks prepared by ionothermal synthesis, Angew. Chem. Int. Ed. 47 (18) (2008) 3450–3453.
[353] L. Rao, R. Ma, S. Liu, L. Wang, Z. Wu, J. Yang, et al., Nitrogen enriched porous carbons from D-glucose with excellent CO2 capture performance, Chem Eng J 362 (January) (2019) 794–801, https://doi.org/10.1016/j.cej.2019.01.093. Available from:.
[354] Y. Zhao, M. Seredych, Q. Zhong, T.J. Bandosz, Aminated graphite oxides and their composites with copper-based metal-organic framework: in search for efficient media for CO2 sequestration, RSC Adv. 3 (25) (2013) 9932–9941.
[355] M. Seredych, T.J. Bandosz, Mechanism of ammonia retention on graphite oxides: role of surface chemistry and structure, J. Phys. Chem. C 111 (43) (2007) 15596–15604.
[356] S. Glomb, D. Woschko, G. Makhloufi, C. Janiak, Metal-organic frameworks with internal urea-functionalized dicarboxylate linkers for SO2 and NH3 adsorption, ACS Appl. Mater. Interfaces 9 (42) (2017) 37419–37434.
[357] C. Cai, N. Fu, Z. Zhou, M. Wu, Z. Yang, R. Liu, Mechanochemical synthesis of tannic acid-Fe coordination compound and its derived porous carbon for CO2 adsorption, Energy Fuels 32 (10) (2018) 10779–10785.
[358] H. Ma, H. Ren, X. Zou, S. Meng, F. Sun, G. Zhu, et al., Post-metalation of porous aromatic frameworks for highly efficient carbon capture from CO2 + N2 and CH4 + N2 mixtures, Polym Chem 5 (1) (2014) 144–152, https://doi.org/10.1039/C3PY00647F. Available from:.

[359] K.L. Mulfort, O.K. Farha, C.L. Stern, A.A. Sarjeant, J.T. Hupp, Post-synthesis alkoxide formation within metal-organic framework materials: a strategy for incorporating highly coordinatively unsaturated metal ions, J. Am. Chem. Soc. 131 (11) (2009) 3866–3868.
[360] K.K. Han, Y. Zhou, Y. Chun, J.H. Zhu, Efficient MgO-based mesoporous CO 2 trapper and its performance at high temperature, J. Hazard Mater. 203–204 (2012) 341–347.
[361] A.M. Pierre-Louis, D.B. Hausner, N. Bhandari, W. Li, J. Kim, J.D. Kubicki, et al., Adsorption of carbon dioxide on Al/Fe oxyhydroxide, J colloid Interface Sci 400 (2013) 1–10, https://doi.org/10.1016/j.jcis.2013.01.047. Available from:.
[362] A.E. Creamer, B. Gao, S. Wang, Carbon dioxide capture using various metal oxyhydroxide-biochar composites, Chem. Eng. J. 283 (2016) 826–832.
[363] S. Hosseini, I. Bayesti, E. Marahel, F. Eghbali, F. Eghbali Babadi, L. Chuah Abdullah, et al., Adsorption of carbon dioxide using activated carbon impregnated with Cu promoted by zinc, J Taiwan Inst Chem Eng 52 (2015) 109–117, https://doi.org/10.1016/j.jtice.2015.02.015. Available from:.
[364] A. Abdedayem, M. Guiza, A. Ouederni, Copper supported on porous activated carbon obtained by wetness impregnation: effect of preparation conditions on the ozonation catalyst's characteristics, Compt. Rendus Chem. 18 (1) (2015) 100–109.
[365] P. Lahijani, M. Mohammadi, A.R. Mohamed, Metal incorporated biochar as a potential adsorbent for high capacity CO2 capture at ambient condition, J CO2 Util 26 (January) (2018) 281–293, https://doi.org/10.1016/j.jcou.2018.05.018. Available from:.
[366] S. Shahkarami, A.K. Dalai, J. Soltan, Enhanced CO2 adsorption using MgO-impregnated activated carbon: impact of preparation techniques, Ind. Eng. Chem. Res. 55 (20) (2016) 5955–5964.
[367] W.J. Liu, H. Jiang, K. Tian, Y.W. Ding, H.Q. Yu, Mesoporous carbon stabilized MgO nanoparticles synthesized by pyrolysis of MgCl2 preloaded waste biomass for highly efficient CO2 capture, Environ. Sci. Technol. 47 (16) (2013) 9397–9403.
[368] S.V. Vassilev, C.G. Vassileva, Extra CO2 capture and storage by carbonation of biomass ashes, Energy Convers Manag 204 (November) (2020) 112331, https://doi.org/10.1016/j.enconman.2019.112331. Available from:.
[369] Y. Guo, C. Zhao, X. Chen, C. Li, CO2 capture and sorbent regeneration performances of some wood ash materials, Appl Energy 137 (X) (2015) 26–36, https://doi.org/10.1016/j.apenergy.2014.09.086. Available from:.
[370] J.H. Kim, W.T. Kwon, Semi-dry carbonation process using fly ash from solid refused fuel power plant, Sustain. Times 11 (3) (2019).
[371] N.R. Galina, G.L.A.F. Arce, I. Ávila, Evolution of carbon capture and storage by mineral carbonation: data analysis and relevance of the theme, Miner Eng 142 (July) (2019) 105879, https://doi.org/10.1016/j.mineng.2019.105879. Available from:.
[372] M.H. Ibrahim, M.H. El-Naas, A. Benamor, S.S. Al-Sobhi, Z. Zhang, Carbon mineralization by reaction with steel-making waste: a review, Processes 7 (2) (2019) 1–21.
[373] F. Fashi, A. Ghaemi, A.H. Behroozi, Piperazine impregnation on Zeolite 13X as a novel adsorbent for CO2 capture: experimental and modeling, Chem. Eng. Commun. 0 (0) (2020) 1–17, https://doi.org/10.1080/00986445.2020.1746657. Available from:.
[374] S. Zhang, S. Ravi, Y.R. Lee, J.W. Ahn, W.S. Ahn, Fly ash-derived mesoporous silica foams for CO2 capture and aqueous Nd3+ adsorption, J. Ind. Eng. Chem. 72 (2019) 241–249, https://doi.org/10.1016/j.jiec.2018.12.024. Available from:.
[375] M. Czaun, A. Goeppert, R.B. May, D. Peltier, H. Zhang, G.K.S. Prakash, et al., Organoamines-grafted on nano-sized silica for carbon dioxide capture, J CO2 Util 1 (2013) 1–7, https://doi.org/10.1016/j.jcou.2013.03.007. Available from:.
[376] J.C. Hicks, J.H. Drese, D.J. Fauth, M.L. Gray, G. Qi, C.W. Jones, Designing adsorbents for CO2 capture from flue gas-hyperbranched aminosilicas capable of capturing CO2 reversibly, J. Am. Chem. Soc. 130 (10) (2008) 2902–2903.
[377] J.H. Drese, S. Choi, R.P. Lively, W.J. Koros, D.J. Fauth, M.L. Gray, et al., Synthesis-structure-property relationships for Hyperbranched aminosilica CO2 adsorbents, Adv. Funct. Mater. 19 (23) (2009) 3821–3832.
[378] J. Yan, C. Zhao, P. Wang, P. Lu, Studies on Several Fly Ashes and Their Modified Materials for CO2 Capture, vol. 1, American Society of Mechanical Engineers, Power Division (Publication) POWER, 2017, https://doi.org/10.1115/POWER-ICOPE2017-3420. Available from:.
[379] Q. Liu, Y. Ding, Q. Liao, X. Zhu, H. Wang, J. Yang, Fast synthesis of Al fumarate metal-organic framework as a novel tetraethylenepentamine support for efficient CO2 capture, Colloids Surfaces A Physicochem Eng Asp 579 (July) (2019) 123645, https://doi.org/10.1016/j.colsurfa.2019.123645. Available from:.
[380] M.M. Maroto-Valer, Z. Tang, Y. Zhang, CO2 capture by activated and impregnated anthracites, in: Fuel Processing Technology, 2005, pp. 1487–1502.
[381] M.B. Yue, Y. Chun, Y. Cao, X. Dong, J.H. Zhu, CO2 capture by as-prepared SBA-15 with an occluded organic template, Adv. Funct. Mater. 16 (13) (2006) 1717–1722.
[382] Y. Cao, F. Song, Y. Zhao, Q. Zhong, Capture of carbon dioxide from flue gas on TEPA-grafted metal-organic framework Mg2(dobdc), J. Environ. Sci. (China) 25 (10) (2013) 2081–2087, https://doi.org/10.1016/S1001-0742(12)60267-8. Available from:.
[383] X. Wang, W. Zeng, M. Song, F. Wang, X. Hu, Q. Guo, et al., Polyetheramine Improves the CO2 Adsorption Behavior of Tetraethylenepentamine-Functionalized Sorbents, Chem Eng J 364 (December 2018) (2019) 475–484, https://doi.org/10.1016/j.cej.2019.02.008. Available from:.
[384] J. Wei, Z. Lin, Z. He, L. Geng, L. Liao, Bagasse activated carbon with TETA/TEPA modification and adsorption properties of CO2, Water Air Soil Pollut. 228 (4) (2017).
[385] J. Wei, D. Mei, Z. Lin, L. Geng, S. Chen, L. Liao, Effects of TETA or TEPA loading on CO2 adsorption properties using pore-expanded KIT-6 as support, Nano 13 (4) (2018) 1–9.
[386] Z. Lin, J. Wei, CO2 adsorption on activated carbon/SBA-15 with TETA/TEPA modification, Key Eng. Mater. 735 KEM (2017) 164–167.
[387] G. Zhang, P. Zhao, L. Hao, Y. Xu, H. Cheng, A novel amine double functionalized adsorbent for carbon dioxide capture using original mesoporous silica molecular sieves as support, Sep Purif Technol 209 (May 2018) (2019) 516–527, https://doi.org/10.1016/j.seppur.2018.07.074. Available from:.
[388] E. Vilarrasa-García, J.A. Cecilia, S.M.L. Santos, C.L. Cavalcante, J. Jiménez-Jiménez, D.C.S. Azevedo, et al., CO2 adsorption on APTES functionalized mesocellular foams obtained from mesoporous silicas, Microporous Mesoporous Mater. 187 (2014) 125–134.
[389] G.P. Knowles, J.V. Graham, S.W. Delaney, A.L. Chaffee, Aminopropyl-functionalized mesoporous silicas as CO2 adsorbents, in: Fuel Processing Technology, 2005, pp. 1435–1448.
[390] J. Pokhrel, N. Bhoria, S. Anastasiou, T. Tsoufis, D. Gournis, G. Romanos, et al., CO2 adsorption behavior of amine-functionalized ZIF-8, graphene oxide, and ZIF-8/graphene oxide composites under dry and wet conditions, Microporous Mesoporous Mater. 267 (March) (2018) 53–67.
[391] N. Minju, P. Abhilash, B.N. Nair, A.P. Mohamed, S. Ananthakumar, Amine impregnated porous silica gel sorbents synthesized from water-glass precursors for CO2 capturing, Chem Eng J 269 (2015) 335–342, https://doi.org/10.1016/j.cej.2015.01.069. Available from:.
[392] T.H. Nguyen, S. Kim, M. Yoon, T.H. Bae, Hierarchical zeolites with amine-functionalized mesoporous domains for carbon dioxide capture, ChemSusChem 9 (5) (2016) 455–461.
[393] S. Salehi, M. Anbia, High CO2 adsorption capacity and CO2/CH4 selectivity by nanocomposites of MOF-199, Energy Fuels 31 (5) (2017) 5376–5384.
[394] Q. Xue, Y. Liu, Mixed-amine modified SBA-15 as novel adsorbent of CO2 separation for biogas upgrading, Separ. Sci. Technol. 46 (4) (2011) 679–686.
[395] D. Zhao, Q. Huo, J. Feng, B.F. Chmelka, G.D. Stucky, Nonionic triblock and star diblock copolymer and oligomeric sufactant syntheses of highly ordered, hydrothermally stable, mesoporous silica structures, J. Am. Chem. Soc. 120 (24) (1998) 6024–6036.
[396] S.G. De Ávila, M.A. Logli, L.C.C. Silva, M.C.A. Fantini, J.R. Matos, Incorporation of monoethanolamine (MEA), diethanolamine (DEA) and methyldiethanolamine (MDEA) in mesoporous silica: an alternative to CO2 capture, J. Environ. Chem. Eng. 4 (4) (2016) 4514–4524.
[397] Z zhu Yang, J jing Wei, G ming Zeng, H qing Zhang, X fei Tan, C. Ma, et al., A review on strategies to LDH-based materials to improve adsorption capacity and photoreduction efficiency for CO 2, Coord Chem Rev 386 (2019) 154–182, https://doi.org/10.1016/j.ccr.2019.01.018. Available from:.
[398] Q. Li, H. Zhang, F. Peng, C. Wang, H. Li, L. Xiong, et al., Monoethanolamine-modified attapulgite-based amorphous silica for the selective adsorption of CO2 from simulated biogas, Energy Fuels 34 (2) (2020) 2097–2106.
[399] S. Mukherjee, Akshay, A.N. Samanta, Amine-impregnated MCM-41 in post-combustion CO2 capture: synthesis, characterization, isotherm modelling, Adv Powder Technol 30 (12) (2019) 3231–3240, https://doi.org/10.1016/j.apt.2019.09.032. Available from:.
[400] A. Kongnoo, P. Intharapat, P. Worathanakul, C. Phalakornkule, Diethanolamine impregnated palm shell activated carbon for CO2 adsorption at elevated temperatures, J Environ Chem Eng 4 (1) (2016) 73–81, https://doi.org/10.1016/j.jece.2015.11.015. Available from:.
[401] K.S.N. Kamarudin, N. Zaini, N.E.A. Khairuddin, CO2 removal using amine-functionalized kenaf in pressure swing adsorption system, J Environ Chem Eng 6 (1) (2018) 549–559, https://doi.org/10.1016/j.jece.2017.12.040. Available from:.
[402] R. Chatti, A.K. Bansiwal, J.A. Thote, V. Kumar, P. Jadhav, S.K. Lokhande, et al., Amine loaded zeolites for carbon dioxide capture: amine loading and adsorption studies, Microporous Mesoporous Mater. 121 (1–3) (2009) 84–89.
[403] R.S. Franchi, P.J.E.E. Harlick, A. Sayari, Applications of pore-expanded mesoporous silica. 2. Development of a high-capacity, water-tolerant adsorbent for CO2, Ind Eng Chem Res 44 (21) (2005 Oct), 8007–13. Available from: https://pubs.acs.org/doi/10.1021/ie0504194.
[404] S. Ahmed, A. Ramli, S. Yusup, CO2 adsorption study on primary, secondary and tertiary amine functionalized Si-MCM-41, Int J Greenh Gas Control 51 (2016) 230–238, https://doi.org/10.1016/j.ijggc.2016.05.021. Available from:.
[405] A. Ramli, S. Ahmed, S. Yusup, Effect of monoethanolamine loading on the physicochemical properties of amine-functionalized Si-MCM-41, Sains Malays. 43 (2) (2014) 253–259.
[406] P. Castellazzi, M. Notaro, G. Busca, E. Finocchio, CO2 Capture by Functionalized Alumina Sorbents: DiEthanolAmine on γ-alumina, Microporous Mesoporous Mater 226 (2016) 444–453, https://doi.org/10.1016/j.micromeso.2016.02.027. Available from:.
[407] J. Wei, L. Liao, Y. Xiao, P. Zhang, Y. Shi, Capture of carbon dioxide by amine-impregnated as-synthesized MCM-41, J Environ Sci 22 (10) (2010) 1558–1563, https://doi.org/10.1016/S1001-0742(09)60289-8. Available from:.
[408] X. Liu, L. Zhou, X. Fu, Y. Sun, W. Su, Y. Zhou, Adsorption and regeneration study of the mesoporous adsorbent SBA-15 adapted to the capture/separation of CO2 and CH4, Chem. Eng. Sci. 62 (4) (2007) 1101–1110.
[409] Y. Zhao, H. Ding, Q. Zhong, Preparation and characterization of aminated graphite oxide for CO 2 capture, Appl Surf Sci 258 (10) (2012) 4301–4307, https://doi.org/10.1016/j.apsusc.2011.12.085. Available from:.

[410] N.I. Kovtyukhova, Layer-by-layer assembly of ultrathin composite films from micron-sized graphite oxide sheets and polycations, Chem. Mater. 11 (3) (1999) 771–778.
[411] H.C. Schniepp, J.L. Li, M.J. McAllister, H. Sai, M. Herrera-Alonson, D. H. Adamson, et al., Functionalized single graphene sheets derived from splitting graphite oxide, J. Phys. Chem. B 110 (17) (2006) 8535–8539.
[412] M. Herrera-Alonso, A.A. Abdala, M.J. McAllister, I.A. Aksay, R.K. Prud'homme, Intercalation and stitching of graphite oxide with diaminoalkanes, Langmuir 23 (21) (2007) 10644–10649.
[413] J. Jiao, J. Cao, Y. Xia, L. Zhao, Improvement of adsorbent materials for CO2 capture by amine functionalized mesoporous silica with worm-hole framework structure, Chem Eng J 306 (2016) 9–16, https://doi.org/10.1016/j.cej.2016.07.041. Available from:.
[414] Y. Li, L. Yang, X. Zhu, J. Hu, H. Liu, Post-synthesis modification of porous organic polymers with amine: a task-specific microenvironment for CO2 capture, Int J Coal Sci Technol 4 (1) (2017) 50–59.
[415] C.F. Martín, M.B. Sweatman, S. Brandani, X. Fan, Wet impregnation of a commercial low cost silica using DETA for a fast post-combustion CO2 capture process, Appl. Energy 183 (2016) 1705–1721.
[416] M.L. Gray, Y. Soong, K.J. Champagne, J. Baltrus, R.W. Stevens, P. Toochinda, et al., CO2 capture by amine-enriched fly ash carbon sorbents, Separ. Purif. Technol. 35 (1) (2004) 31–36.
[417] N.P. Wickramaratne, J. Xu, M. Wang, L. Zhu, L. Dai, M. Jaroniec, Nitrogen enriched porous carbon spheres: attractive materials for supercapacitor electrodes and CO2 adsorption, Chem. Mater. 26 (9) (2014) 2820–2828.
[418] P. Puthiaraj, Y.R. Lee, W.S. Ahn, Microporous amine-functionalized aromatic polymers and their carbonized products for CO2 adsorption, Chem Eng J 319 (2017) 65–74, https://doi.org/10.1016/j.cej.2017.03.001. Available from:.
[419] K. Li, J. Jiang, S. Tian, F. Yan, X. Chen, Polyethyleneimine-nano silica composites: a low-cost and promising adsorbent for CO2 capture, J. Mater. Chem. 3 (5) (2015) 2166–2175.
[420] H. Zhang, A. Goeppert, M. Czaun, G.K.S. Prakash, G.A. Olah, CO2 capture on easily regenerable hybrid adsorbents based on polyamines and mesocellular silica foam. Effect of pore volume of the support and polyamine molecular weight, RSC Adv. 4 (37) (2014) 19403–19417.
[421] A. Houshmand, M.S. Shafeeyan, A. Arami-Niya, W.M.A.W. Daud, Anchoring a halogenated amine on the surface of a microporous activated carbon for carbon dioxide capture, J Taiwan Inst Chem Eng 44 (5) (2013) 774–779, https://doi.org/10.1016/j.jtice.2013.01.014. Available from:.